COMBUSTION AND CO-COMBUSTION OF OLIVE CAKE AND COAL IN A FLUIDIZED BED

A THESIS SUBMITTED TO
THE GRADUATE SCHOOL OF NATURAL AND APPLIED SCIENCES
OF
MIDDLE EAST TECHNICAL UNIVERSITY

BY

MURAT VAROL

IN PARTIAL FULLFILLMENT OF THE REQUIREMENTS
FOR
THE DEGREE OF MASTER OF SCIENCE
IN
ENVIRONMENTAL ENGINEERING

APRIL 2006

Approval of the Graduate School of Natural and Applied Sciences

Prof. Dr. Canan Özgen
Director

I certify that this thesis satisfies all the requirements as a thesis for the degree of Master of Science.

Prof. Dr. Filiz B. Dilek
Head of Department

This is to certify that we have read this thesis and that in our opinion it is fully adequate, in scope and quality, as a thesis for the degree of Master of Science.

Prof. Dr. Aysel Atımtay
Supervisor

Examining Committee Members

Assoc. Prof. Dr. F. Dilek Sanin (METU, ENVE) _____

Prof. Dr. Aysel Atımtay (METU, ENVE) _____

Prof. Dr. Timur Doğu (METU, CHE) _____

Assist. Prof. Dr. Ayşegül Aksoy (METU, ENVE) _____

Assist. Prof. Dr. İpek İmamoğlu (METU, ENVE) _____

I hereby declare that all information in this document has been obtained and presented in accordance with academic rules and ethical conduct. I also declare that, as required by these rules and conduct, I have fully cited and referenced all material and results that are not original to this work.

Name, Last name : Murat VAROL

Signature :

ABSTRACT

COMBUSTION AND CO-COMBUSTION OF OLIVE CAKE AND COAL IN A FLUIDIZED BED

VAROL, Murat
M.Sc., Department of Environmental Engineering
Supervisor: Prof. Dr. Aysel T. ATIMTAY

April 2006, 155 pages

In this study, combustion performances and emission characteristics of olive cake and olive cake+coal mixture are investigated in a bubbling fluidized bed of 102 mm inside diameter and 900 mm height. The average particle sizes of coal and olive cake used in the experiments were 1.57 mm and 1.52 mm, respectively. Flue gas concentrations of O_2, CO, SO_2, NO_x, and total hydrocarbons (C_mH_n) were measured during combustion experiments. Operational parameters (excess air ratio, secondary air injection) were changed and variation of pollutant concentrations and combustion efficiency with these operational parameters were studied.

The temperature profiles measured along the combustor column was found higher in the freeboard for olive cake than coal due to combustion of hydrocarbons mostly in the freeboard. The location of the maximum temperature in the freeboard shifted to the upper part of the column, as the volatile matter content in the fuel mixture increased.

Combustion efficiencies in the range of 83.6-90.1% were obtained for olive cake with the excess air ratio of 1.12-2.30. The corresponding combustion efficiency for coal was 98.4-99.7% under the same conditions. As the CO and hydrocarbon concentration in the flue gas increased, the combustion efficiency decreased.

Also co-combustion experiments of olive cake and coal for various mixing ratios were carried out. As the amount of olive cake in the fuel mixture increased, SO_2 emissions decreased because of the very low sulfur content of olive cake.

In order to increase the combustion efficiency, secondary air was injected into the freeboard which was a good solution to decrease the CO and hydrocarbon emissions, and to increase the combustion efficiency.

For the setup used in this study, the optimum operating conditions with respect to NO_x and SO_2 emissions were found as 1.35 for excess air ratio, and 30 L/min for secondary air flowrate for the combustion of 75 wt% olive cake and 25 wt% coal mixture. Highest combustion efficiency of 99.8% was obtained with an excess air ratio of 1.7, secondary air flow rate of 40 L/min for the combustion of 25 wt% olive cake and 75 wt% coal mixture.

Key Words: Olive cake combustion, Bubbling fluidized bed, Co-combustion, Emissions, Secondary air injection

ÖZ

PRİNA, KÖMÜR VE PRİNA-KÖMÜR KARIŞIMLARININ AKIŞKAN YATAKTA YAKILMASI

VAROL, Murat
Yüksek Lisans, Çevre Mühendisliği Bölümü
Tez Danışmanı: Prof. Dr. Aysel T. ATIMTAY

April 2006, 155 sayfa

Bu çalışmada, prinanın ve prina+kömür karışımının 102 mm iç çapında ve 900 mm yüksekliğinde olan bir kabarcıklı akışkan yatak sisteminde yanma ve emisyon davranışları incelenmiştir. Deneylerde kullanılan kömür ve prinanın ortalama parçacık boyutları sırasıyla 1.57 mm ve 1.52 mm'dir. Yakma deneyleri sırasında oluşan baca gazında O_2, CO, SO_2, NO_x ve toplam hidrokarbon (C_mH_n) konsantrasyonları ölçülmüştür. İşletme parametreleri (fazla hava oranı, ikincil hava ilavesi) değiştirilerek bu parametrelerin kirletici konsantrasyonları ve yanma verimi üzerindeki etkileri incelenmiştir.

Yakma testleri esnasında yakıcı kolon boyunca yapılan sıcaklık ölçümler, prina yakıldığında oluşan serbest bölge (freeboard) sıcaklıklarının kömür yakıldığında oluşan sıcaklıklardan daha yüksek olduğunu göstermiştir. Bu da yakıttaki hidrokarbonların daha çok serbest bölgede yanmasından kaynaklanmaktadır. En

yüksek sıcaklığın gözlendiği bölge, yakıt içindeki uçucu madde miktarı arttıkça yatağın daha üst kısımlarına kaymaktadır.

Prina yakıldığında 1.12-2.30 aralığındaki fazla hava oranı için %83.6-90.1 arasında değişen yanma verimleri elde edilmiştir. Kömür için aynı koşullarda bu değerler %98.4-99.7 olarak tespit edilmiştir. Baca gazındaki CO ve hidrokarbon konsantrasyonları arttıkça yanma veriminin düştüğü gözlenmiştir

Ayrıca, prina ile kömürün farklı karışım oranları için de yanma deneyleri yapılmıştır. Yakıt karışımında prina oranı arttıkça, prinadaki çok düşük kükürt oranından dolayı baca gazında SO_2 emisyonları azalmıştır.

Yanma verimini arttırabilmek için yatak üzerindeki serbest bölgeye ikincil hava enjeksiyonu yapılmıştır. Bu uygulama, yanma gazları içinde bulunan CO ve hidrokarbon konsantrasyonlarını azaltan iyi bir çözüm olmuştur.

Bu çalışmada kullanılan deney sistemi için, NO_x ve SO_2 emisyonlarının en aza indiği optimum koşullar, %75 prina-%25 kömür içeren karışımın 1.35 fazla hava oranı ve 30 L/dak ikincil hava miktarı ile yakıldığı koşullar olmuştur. Ayrıca, en yüksek (%99.8) yanma verimi, 1.7 fazla hava oranı ve 40 L/dak ikincil hava miktarı ile yakıldığı durumda elde edilmiştir.

Anahtar Sözcükler: Prina yanması, Kabarcıklı akışkan yatak, Birlikte yanma, Emisyonlar, İkincil hava ilavesi

To my parents,

ACKNOWLEDGMENTS

I would like to express my deepest gratitude to my supervisor Prof. Dr. Aysel Atımtay for her guidance, advice, criticism and encouragement and insight throughout the research.

I also would like to thank Assist. Prof. Dr. Hüseyin Topal from Gazi University for providing and preparation of coal samples, and helping in some technical details at the beginning of the experiments.

I would like to thank my committee members, Prof. Dr. Timur Doğu, Assoc. Prof. Dr. F. Dilek Sanin, Assist. Prof. Dr. Ayşegül Aksoy, and Assist. Prof. Dr. İpek İmamoğlu for their suggestions and comments.

I would also like to thank my mother, Hükmiye Varol, my father, A. Fikri Varol, and my sister, Selen Varol for their support and confidence in me.

TABLE OF CONTENTS

LIST OF TABLES

TABLES

LIST OF FIGURES

FIGURES

ABBREVIATIONS

BFBC	: Bubbling fluidized bed combustor
BFB	: Bubbling fluidized bed
CFB	: Circulating fluidized bed
C_mH_n	: Hydrocarbon emissions measured as C_3H_8
d_p	: Particle diameter (mm)
HHV	: Higher heating value (kJ/kg)
L_{CH}	: Heating value of combustible material lost as hydrocarbons in flue gas (%)
L_{CO}	: Heating value of combustible material lost as CO in flue gas (%)
$L_{C,bed}$	: Heating value of combustible material lost as C in bottom ash (%)
$L_{C,cylone}$	: Heating value of combustible material lost as C in fly ash (%)
L_{mf}	: Height of bed at minimum fluidization (mm)
LHV	: Lower heating value (kJ/kg)
M_f	: Fuel feeding rate (kg fuel/h)
Nm^3	: Volume (m^3) at normal conditions (0^oC, 1 Atm)
O_2 atm	: Atmospheric oxygen concentration (20.90 %)
$O_{2,th}$	: Theoretical oxygen requirement for the combustion of one kg of fuel (Nm^3/kg fuel)
ΔP_{bed}	: Pressure drop across the bed (mm water)
Q_f	: Total thermal capacity of combustor (kW)
SMR	: Saturation mixing ratio (g H_2O/kg of air)
$T_{average}$	: Average bed temperature (^oC)
TC	: Thermocouple
u_{mf}	: Minimum fluidization velocity at room temperature (m/s)
u_o	: Superficial gas velocity (m/s)

W/A	: Weight of particles / cross sectional area of the column
$V_{air,actual}$	: Actual volume of air required for the combustion of one kg of fuel (Nm^3/kg fuel)
$V_{air,th}$	: Volume of air theoretically required for the combustion of one kg of fuel (Nm^3/kg fuel)
V_{CO2}	: Volume of CO_2 in flue gas (Nm^3/kg fuel)
$V_{fluegas,actual}^{0}$	: Actual amount of flue gas formed (Nm^3/kg fuel)
$V_{fluegas,th(d.b)}$	: Volume of flue gas formed on dry basis for the combustion of one kg of fuel (Nm^3/kg fuel)
$V_{fluegas,th(w.b)}$	: Volume of flue gas formed on wet basis for the combustion of one kg of fuel (Nm^3/kg fuel)
V_g	: Volume of gas per kg of fuel (Nm^3/kg fuel)
$V_{H2O\ in\ air}$	: Volume of water vapor formed by the moisture content of air (Nm^3/kg fuel)
$V_{H2O\ in\ flue\ gas}$	: Volume of H_2O in flue gas (Nm^3/kg fuel)
$V_{moisture\ in\ fuel}$	: Volume of water vapor formed by the moisture content of fuel (Nm^3/kg fuel)
V_{NO}	: Volume of NO in flue gas (Nm^3/kg fuel)
V_{N2}	: Volume of nitrogen supplied from air for the combustion of one kg of fuel (Nm^3/kg fuel)
V_{O2}	: Volume of O_2 in flue gas (Nm^3/kg fuel)
V_{SO2}	: Volume of SO_2 in flue gas (Nm^3/kg fuel)
$V_{total,\ H2O}$	: Total volume of water vapor formed for the combustion of one kg of fuel (Nm^3/kg fuel)
VM	: Volatile Matter
ε	: Void fraction of bed (-)
ε_{mf}	: Void fraction at minimum fluidization (-)
η	: Combustion efficiency (%)
μ	: Fluid viscosity (g-cm/s)
λ	: Excess air ratio (-)

CHAPTER 1

INTRODUCTION

1.1. General

Energy is an indispensable component of life. The need for energy has continuously increased throughout the history firstly due to increase in human population and secondly due to industrialization. World's energy supply is not infinite and fossil fuels used today to supply the energy demand of the world will not last very long. Besides, fossil fuels generate air pollution which increases every year at a very fast rate. In order to supply the increasing demand for energy, fossil fuels should be replaced with new and alternative energy sources such as solar, wind, hydraulic and biomass energies. Biomass energy, or bioenergy, is defined as energy derived from plant materials and animal wastes, and this energy obtained from biomass can be considered as "CO_2 – neutral". The amount of CO_2 released from combustion of biomass sources is absorbed by plants during photosynthesis in their lifetimes. Consequently, CO_2 absorbed from atmosphere via photosynthesis is returned to the atmosphere during combustion. Thus, there is no net input of CO_2 into the atmosphere by biomass.

Many countries head towards new and renewable energy resources in addition to the conventional resources. New and renewable energy sources can be listed as biomass, wind, solar, hydrogen, geothermal and wave energy. Biomass energy has a worldwide usage in the developing countries to produce energy and our country is also rich regarding biomass. Biomass has an advantage of minimizing greenhouse gas emissions which cause global warming. CO_2 is one of the

greenhouse gases and it is possible to decrease the CO_2 emissions with energy production from biomass.

Turkey has decided to be a part of the United Nations Framework Convention on Climate Change (UNFCCC) as of October 2003, and this agreement was signed on the 24th of May in 2004 (UNFCCC, 2006). This decision will be followed by ratification of the KYOTO protocol which aims to decrease the emissions of greenhouse gases, especially CO_2, to the level of 1990's. In this scope, the protocol brings legal obligations to the countries. For the protocol to enter into force, it was needed to be signed by not less than 55 countries of the Convention, incorporating countries included in Annex I which accounted in total for at least 55 per cent of the total carbon dioxide emissions of the countries included in Annex I.

One of the most important objectives of this century is to develop new technologies to increase the energy production efficiency while protecting the environment by minimizing the emissions. It is obvious that energy obtained from biomass serves to that objective.

1.2. Energy Outlook of Turkey

The energy statistics prepared by the World Energy Council, Turkish National Committee (WEC/TNC) in 2003 states that: "Turkey is an energy importing country as far as the total primary energy supply is concerned. Turkey meets **19.7 %** of its total primary energy supply from national solid fuels, **71.97 %** from imports, and **6.8 %** from biomass sources such as wood, animal waste and vegetable residues. It is expected that the energy dependency to imported fuel sources will increase in the future. Turkey is also extremely dependent to developed countries for the energy conversion and environment protection technologies" (WEC/TNC, 2006).

The general energy outlook of Turkey from 1985 to 2003 is given in Table 1.1. Total energy production and total energy supply is shown in units of MTOE (million tones of oil equivalent). The total shares of the production and net imports in the total supply of energy are also shown as percentages in the last two rows of this table in order to emphasize the increase of energy imports. The total net % of imports was 72% in 2003 and this number is expected to reach to 74 % in 2005. Energy demand and supply equilibrium of Turkey between 1985 and 2003 is given in Figure 1.1. Data is provided from the WEC/TNC.

Table 1.1 Energy outlook of Turkey between 1985 and 2003 (WEC/TNC, 2006)

	1985	1990	1995	2000	2001	2002	2003
Total Production, MTOE	**21.70**	**25.14**	**26.20**	**26.87**	**25.17**	**24.57**	**23.81**
Total Net Import, MTOE	**17.39**	**27.16**	**36.14**	**54.23**	**49.47**	**53.94**	**60.46**
Total Supply, MTOE	**39.09**	**52.30**	**62.34**	**81.27**	**75.96**	**78.41**	**84.00**
Total Production, %	**55.52%**	**48.07%**	**42.03%**	**33.06%**	**33.14%**	**31.34%**	**28.35%**
Total Net Import, %	**44.48%**	**51.93%**	**57.97%**	**66.73%**	**65.13%**	**68.79%**	**71.97%**

In 2003, the total primary energy production of Turkey is 23.81 Mtoe which meets 28.35 % of the total primary energy supply. It can be seen from Figure 1.1 that there is a gradual increase in the energy supply between the years 1985 and 2000. However, a decrease in the total supply is observed in 2001 due to the economical crisis in that year. The total primary energy supply in 2000 was 81.27 Mtoe and it became 75.96 Mtoe in 2001 by decreasing 6.5%. After that year with the recovery of the economical situation, the increasing trend on the total primary energy supply continued, being 78.41 Mtoe in 2002 and 84.00 Mtoe in 2003.

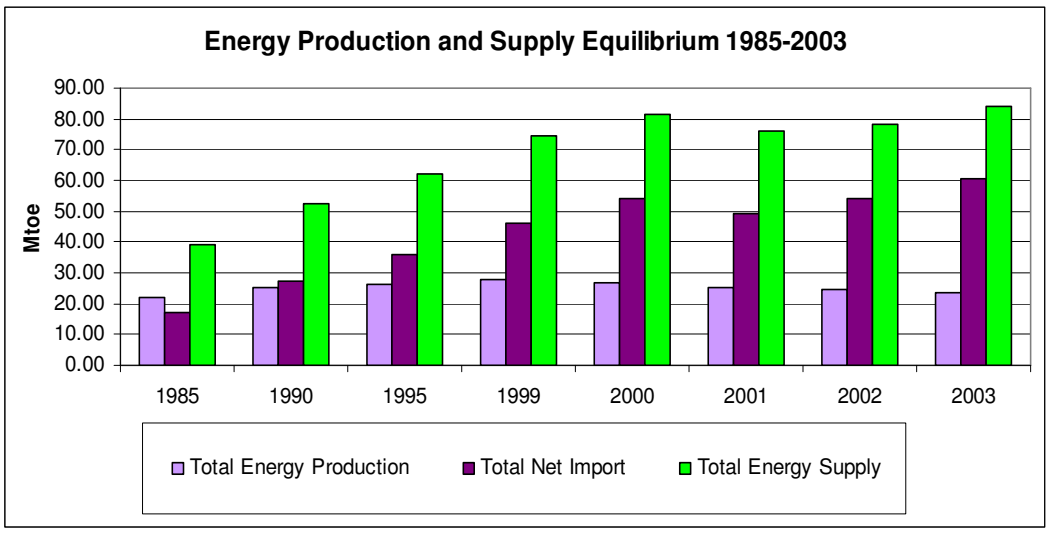

Figure 1.1 Energy production, imports and the total supply between 1985 and 2003 in Turkey (WEC/TNC, 2006)

Energy production in Turkey is not sufficient to meet the energy demand. As a result of a rapid increase in the energy demand and a slow increase in the energy production, the energy imports have increased rapidly. The total imported energy was 17.39 Mtoe in 1985. The energy import has increased at about 2.39 Mtoe annually and reached to 60.46 Mtoe in the 2003. The rate of increase of the total energy imports is approximately 7.2% per year between 1985 and 2003. The share of imports has increased up to 71.97% in 2003. It still keeps increasing with the growth in economy. The increasing share of imports in Turkey's energy supply between 1985 and 2003 is seen in Figure 1.2.

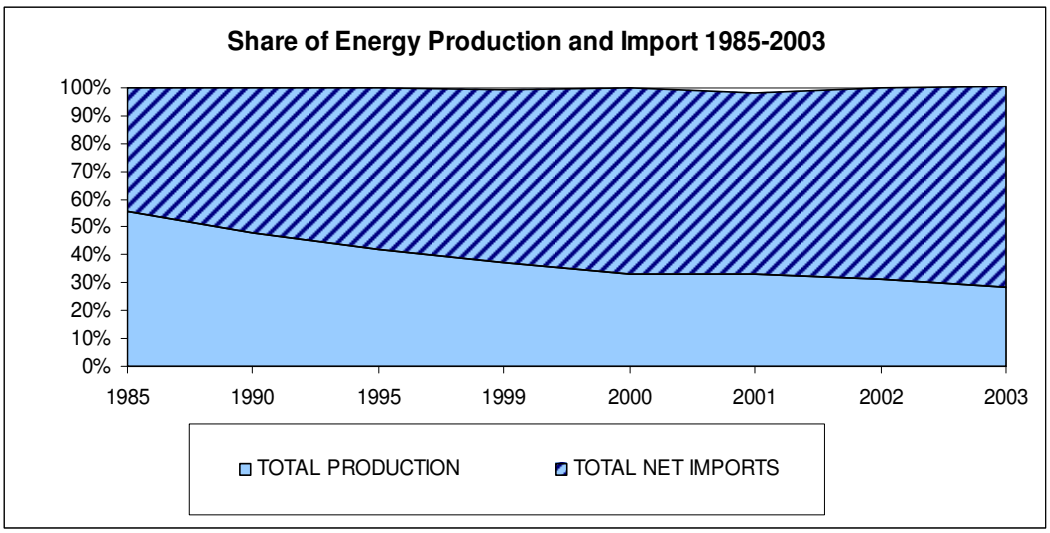

Figure 1.2 Shares of energy production and net imports in Turkey between 1985 and 2003 (WEC/TNC, 2006)

When Turkey's total primary energy supply is examined between 1990 and 2003, it can be seen that the share of gas (natural gas) on the total primary energy supply (TPES) has increased from 3.11 Mtoe in 1990 to 19.45 Mtoe in 2003 with an increasing rate of 1.26 Mtoe per year. Although the shares of combustibles, renewables, wastes and hydropower resources on TPES decrease, the shares of geothermal and solar and wind resources in TPES have increased from 1990 to 2003. The combustible, renewable and wastes include the wood and woody residues, agricultural residues, and animal wastes.

Table 1.2 Total primary energy supply of Turkey between 1990 and 2003 with respect to energy resources (WEC/TNC, 2006)

	TOTAL PRIMARY ENERGY SUPPLY (TPES), MTOE					
	1990	**1995**	**2000**	**2001**	**2002**	**2003**
Total	**52.30**	**62.34**	**80.98**	**75.60**	**78.14**	**84.00**
Coal	16.00	16.50	24.85	20.46	21.22	22.70
Oil	23.86	29.30	32.30	30.94	30.78	31.81
Gas	3.11	6.20	13.73	14.87	16.13	19.45
Comb.Ren.&Wastes	7.20	7.07	6.46	6.21	5.97	5.75
Hydropower	2.00	3.05	2.66	2.07	2.90	3.04
Geothermal	0.09	0.14	0.71	0.76	0.82	0.86
Solar and Wind	0.02	0.09	0.27	0.29	0.32	0.36

The progress and evolution of total primary energy supply in Turkey between 1985 and 2003 can be seen from Figure 1.3. The natural gas usage in the production of energy has increased every year, especially after 1990. There is also an increase in the energy produced from coal and oil resources.

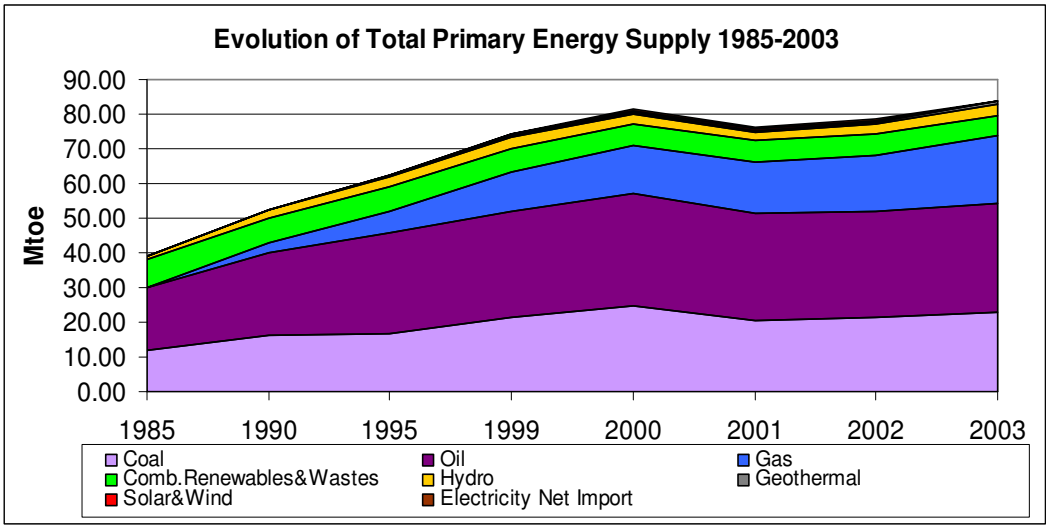

Figure 1.3 Evolution of total primary energy supply between 1985 and 2003 in Turkey (WEC/TNC, 2006)

According to the total primary energy supply data in 2003, 37.88% of the total primary energy supply is met by oil resources, 27.04% by coal resources, 23.17% by natural gas, 6.85% by combustibles, renewables and wastes, 3.62% by hydropower resources and the rest by geothermal (1.02%) and solar and wind resources (0.42%).

The energy supplied from renewable energy resources has reached to10.01 Mtoe in 2003 including hydropower (3.04 Mtoe), geothermal (0.86 Mtoe) and solar and wind energies (0.36 Mtoe). The share of the renewable energy resources on TPES is 11.92% for 2003.

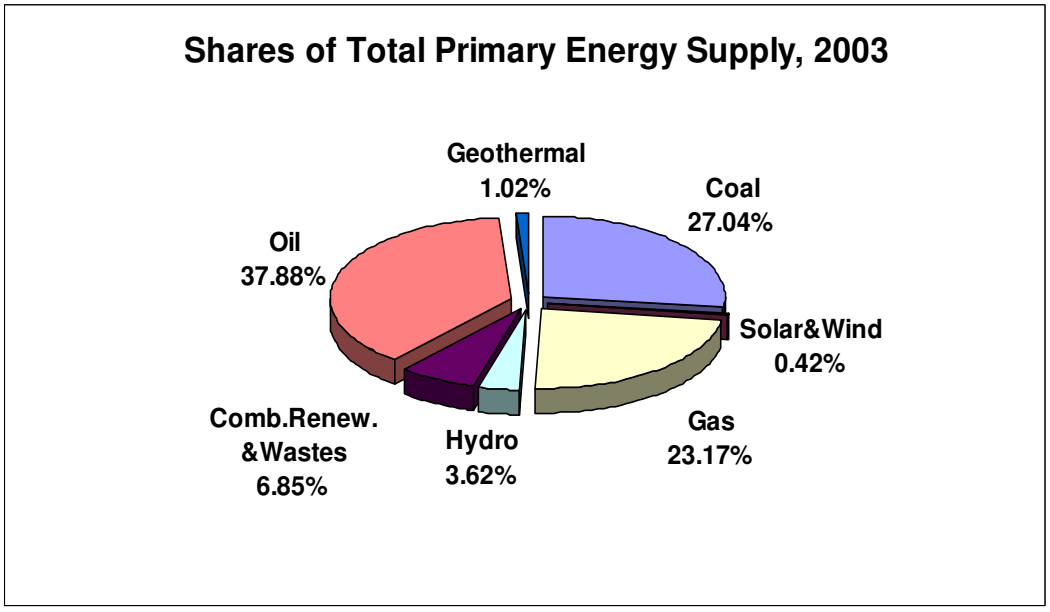

Figure 1.4 Shares of total primary energy supply of Turkey in 2003 (WEC/TNC, 2006)

Shares of different resources in the total energy production for Turkey in 2003 are shown in Figure 1.5. According to the total energy production data in 2003, coal approximately meets the half (45.38%) of the total energy production. Although

Turkey benefits from combustibles and wastes much less than the other resources, this energy resource is commonly used in energy production.

Next to coal, the combustibles and wastes are the main energy resource of Turkey, especially in rural areas. Their share in the total energy production is 24.30% in 2003. Another important energy resource is the hydropower. 12.76% of the total energy production is met by hydropower in 2003.

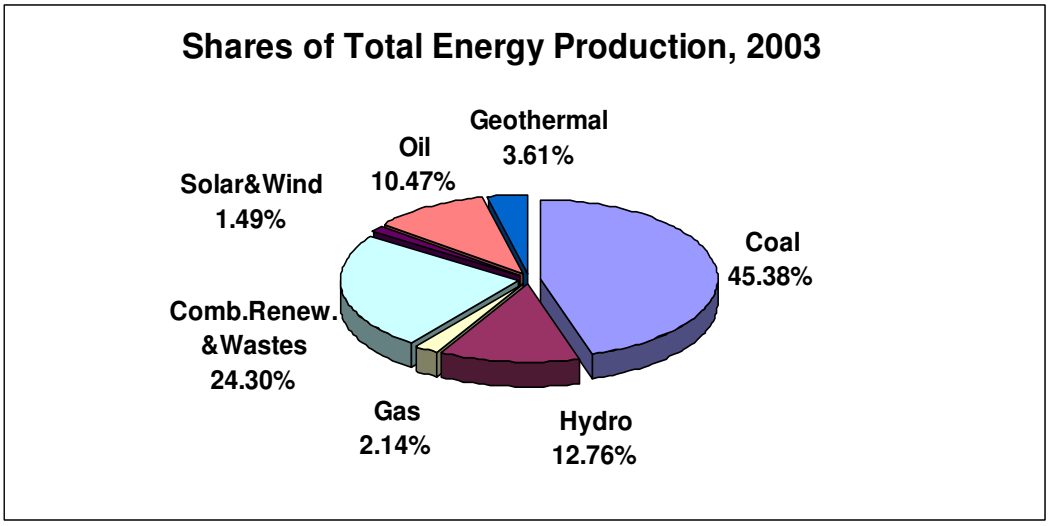

Figure 1.5 Shares of different resources in the total energy production of Turkey in 2003 (WEC/TNC, 2006)

1.3. Biomass Energy Potential of Turkey

The annual biomass energy potential of Turkey is estimated as 32 Mtoe (Balat, 2005). The total recoverable biomass energy potential is estimated to be about 16.92 Mtoe. The estimate is based on the recoverable biomass energy potential from the main agricultural residues, livestock farming wastes, forestry and wood processing residues and municipal wastes (Kaygusuz, 2002). The biomass energy production for the year 2003 is 5.75 Mtoe. The largest portion of that production

is used in rural areas for heating and cooking. It can be said that the classical biomass energy is produced by burning wood and dried dung in rural areas.

The total annual amount of agricultural residues in Turkey is estimated to be 50-65 million tons. Total calorific value of field crop residues is 228 PJ /year. The major crops produced in Turkey are maize (33.4% of the total production), wheat (27.6% of the total production), and cotton (18.1% of the total production). Also there are a lot of fruit crop residues in Turkey. The total calorific value of fruit crop residues is 75 PJ/year. The major crops produced in Turkey with shell are hazelnut 55.8% and olive 25.9% (Exploitation of Agricultural Residues in Turkey, 2005).

In order to understand the energy potential of olive, it is beneficial to investigate the olive production in Turkey as well as in the world.

1.3.1. Olive and Olive Cake Production in Turkey

Olive (Olea europaea L.) is a member of Oleacea family. The homeland of olive is the South-Front Asia and the upper side of the Mesopotamia including the South-East Anatolian region. Olive plant has spread out from two branches. The first one is to Tunisia and Morocco through Egypt; the other is to Aegean islands, Greece, Italy and Spain along the Anatolia. The first cultivation and improvement of olive was achieved by Semitics (Özkaya, 2006).

Turkey has an agricultural area of 27 million hectares and 2.2% of it is used for olive groves. The product, olive, which is obtained from these olive groves, is a very valuable product for the national economy. Besides, it is important for the preservation of land, for the employment of manpower, and for producing valuable nutrients for human health (Kutkan, 2002).

Countries of the European Union (EU) like Italy, Spain, and France produce about 70% of olive in the world. Turkey, Tunisia, Syrian Arab Republic and Morocco are the other important producers.

Olive production in the world, between 2001 and 2004, is shown in Table 1.3. There is a fluctuation tendency of olive production for each year because of the alternate behavior of olive trees. For that reason, there can be a big difference between the years. Because of the fluctuation regime of olive production, the last 11 years' average of olive production has been calculated and is given in Table 1.3 and the percentage shares of countries in the total olive production in the world are shown in Figure 1.6.

Table 1.3 World olive production between 2001 and 2004 and last 11-years' average (Food and Agriculture Organization of the United Nations (FAO)) (FAO, 2005)

	Olive Production (tons)				
	2001	**2002**	**2003**	**2004**	**1994-2004 (Average)**
World	15,254,290	15,573,609	16,636,685	15,340,488	14,443,786
Spain	6,762,600	4,290,700	7,290,900	4,556,000	4,588,484
Italy	2,894,097	3,231,300	3,149,830	3,149,830	3,020,636
Greece	2,249,430	2,573,835	2,050,260	2,300,000	2,193,764
Turkey	600,000	1,800,000	900,000	1,800,000	1,214,164
Syrian	496,952	998,988	580,000	950,000	642,668
Morocco	420,000	455,200	470,000	470,000	523,796
Algeria	200,339	191,926	167,627	170,000	215,325
Portugal	271,000	240,000	280,000	270,000	277,814
Tunisia	150,000	350,000	500,000	350,000	606,818
France	18,127	21,420	24,231	24,231	17,893

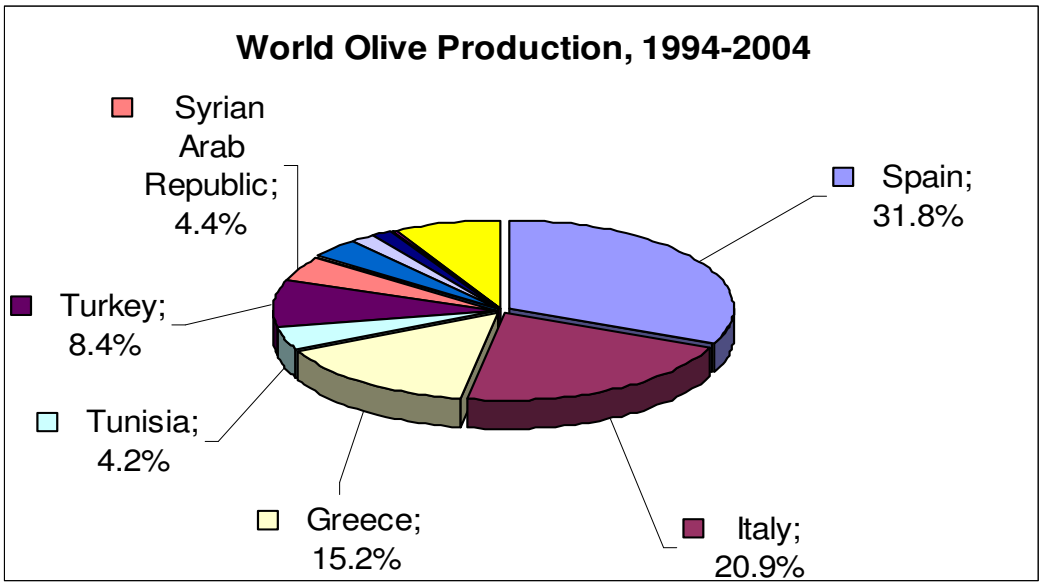

Figure 1.6 Shares of countries in the total olive production between 1994 and 2004 (FAO, 2005)

The amount of olive and olive cake produced in Turkey between 1999 and 2004 are given in Table 1.4 and in Figure 1.7.

Table 1.4 Olive and olive cake production in Turkey between 1999 and 2004 (FAO, 2005)

Products	**Production, tons**					
	1999	**2000**	**2001**	**2002**	**2003**	**2004**
Olive	600,000	1,800,000	600,000	1,800,000	900,000	1,800,000
***Olive Cake**	240,000	720,000	240,000	720,000	360,000	720,000

* 35-45 kg olive cake can be obtained from 100 kg olive.

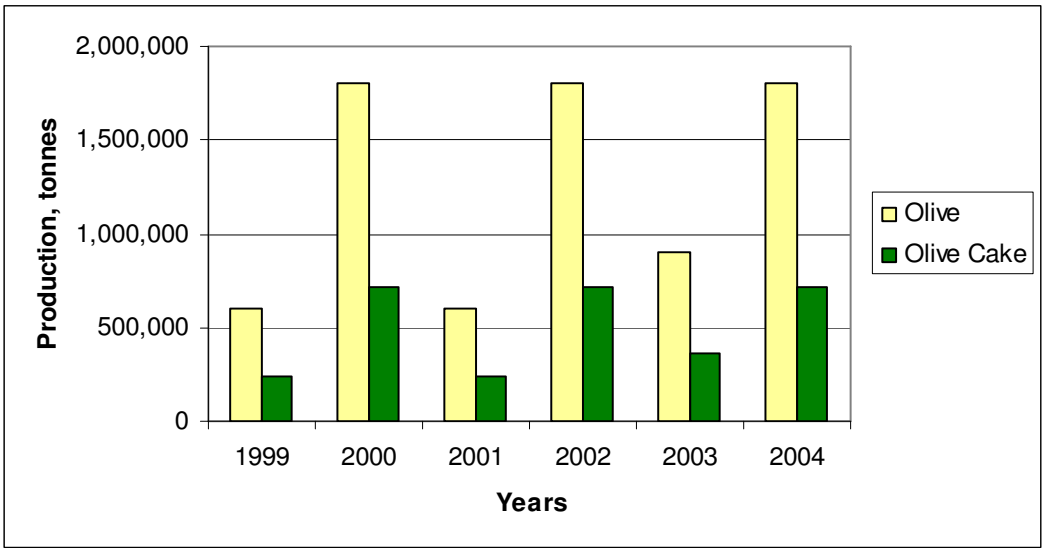

Figure 1.7 Graphical representation of olive and olive cake production in Turkey between 1999 and 2004 (FAO, 2005)

In Turkey, there are about 101.6 million olive trees in an area of about 600,000 ha. 91.7 million of these are productive. Turkey produces 8.41% of the total olive in the world (1,250,000 tons according to the last 11-years' average (1994-2004)). Therefore, Turkey is the 4th biggest olive producer in the world.

According to the data of Institute of Olive Researches, 15-22 kg of olive oil and 35-45 kg of olive cake are obtained for a 100 kg of olive (IOR, 2005). Approximately 70% of olive harvested is used in the production of olive oil and from this production about 500,000 (1,250,000 * 0.4) tons of olive cake is formed. This given amount of olive cake is based on wet basis. If it is assumed that the moisture content of raw olive cake is about 50 %, the amount of olive cake on dry basis is found as 250,000 tons per year. The calorific value (lower heating value) of olive cake is about 20 MJ/kg. As a rough estimate, the total recoverable energy potential of olive cake is considered as 5 PJ which is equivalent to 119.4 ktoe. This energy potential of olive cake is an amount which can not be neglected.

1.4. Aim of the Study

Olive cake, as a possible source of renewable energy, is a potential source of environmental pollution in its raw form. Combustion of olive cake in ordinary combustion units results in production of hydrocarbons and CO which causes a lot of inefficiency and energy loss due to incomplete combustion. Moreover, complete combustion of olive cake is possible, while complete combustion of coal is more difficult to achieve. Therefore, studies concerning utilization of olive cake as a potential renewable source of energy must be highly appreciated (Alkhamis and Kablan, 1999a).

This study aims to obtain energy by directly combusting olive cake, which has **high energy content** and is a **waste from olive oil production process**, in a bubbling fluidized bed. It is also the aim of this study to investigate the flue gas emissions. Generally, olive cake is combusted without any control in the Aegean and the South-Eastern Anatolian region of Turkey in conventional systems. At the end of this un-controlled combustion process, CO and hydrocarbons are formed at considerable amounts in the flue gas. These emissions create environmental pollution. Moreover, untreated olive cake has high moisture content. Every combustion system is not suitable for high moisture fuels. For example, classical grated combustors which are mostly used in olive cake combustion in Turkey, are not suitable to combust olive cake at all. For that reasons, a new combustion technology should be applied for the combustion of olive cake to generate energy.

Furthermore, olive cake is a seasonal residue. It is not easy to supply olive cake to an energy production company for the whole year. Therefore, co-combustion of olive cake and coal should be considered for energy production. However, lignite coals in Turkey contain high ash and moisture and high sulfur. Combustion of lignite coal causes air pollution especially because of its high sulfur content. One of the solutions for this problem is co-combustion of lignite coal with biomass which has almost zero sulfur and low ash content. In this respect, this study also

aims to investigate the co-combustion of olive cake and coal at certain mixing ratios and to determine the emissions from the combustion of the mixture.

In summary, the objectives of this study are:

- To investigate the combustion of olive cake in a bubbling fluidized bed,
- To investigate the emissions during combustion of the olive cake in bubbling fluidized bed,
- To determine the combustion efficiencies at different excess air ratios,
- To investigate the co-combustion of olive cake at different mixing ratios,
- To determine the effect of the secondary air on combustion efficiency and emissions at different mixing ratios of olive cake and coal.

CHAPTER 2

THEORETICAL BACKGROUND

2.1. Biomass and Bioenergy

Biomass is one of the few renewable, indigenous, widely dispersed, natural resources that can be utilized to reduce both the amount of fossil fuels burned and several greenhouse gases emitted during fossil fuel combustion processes. Carbon dioxide, for example, is one of the primary products of fossil fuel combustion and is a greenhouse gas that is widely believed to be associated with global warming. It is removed from the atmosphere via carbon fixation by photosynthesis (Klass, 1998).

It takes millions of years to convert organic materials into fossil fuels and they are not renewable sources. Burning fossil fuels converts the 'old' biomass into CO_2, thus the carbon content in the lithosphere is transferred into the atmosphere. There is a continuous transportation of carbon from the lithosphere to the atmosphere due to the combustion of fossil fuels. This causes accumulation and the increase of the carbon dioxide concentration in the atmosphere.

The contribution of biomass to CO_2 emissions is almost zero. Because replanting biomass ensures that CO_2 is absorbed by the plants and used in their growth process. CO_2 given to the atmosphere during the combustion process is taken back by the new replanted biomass by the photosynthesis process. So, the net CO_2 emission due to biomass combustion is almost zero.

Biomass sources with their low sulphur content do not have any negative effect on the SO_2 pollution.

2.1.1. What is Biomass?

Biomass can be defined as the carbonaceous organic material which originates from plants and animals. These include the residues of agriculture and forestry, animal wastes and wastes from food processing operations (Kaygusuz and Türker, 2002).

In many ways plant-originated biomass can be considered as a form of stored solar energy (Task 29: IEA, 2006). When "Biomass" is used in the text of this thesis, plant-originated biomass will be meant from this point on.

The reaction between CO_2 in the air, water and sunlight via photosynthesis produces carbohydrates that form the building blocks of biomass. Typically photosynthesis converts less than 1% of the available sunlight to stored, chemical energy. The solar energy is stored in the chemical bonds of the structural components of biomass. If biomass is processed efficiently, either chemically or biologically, the energy stored in the chemical bonds of the biomass is extracted. Hydrocarbons in the structure are oxidized to produce CO_2 and water. The process is cyclical, as the CO_2 is then available to produce new biomass. Biomass has always been a major energy source of the mankind (McKendry, 2002a).

There are three main advantages for the use of local biomass in energy production:

- Political benefits - the reduction of dependency on imported fuels;
- Creating new jobs - biomass fuels create up to 20 times more employment than coal and oil;
- Environmental benefits - such as mitigation of greenhouse gas emissions, reduction of acid rain, and soil improvement (Task 32: IEA, 2006).

Already, around 12-14% of the global energy demand is generated by combustion of biomass sources, which vary from wood to animal by-products and black liquor. A wide variety of appliances is used to convert this biomass into useful energy. In developing countries, around 35% of the total energy used originates from biomass, but most of it is for non-commercial use in traditional applications (such as cooking). In a country such as Nepal, over 90% of the primary energy is produced from traditional biomass fuels (Task 32: IEA, 2006).

In industrialized countries, the total contribution of biomass to the primary energy production is only 3%. This mainly involves the combustion of commercial biomass fuels in modern devices - for example, woodchip-fired cogeneration plants for heat and power. Other applications are domestic space heating and cooking, industrial heat supply, and large-scale power generation in coal-fired plants (Task 32: IEA, 2006). However, EU countries have published a **"White Paper"** and planned to produce 12% of the total energy supply from renewable resources by 2010 from the present value of 6%. In the medium terms, according to the Directive 2001/77/EC, the share of renewable sources in the total consumption of the electrical energy will be raised to 22.1% from the present value of 14% by 2010.

2.1.2. Types of Biomass

Biomass is a very broad term which is used to describe materials of recent biological origin that can be used either as a source of energy or as a source of chemicals. It includes trees, crops, algae and other plants, as well as agricultural and forest residues. It also includes many materials that are considered as waste by our society including the wastes from food and drink manufacturing processes, sludge, manures, industrial (organic) by-products and the organic fraction of household waste (Task 29: IEA, 2006).

Information on the several groups of biomass is given below.

Woody Biomass

- *Forest residues;* examples include: thinning, pruning or any other leftover plant material after cutting.
- *Fuel wood;* examples include: logs or any other form to be used in small stoves.
- *Wood waste from wood-processing industry;* examples include: bark, sawdust, shaving, off cuts, black liquor, etc.
- *Short rotation forestry;* examples include: willow (Salix) or eucalyptus.
- *Woodlands/Urban biomass;* examples include tree trimmings and gardening waste, both domestic and municipal, as well as the green and woody portion of municipal solid waste.

Non-Woody Biomass

- *Agricultural crops;* examples include various annual and perennial crops like Miscanthus, Switchgrass, but also many traditional agricultural crops like maize, rapeseed, sunflowers, both for direct utilization or liquid biofuels production.
- *Crop residues;* examples include: rice or coconuts husks, maize cobs, cereal straw.
- *Process residues,* examples include: bagasse from sugar cane processing, olive cake from olive oil extraction, etc.

Other Organic Wastes

- *Animal waste;* manure from pigs, chickens and cattle (in feed lots) because these animals are reared in confined areas.
- *Municipal Solid Waste (MSW);*
- *Sewage sludge;* domestic and municipal sewage from mainly human waste.
- *Industrial wastes (organic)*

2.1.3. Biomass Properties

While covering the biomass properties, the review paper by McKendry, 2002a was used as a reference material in this section.

It is the inherent properties of the biomass source that determines both the choice of conversion process and any subsequent processing difficulties that may arise. Equally, the choice of biomass source is influenced by the form in which the energy is required and it is the interplay between these two aspects that enables flexibility to be introduced into the use of biomass as an energy source.

The main material properties of interest, during subsequent processing as an energy source, relate to:

- moisture content (intrinsic and extrinsic),
- calorific value,
- proportions of fixed carbon and volatiles (FC/VM ratio),
- ash/residue content,
- alkali metal content,
- cellulose/lignin ratio.

For dry biomass conversion processes, the first five properties are of interest, while for wet biomass conversion processes, the first and last properties are of prime concern.

Moisture content

Two forms of moisture content are of interest in biomass:

- Intrinsic moisture: the moisture content of the material without the influence of weather effects,
- Extrinsic moisture: the influence of prevailing weather conditions during harvesting on the overall biomass moisture content.

In practical terms, it is the extrinsic moisture content that is of concern, as the intrinsic moisture content is usually only determined under laboratory conditions.

Table 2.1 lists the typical (intrinsic) moisture contents of a range of biomass materials.

Table 2.1 Proximate analysis and heating values of some biomass feedstocks and bituminous coal (McKendry, 2002a)

Biomass	Moisture[a] (wt%)	VM (wt%)	FC (wt%)	Ash (wt%)	LHV (MJ/kg)	HHV (MJ/kg)
Wood	20	82	17	1	18.6	18.6
Wheat straw	16	59	21	4	17.3	17.3
Barley straw	30	46	18	6	16.1	16.1
Lignite	34	29	31	6	26.8	26.8
Fir	6.5	17.2	82	0.8	-	21.0
Danish pine	8.0	19.0	71.6	1.6	-	21.2
Willow	60.0	-	-	1.6	-	20.0
Poplar	45.0	-	-	2.1	-	18.5
Cereal straw	6.0	10.7	79.0	4.3	-	17.3
Miscanthus	11.5	15.9	66.8	2.8	-	18.5
Bagasse	45-50	-	-	3.5	-	19.4
Switchgrass	13-15	-	-	4.5	-	17.4
Bituminous coal	8-12	57.0	35	8	34	26.2

[a] Intrinsic.

Based on the proximate analysis, woody and low moisture content herbaceous plant species are the most efficient biomass sources for thermal conversion to liquid fuels, such as methanol. For the production of ethanol by biochemical conversion (fermentation), high moisture herbaceous plant species, such as sugarcane, are more suited: such species can also be fermented via another biochemical process, anaerobic digestion (AD), to produce methane.

Calorific value

The calorific value of a material is an expression of the energy content, or heat value, released when burned in air. The calorific value of a fuel can be expressed

in two forms, the gross calorific value, or higher heating value (HHV) and the net calorific value, or lower heating value (LHV).

The HHV is the total energy content released when the fuel is burnt in air, including the latent heat contained in the water vapor and therefore, represents the maximum amount of energy potentially recoverable from a given biomass source. The actual amount of energy recovered will vary with the conversion technology, as will the form of that energy i.e. combustible gas, oil, steam, etc. In practical terms, the latent heat contained in the water vapor cannot be used effectively and therefore, the LHV is the appropriate value to use for the energy available for subsequent use.

Table 2.1 also lists the calorific values of a range of biomass materials. When quoting a calorific value, the moisture content needs to be stated, as this reduces the available energy from the biomass.

Proportions of fixed carbon and volatile matter

Fuel analysis has been developed based on solid fuels, such as coal, which consists of chemical energy stored in two forms, fixed carbon and volatiles:

- the volatiles content, or volatile matter (VM) of a solid fuel, is that portion driven-off as a gas after moisture determination by heating the solid fuel to 950 ^{o}C for 7 min (TS ISO 5071, 1999)
- the fixed carbon content (FC), is the mass remaining after the release of volatiles by burning the material at 950 ^{o}C. The remainder after the FC is ash.

Laboratory tests are used to determine the VM and FC contents of the biomass fuels. Fuel analysis based upon the VM content, ash and moisture, with the FC determined by difference, is termed as the “proximate analysis” of a fuel. The FC/VM ratios of some typical biomass sources are given in Table 2.2. FC/VM ratios for biomass are generally smaller than one. However, this ratio is greater than one for coal. FC/VM ratios for typical lignite and bituminous coals are also shown in the table for comparison with the biomass.

Table 2.2 FC/VM ratios for typical biomass sources, lignite and bituminous coals (McKendry, 2002a)

Biomass	FC (wt%)	VM (wt%)	FC/VM (-)
Wood	17	82	0.207
Wheat straw	21	59	0.356
Barley straw	18	46	0.391
Lignite	31	29	1.069
Bituminous coal	45	35	1.286

Elemental analysis of a fuel, presented as C, N, H, O and S together with the ash content as wt%, is termed the "ultimate analysis" of a fuel. Table 2.3 gives the ultimate analyses for some biomass materials.

The VM and FC contents of a fuel is significant, because they provide a measure of the ease with which the biomass can be ignited and subsequently gasified, or oxidized, depending on how the biomass is to be utilized as an energy source. This type of fuel analysis is of value for biological conversion processes, enabling a comparison of different fuels to be undertaken.

Table 2.3 Ultimate analysis for biomass materials and coals on dry basis (McKendry, 2002a)

Material	wt % on dry basis					
	C	**H**	**O**	**N**	**S**	**Ash**
Cypress	55.0	6.5	38.1	-	-	0.4
Beech	51.6	6.3	41.4	-	-	-
Wood (average)	51.6	6.3	41.5	0.0	0.1	1.0
Miscanthus	48.1	5.4	42.2	0.5	<0.1	2.8
Wheat straw	48.5	5.5	3.9	0.3	0.1	4.0
Barley straw	45.7	6.1	38.3	0.4	0.1	6.0
Rice straw	41.4	5.0	39.9	0.7	0.1	
Bituminous coal	73.1	5.5	8.7	1.4	1.7	9.0
Lignite	56.4	4.2	18.4	1.6[a]	-	5.0

[a] Combined N and S.

Ash/residue content

The chemical breakdown of a biomass fuel, by either thermo-chemical or bio-chemical processes, produces a solid residue. When produced by combustion in air, this solid residue is called 'ash' and forms a standard measurement parameter for solid and liquid fuels. The ash content of biomass affects both the handling and processing costs of the overall biomass energy conversion cost. During biochemical conversion, the percentage of solid residue will be greater than the solid residue formed during combustion of the same material.

In a thermo-chemical conversion process, the chemical composition of the ash can present significant operational problems. This is especially true for combustion processes, where the ash can react to form a 'slag', a liquid phase formed at elevated temperatures, which can reduce plant throughput and result in increased operating costs.

Ash content of a biomass can be determined by proximate or ultimate analysis. Ultimate analysis carried out with a CHN Analyzer can reveal many more information than the proximate analysis. Ultimate analyses for several biomass materials as well as some typical coal samples are given in Table 2.3.

Alkali metal content

The alkali metal content of biomass i.e. Na, K, Mg, P and Ca, is especially important for any thermo-chemical conversion processes. The reaction of alkali metals with silica present in the ash produces a sticky, mobile liquid phase, which can lead to blockages of airways in the furnace and the boiler plant. It should be noted that while the intrinsic silica content of a biomass source may be low, contamination with soil introduced during harvesting can increase the total silica content significantly, such that while the content of intrinsic silica in the material may not be a cause for concern, but the increased total silica content may lead to operational difficulties.

The alkali metal contents of typical biomass materials are given in Table 2.4. As can be seen from this table Na and K contents of willow and poplar trees are in considerable amounts.

Table 2.4 Alkali metal contents of typical biomass materials (McKendry, 2002a)

Material	**Alkali metal**
	(as Na and K oxides) (wt%)
Fir	-
Danish pine	4.8
Willow	15.8
Poplar	16.0
Cereal straw	11.8
Miscanthus	-
Bagasse	4.4
Switchgrass	14.0
Bituminous coal	-

Cellulose/lignin ratio

The proportions of cellulose and lignin in biomass are important only in biochemical conversion processes. The biodegradability of cellulose is greater than that of lignin, hence the overall conversion of the carbon-containing plant material in the form of cellulose is greater than the material in the form of lignin, a determining factor when selecting biomass plant species for biochemical processing. Table 2.5 gives the proportions of cellulose/hemicellulose/lignin contents for softwoods and hardwoods and for comparison for wheat straw and switchgrass.

Table 2.5 Cellulose/lignin content of selected biomass (McKendry, 2002a)

Biomass	Lignin, (wt%)	Cellulose, (wt%)	Hemi-cellulose, (wt%)
Softwood	27-30	35-40	25-30
Hardwood	20-25	45-50	20-25
Wheat straw	15-20	33-40	20-25
Switchgrass	5-20	30-50	10-40

Bulk density

An important characteristic of biomass materials is their bulk density both as-produced and as-subsequently processed basis (Table 2.6). The density as-produced (bulk density) is important in relation to transport and storage costs. The density of the processed product has impacts on fuel storage requirements, the sizing of the materials handling system and how the material is likely to behave during subsequent thermo-chemical/biological processing as a fuel/feedstock.

Table 2.6 Bulk volume and density of selected biomass sources (McKendry, 2002a)

Biomass	Bulk volume (m^3/ton, daf)[a]	Bulk density (ton/m^3, daf)
Wood		
Hardwood chips	4.4	0.23
Softwood chips	5.2-5.6	0.18-0.19
Pellets	1.6-1.8	0.56-0.63
Sawdust	6.2	0.12
Planer shavings	10.3	0.10
Straw		
Loose	24.7-49.5	0.02-0.04
Chopped	12.0-49.5	0.02-0.08
Baled	4.9-9.0	0.11-0.20
Moduled	0.8-10.3	0.10-1.25
Hammermilled	9.9-49.5	0.02-0.11
Cubed	1.5-3.1	0.32-0.67
Pelleted	1.4-1.8	0.56-0.71

[a] Dry, ash-free.

2.2. Biomass Conversion Technologies

The conversion of biomass to energy encompasses a wide range of different types and sources of biomass, conversion options, end-use applications and infrastructure requirements (McKendry, 2002b). Whatever the conversion technology, the biomass feedstock has to be collected and transported from the source to the conversion unit. Because of its seasonal production, biomass should be stored before it is used as an energy source for the selected conversion unit in order to obtain continuous energy production.

Biomass is used to extract its stored energy by using different conversion technologies.

Factors that influence the choice of the conversion process are (McKendry, 2002b):

- The type and quantity of biomass feedstock,
- The desired form of the energy,
- End-use requirements,
- Environmental standards,
- Economic conditions,
- Project specific factors.

A distinction can be made between the energy carriers produced from biomass by their ability to provide heat, electricity and engine fuels. A useful means of comparing biomass and fossil fuels is in terms of their O/C and H/C ratios, known as a Van Krevelen diagram as shown in Figure 2.1. The lower the respective ratios, the greater the energy content of the material (McKendry, 2002b).

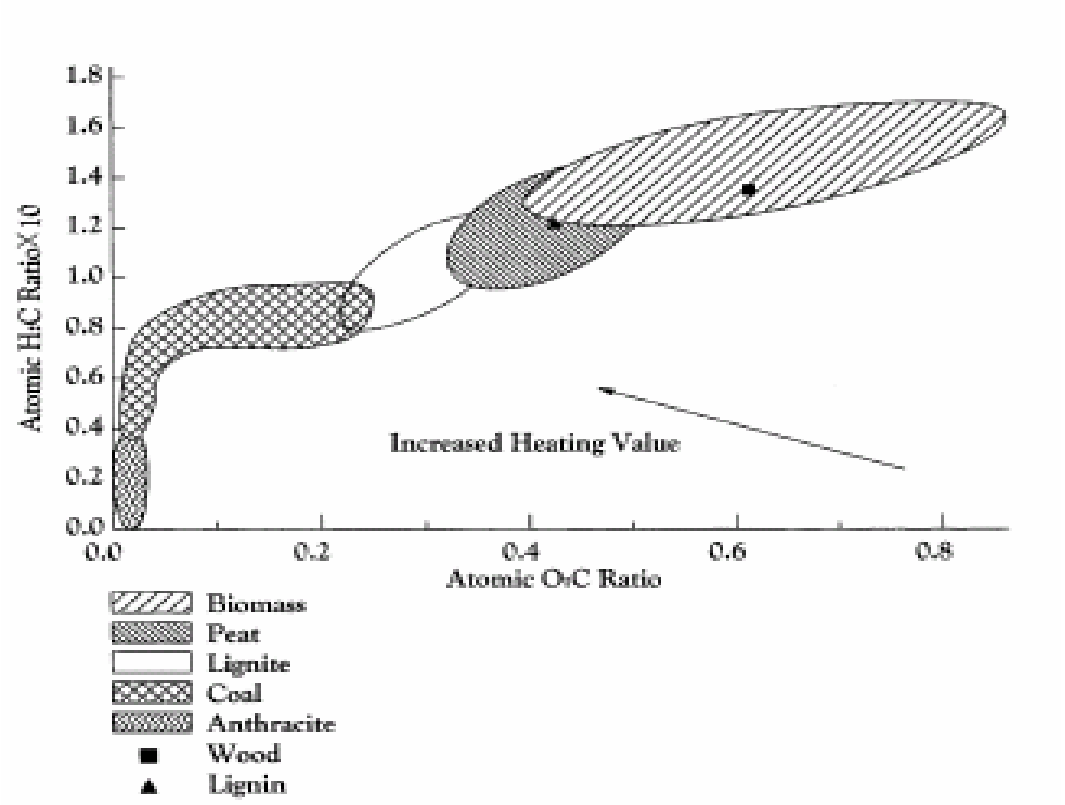

Figure 2.1 Van Krevelen diagram for various solid fuels (McKendry, 2002b)

The biomass conversion technologies are mainly separated into two groups:

- Bio-chemical conversion and,
- Thermo-chemical conversion.

Mechanical Extraction is the third technology as means of common usage. Although the main focus is the combustion process of biomass in fluidized bed combustors, the other conversion technologies are briefly explained to give general background information.

2.2.1. Bio-chemical Conversion Technologies

Fermentation and anaerobic digestion are the two main bio-chemical conversion technologies used.

2.2.1.1. Fermentation

Fermentation is a process in which ethanol is produced as an end-product from sugar and starch crops. Use of fermentation in industry is very common.

The biomass is ground and the starch in the biomass is converted to sugars by enzymes. Then sugars are converted to ethanol with yeast. Purification of ethanol by distillation is an energy-intensive step. About 450 L of ethanol is produced per ton of dry corn. The solid residue from the fermentation process can be used as cattle-feed and in the case of sugar cane; the bagasse can be used as a fuel for boilers for subsequent gasification (McKendry, 2002b).

The conversion of lignocellulosic biomass (such as wood and grasses) is more complex, due to the presence of longer-chain polysaccharide molecules and requires acid or enzymatic hydrolysis before the resulting sugars can be fermented to ethanol. Such hydrolysis techniques are currently at the pre-pilot stage (McKendry, 2002b).

2.2.1.2. Anaerobic Digestion

Anaerobic digestion is the process in which organic material is directly converted to a mixture of gas; mainly methane and carbon dioxide. This gas is termed as "biogas". It also includes small quantities of other gases such as hydrogen sulphide. The biomass is produced by bacteria under anaerobic conditions. The produced gas has an energy content of about 20-40% of the lower heating value of the feedstock. Anaerobic digestion is a commercially proven technology and is widely used for treating the high moisture content (80-90%) organic wastes (McKendry, 2002b).

Biogas can be used directly in spark ignition gas engines and in gas turbines. It can be upgraded to higher quality i.e. natural gas quality, by the removal of CO_2. If it is used as a fuel in spark ignition gas engines to produce electricity, the

overall conversion efficiency from biomass to electricity is about 10–16%. As with any power generation system using an internal combustion engine as the prime mover, waste heat from the engine oil and water-cooling systems and the exhaust could be recovered using a combined heat and power system (McKendry, 2002b).

2.2.2. Mechanical Extraction

Extraction is a mechanical conversion process used to produce oil from the seeds of various biomass crops, such as oilseed rape, cotton and groundnuts. The process produces not only oil but also a residual solid or 'cake', which is suitable for animal fodder. Three tons of rapeseed is required per ton of rapeseed oil produced. Rapeseed oil can be processed further by reacting it with alcohol using a process called "esterification" in order to obtain bio-diesel (McKendry, 2002b).

2.2.3. Thermo-chemical Conversion Technologies

Within the thermo-chemical conversion of biomass, there are three main processes, namely "gasification", "pyrolysis" and "combustion". These processes and their intermediate and final products are shown in Figure 2.2. However, the liquefaction process, another thermo-chemical process, is not covered in this report because of its not extensive usage (McKendry, 2002b).

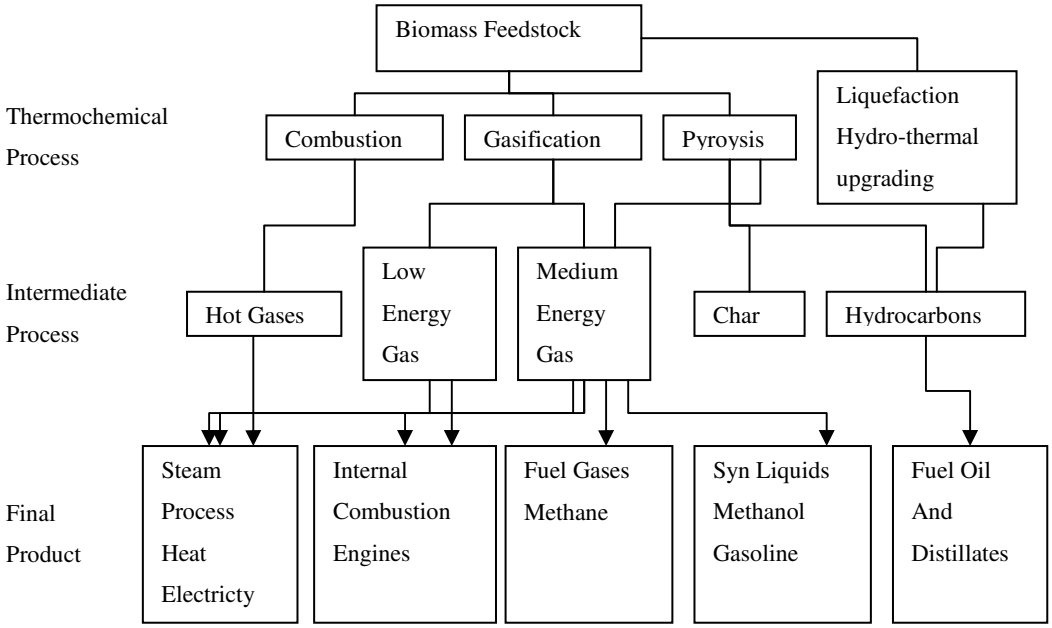

Figure 2.2 Main processes, intermediate energy carriers and final products from thermo-chemical conversion of biomass (McKendry, 2002b)

2.2.3.1. Gasification

Gasification is the conversion of biomass into a combustible gas mixture by the partial oxidation of biomass at high temperatures, typically in the range of 800–900 ^{o}C. The low calorific value (CV) gas produced (about 4–6 MJ/Nm^{3}) can be burnt directly or used as a fuel for gas engines and gas turbines. The product gas can be used as a feedstock (syngas) in the production of chemicals (e.g. methanol) (McKendry, 2002b).

End-products, methanol and hydrogen, are obtained from the gasification of biomass. Each of them has a big potential and future to be used as a fuel for transportation (McKendry, 2002b).

2.2.3.2. Pyrolysis

Pyrolysis is the conversion of biomass to liquid (called bio-oil or bio-crude), solid and gaseous fractions, by heating the biomass in the absence of air to around 500 ^{o}C. Figure 2.3 shows the range and possible yields of pyrolysis products. Pyrolysis can be used to produce predominantly bio-oil if flash pyrolysis is used, enabling the conversion of biomass to bio-crude with an efficiency of up to 80%. The bio-oil can be used in engines and turbines and its use as a feedstock for refineries is also being considered (McKendry, 2002b).

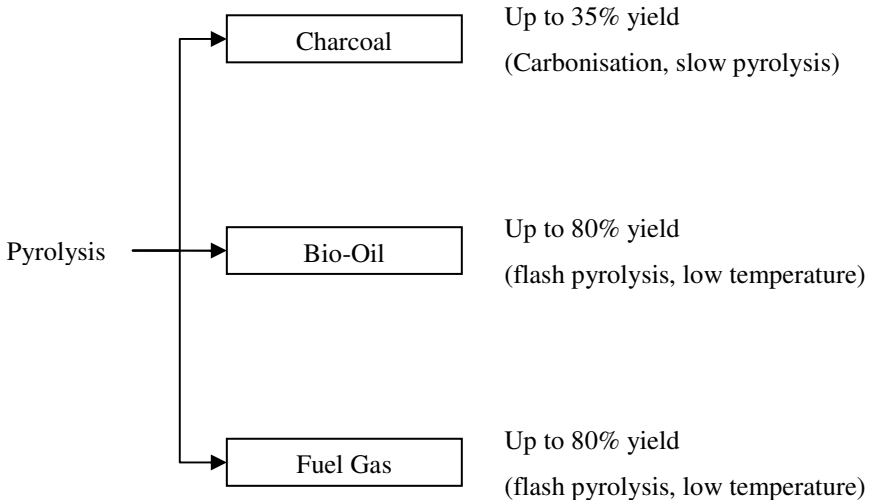

Figure 2.3 Products obtained from pyrolysis (McKendry, 2002b)

2.2.3.3. Combustion

The combustion of biomass is used to convert the chemical energy stored in biomass to valuable products such as heat, power or electricity. Direct combustion of any type of biomass is possible but it is not efficient to burn biomass with the moisture content higher than 50%. In order to burn biomass of high moisture content, it is necessary to dry the biomass before burning. Otherwise, high

moisture content biomass is more suitable energy source for biological conversion processes (McKendry, 2002b).

Combustion is the most common way of converting biomass to energy. It is well understood, relatively straightforward, and commercially available, and can be regarded as a proven technology. However, the desire to burn uncommon fuels, improve efficiencies, cut costs, and decrease emission levels continuously results in new technologies being developed (Task 32: IEA, 2006).

2.3. Combustion of Biomass

Biomass can be converted into energy (heat or electricity) or energy carriers (charcoal, oil, or gas) using both thermo-chemical and biochemical conversion technologies. Combustion is the most developed and most frequently applied process because of its low costs and high reliability. However, combustion technologies deserve continuous attention from developers in order to remain competitive with the other options (Task 32: IEA, 2006).

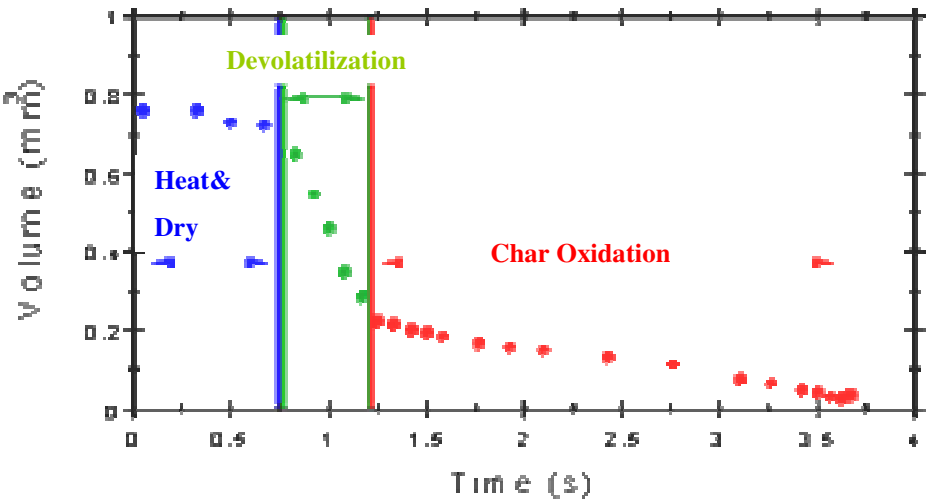

Figure 2.4 Distinct stages in the process of combustion of a particle; 1) heating and drying, 2) devolatilization and 3) char oxidation (Task 32: IEA, 2006)

Distinct stages during the combustion of biomass fuel particle are shown in Figure 2.4. As can be seen from the figure, the first stage is heating and drying. During this stage, the biomass first loses its moisture at temperatures up to 100°C, using heat from other particles that have already released their heating value. As the dried particle heats up, volatile gases containing hydrocarbons, CO, CH_4 and other gaseous components are released. This stage is called "devolatilization" stage. During devolatilization stage, the gases released contain about 70% of the heating value of the biomass. Finally, at the last stage, called "char oxidation", the remaining char burns and the final material is ash (Task 32: IEA, 2006).

Emissions caused by incomplete combustion are usually as a result of either (Task 32: IEA, 2006):

- poor mixing of combustion air and fuel in the combustion chamber, giving local fuel-rich combustion zones,
- an overall lack of available oxygen,
- combustion temperatures that are too low,
- residence times that are too short,
- radical concentrations that are too low.

In an ideal situation of combustion process, the fuel is assumed to be consisting of pure hydrocarbons and it completely burns with the required excess air. The combustion products form at the end of the combustion process. They are mainly CO_2, H_2O, N_2 and excess O_2. They leave the system in the exhaust gas, while the heat is transferred to the surrounding from the system (Howard, 1989).

However, all the solid fuels are not fully originated from hydrocarbons. They are very complex compounds of carbon, hydrogen, oxygen, nitrogen, sulphur and other inert and active components such as chlorine, alkali metal salts and moisture. Besides the combustion products in the ideal situation, some atmospheric pollutants such as SO_x and NO_x can be formed during the combustion. Moreover, acidic vapors of H_2SO_4 and HCl, which are very reactive, corrosive and harmful for the reactor material, can be formed. Furthermore, the

inert ash in the fuel does not vanish; part of it will be elutriated as particulates in the exhaust gases, adding pollutants to be discharged, while part may remain in the system and may have to be removed mechanically (Howard, 1989).

2.3.1. Advantages of Biomass Combustion

Unlike any other energy resource, using biomass to produce energy is often a way to dispose of biomass waste materials that otherwise would create environmental risks. In the following ways, using biomass for energy can deliver unique environmental advantages as well as production of useful energy (Oregon, 2006).

- ***Reducing Greenhouse Gases: Carbon Dioxide***

Carbon dioxide (CO_2), methane, nitrous oxide and certain other gases are called greenhouse gases because they trap heat in the Earth's atmosphere. The global concentration of CO_2 and other greenhouse gases is increasing. (Oregon, 2006).

- ***Reducing Greenhouse Gases: Methane***
- ***Keeping Waste Out of Landfills***
- ***Reducing Acid Rain and Smog***

2.4. Fluidized Bed Combustion of Biomass

In a fluidized bed, biomass fuel is burned in a self-mixing suspension of gas and solid bed material (usually silica sand and dolomite) in which air for combustion enters from below. Depending on the fluidization velocity, bubbling and circulating fluidized bed combustion can be distinguished. The intense heat transfer and mixing provide good side conditions for complete combustion with low excess air demand. Using internal heat exchanger surfaces, flue gas re-circulation, or water injection, a relatively low combustion temperature is maintained in order to prevent ash sintering in the bed (Task 32: IEA, 2006).

Due to the good mixing achieved, fuel flexibility is high, although attention must be paid to particle size and impurities contained in the fuel (Task 32: IEA, 2006).

Low NO_x emissions can be achieved by good air-staging, good mixing, and a low requirement for excess air. Moreover, additives (e.g. limestone for sulphur removal) work well due to the good mixing behavior. The low excess air amounts required reduce the flue gas volume flow and increase combustion efficiency. Fluid bed combustion plants are of special interest for large-scale applications (normally exceeding 30 MW_{th}). For smaller plants, fixed bed systems are usually more cost-effective. One disadvantage is the high dust loads taken in with the flue gas, which make efficient dust precipitators and boiler cleaning systems necessary. Bed material is also lost with the ash, making it necessary to periodically add new bed material (Task 32: IEA, 2006).

2.4.1. Fluidization

2.4.1.1. The Phenomenon of Fluidization

Fluidization is defined as the process by which solid particles are transformed into a fluidlike state through suspension in a gas or liquid. When the solid particles are confined in a vessel and remain localized they form a composite material that is referred to as a "fluidized bed". This method of contacting has advantages for heat and mass transfer between fluid and solid phases, which can be exploited through fluidization engineering (Kunii and Levenspiel, 1991).

Various forms of contacting of a batch of solids by fluid are shown in Figure 2.5. If a fluid is passed upward through a bed of fine particles at a low flow rate, the fluid merely percolates through the void spaces between stationary particles. This is a *fixed bed*. With an increase in flow rate, particles move apart and a few vibrate and move in restricted regions. This is the *expanded bed* (Kunii and Levenspiel, 1991).

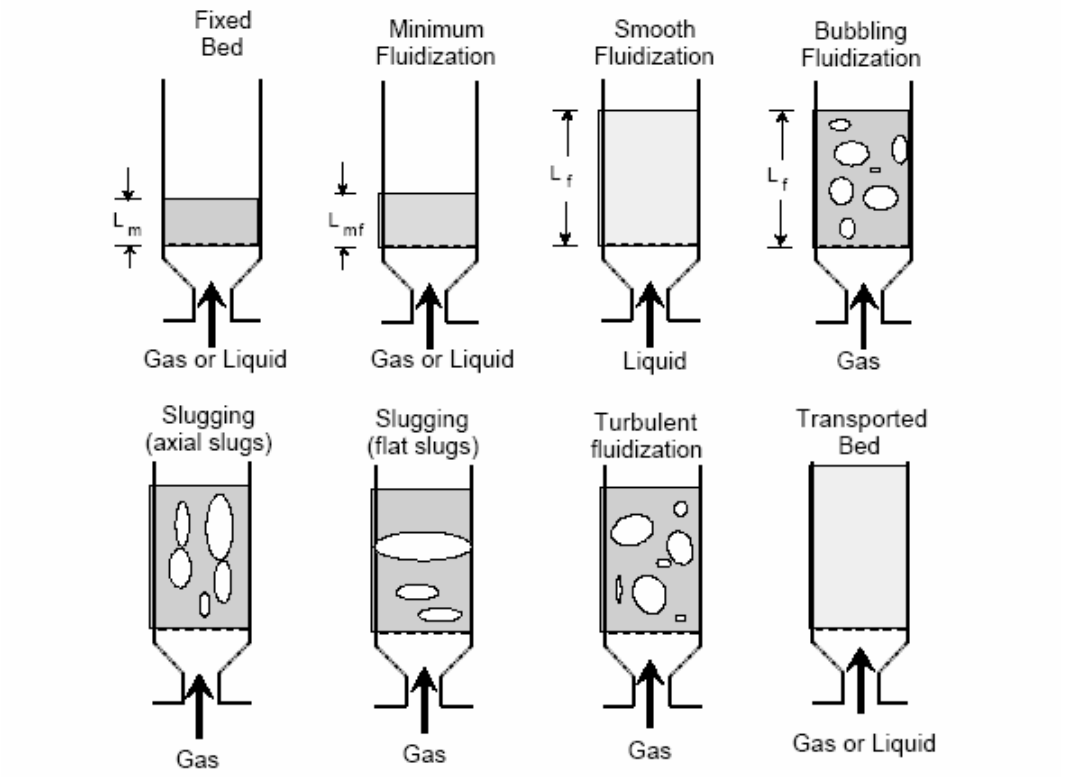

Figure 2.5 Types of solid-fluid flows (Kunii and Levenspiel, 1991)

At a still higher velocity, a point is reached where all the particles are just suspended by the upward-flowing gas or liquid. At this point the fractional force between particle and fluid just counterbalances the weight of the particles, the vertical component of the compressive force between adjacent particles disappears, and the pressure drop through any section of the bed about equals the weight of the fluid and particles in that section. The bed is considered to be just fluidized and is referred to as *incipiently fluidized bed* or a bed at *minimum fluidization* (Kunii and Levenspiel, 1991).

With an increase in flow rate beyond minimum fluidization, large instabilities with bubbling and channeling of gas are observed. At higher flow rates, agitation becomes more violent and the movement of solids becomes more vigorous. In addition, the bed does not expand much beyond its volume at minimum

fluidization. Such a bed is called as an *aggregative fluidized bed*, a *heterogeneous fluidized bed*, or a *bubbling fluidized bed* (Kunii and Levenspiel, 1991).

In gas-solid systems, gas bubbles coalesce and grow as they rise, and in a deep enough bed of small diameter they may eventually become large enough to spread across the vessel. In the case of fine particles, they flow smoothly down by the wall around the rising void of gas. This is called *slugging*, with *axial slugs*. For coarse particles, the portion of the bed above the bubble is pushed upward, like a piston. Particles rain down from the slug, which finally disintegrates. At about this time another slug forms, and this unstable oscillatory motion is repeated. This is called a *flat slug*. Slugging is especially serious in long, narrow fluidized beds (Kunii and Levenspiel, 1991).

When fine particles are fluidized at a sufficiently high gas flow rate, the terminal velocity of the solids is exceeded, the upper surface of the bed disappears, entrainment becomes appreciable, and, instead of bubbles, one observes a turbulent motion of solid clusters and voids of gas of various sizes and shapes. This is the *turbulent fluidized bed*. With a further increase in gas velocity, solids are carried out of the bed with the gas. In this state we have a *disperse-*, *dilute-*, or *lean-phase fluidized bed* with pneumatic transport of solids (Kunii and Levenspiel, 1991).

A dense-phase gas fluidized bed looks very much like a boiling liquid and in many ways exhibits liquidlike behavior. For example, a large, light object is easily pushed into a bed and, on release, will pop up and float on the surface. When the container is tipped, the upper surface of the bed remains horizontal, and when two beds are connected their levels equalize. Also, the difference in pressure between any two points in a bed is roughly equal to the static head of bed between these points. The bed also has liquidlike flow properties. Solids will gush in a jet from a hole in the side of a container and can be made to flow like a liquid from vessel to vessel (Kunii and Levenspiel, 1991).

At fluid velocities exceeding that corresponding to minimum fluidization, u_{mf}, the bed behaves differently depending upon the density difference between the solid and fluid, the size of the particles, and the fluid velocity (Kunii and Levenspiel, 1991).

2.4.1.2. Advantages and Disadvantages of Fluidized Beds

There are of course many advantages and disadvantages associated with using fluidized beds. The advantages include (Kunii and Levenspiel, 1991):

1. The smooth, liquidlike flow of particles allows continuous automatically controlled operations with easy handling.
2. The rapid mixing of solids leads to close to isothermal conditions throughout the reactor; hence the operation can be controlled simply and reliably.
3. In addition, the whole vessel of well-mixed solids represent a large thermal flywheel that resists rapid temperature changes, responds slowly to abrupt changes in operating conditions, and gives a large margin of safety in avoiding temperature runaways for highly exothermic reactions.
4. The circulation of solids between two fluidized beds makes it possible to remove (or add) the vast quantities of heat produced (or needed) in large reactors.
5. It is suitable for large-scale operations.
6. Heat and mass transfer rates between gas and particles are high when compared with other modes of contacting.
7. The rate of heat transfer between a fluidized bed and an immersed object is high; hence heat exchangers within fluidized beds require relatively small surface areas.

Its disadvantages are:

1. The rapid mixing of solids in the bed leads to non-uniform residence times of solids in the reactor.
2. Friable solids are pulverized and entrained by the gas and must be replaced.

3. Erosion of pipes and vessels from abrasion by particles can be serious.
4. For non-catalytic operations at high temperature, the agglomeration and sintering of fine particles can require a lowering in temperature of operations, thereby reducing the reaction rate considerably.

The desirability of using fluidized beds is dependent on achieving good mixing between the solids and the suspending fluid. By controlling the way in which the fluid and solids interact, it is possible to control the heat and mass transfer characteristics between the two phases. The macroscopic observables in fluidized beds are the fluid pressure drop needed to cause the fluid to flow through the bed of solids, the fluid velocity, and the density of the solids (Kunii and Levenspiel, 1991).

2.4.2. Biomass co-combustion

Co-firing biomass with coal in traditional coal-fired boilers is becoming increasingly popular, as it capitalizes on the large investment and infrastructure associated with the existing fossil-fuel-based power systems while traditional pollutants (SO_x, NO_x, etc.) and net greenhouse gas (CO_2, CH_4, etc.) emissions are decreased (Task 32: IEA, 2006).

Co-firing biomass with coal can have a substantial impact on emissions of sulphur and nitrous oxides. SO_x emissions almost uniformly decrease when biomass is fired with coal, often in proportion to the biomass thermal load, because most biomass fuels contain far less sulphur than coal (Task 32: IEA, 2006).

An additional incremental reduction is sometimes observed due to sulphur retention by alkali and alkaline earth compounds in the biomass fuels. The effects of co-firing biomass with coal on NO_x emissions are more difficult to anticipate (Task 32: IEA, 2006).

High-temperature corrosion of super heaters is of great concern when burning high-chlorine or high-alkali fuels, such as herbaceous or intensely cultivated fuels, since species containing chlorine (generally alkali chlorides) may deposit it on heat transfer surfaces and greatly increase surface chlorine concentration. However, research has indicated that the corrosion potential can be reduced if alkali chlorides (primarily from the biomass) can interact with sulphur (primarily from the coal) to form alkali sulphates. As a result, highly corrosive alkali chlorides on super heater tubes are converted to HCl and other gas-phase products that are less corrosive and that leave the surface relatively easily. The HCl may condense on lower-temperature surfaces such as air heaters. However, this problem is generally less serious and more manageable than super heater corrosion (Task 32: IEA, 2006).

2.4.3. Review of EU and Turkey Legislations about Biomass Energy

Turkey is a candidate country to European Union (EU). In the process of adaptation to EU, Turkey has prepared and will still prepare some laws, regulations, legislations and directives. Turkey mostly translates EU directives and adapts them to the situation in Turkey. Although several directives have been translated from English to Turkish, there are still some industrial fields which are not included in any directive.

From the point of view, **DIRECTIVE 2001/80/EC** OF THE EUROPEAN PARLIAMENT AND OF THE COUNCIL of 23 October 2001 on the limitation of emissions of certain pollutants from large combustion plants is approved as a reference legislation for the “fluidized bed combustion” system.

This Directive is prepared for the combustion plants, the rated thermal input of which is equal to or greater than 50 MW, irrespective of the type of fuel used (solid, liquid or gaseous).

This Directive is applied only to combustion plants designed for production of energy with the exception of those which make direct use of the products of combustion in manufacturing processes. In particular, this Directive shall not apply to the following combustion plants:
(a) plants in which the products of combustion are used for the direct heating, drying, or any other treatment of objects or materials e.g. reheating furnaces, furnaces for heat treatment;
(b) post-combustion plants i.e. any technical apparatus designed to purify the waste gases by combustion which is not operated as an independent combustion plant;
(c) facilities for the regeneration of catalytic cracking catalysts, facilities for the conversion of hydrogen sulfide into sulphur;
(d) reactors used in the chemical industry, coke battery furnaces, coopers;
(e) any technical apparatus used in the propulsion of a vehicle, ship or aircraft, gas turbines used on offshore platforms;

Plants powered by diesel, petrol and gas engines shall not be covered by this Directive.

2.4.3.1. Emission Limit Values for SO_2

Solid Fuel

A. SO_2 emission limit values expressed in mg/Nm^3 (O_2 content 6 %) to be applied by new and existing plants (which has been licensed before 27 November 2002 and provided that the plant is put into operation no later than 27 November 2003):

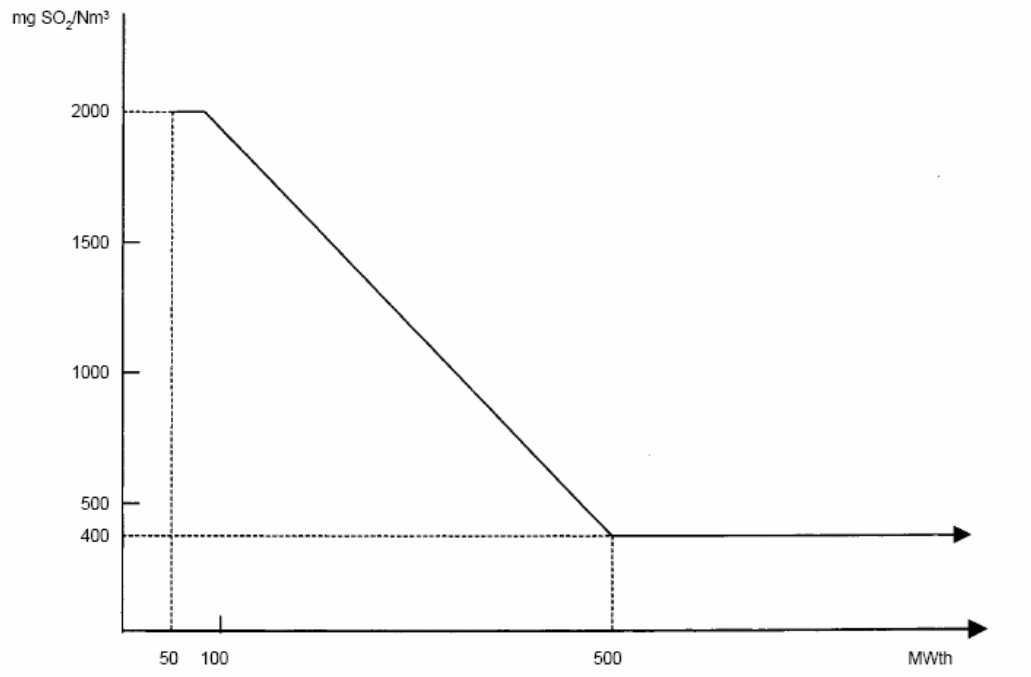

NB. Where the emission limit values above cannot be met due to the characteristics of the fuel, a rate of desulphurization of at least 60 % shall be achieved in the case of plants with a rated thermal input of less than or equal to 100 MWth, 75 % for plants greater than 100 MWth and less than or equal to 300 MWth and 90 % for plants greater than 300 MWth. For plants greater than 500 MWth, a desulphurization rate of at least 94 % shall apply or of at least 92 % where a contract for the fitting of flue gas desulphurization or lime injection equipment has been entered into, and work on its installation has commenced, before 1 January 2001.

Figure 2.6 SO_2 emission limit values to be applied by existing plants for EU-DIRECTIVE 2001/80/EC

B. SO_2 emission limit values expressed in mg/Nm^3 (O_2 content 6 %) to be applied by new plants (others than covered by in section A):

Table 2.7 SO_2 emission limit values to be applied by new plants for EU-DIRECTIVE 2001/80/EC

Type of fuel	50 to 100 MWth	100 to 300 MWth	> 300 MWth
Biomass	200	200	200
General Case	850	200[(1)]	200

[(1)] Except in the case of the 'Outermost Regions' where 300 mg/Nm^3 shall apply.

NB. Where the emission limit values above cannot be met due to the characteristics of the fuel, installations shall achieve 300 mg/Nm^3 SO_2, or a rate of desulphurization of at least 92 % shall be achieved in the case of plants with a rated thermal input of less than or equal to 300 MWth and in the case of plants with a rated thermal input greater than 300 MWth a rate of desulphurization of at least 95 % together with a maximum permissible emission limit value of 400 mg/Nm^3 shall apply.

2.4.3.2. Emission Limit Values for NO_X (Measured as NO_2)

A. NO_x emission limit values expressed in mg/Nm^3 (O_2 content 6 % for solid fuels) to be applied by new and existing plants (which has been licensed before 27 November 2002 and provided that the plant is put into operation no later than 27 November 2003):

Table 2.8 NO_x emission limit values to be applied by existing plants for EU-DIRECTIVE 2001/80/EC

Type of fuel:	Limiting values (mg/Nm^3)
Solid:	
50 to 500 MWth	600
> 500 MWth	500
From 1 January 2016	
50 to 500 MWth	600
> 500 MWth	200

B. NO_x emission limit values expressed in mg/Nm^3 to be applied by new plants (other than covered by in section A):

Table 2.9 NO_x emission limit values to be applied by new plants for EU-DIRECTIVE 2001/80/EC

Solid fuels (O_2 content 6 %)

Type of fuel	50 to 100 MWth	100 to 300 MWth	> 300 MWth
Biomass	400	300	200
General Case	400	200[(1)]	200

[(1)] Except in the case of the 'Outermost Regions' where 300 mg/Nm^3 shall apply.

Air emissions limits for facilities using biomass as a fuel are summarized below according to the Turkish Regulation for Air Pollution Control from Industrial Sources (RAPCIS, 2004).

As mentioned in the item-43 of Article 5 of Turkish Air Pollution-Industry Control Regulation, the air pollutant emissions can not exceed the limit values given in Table 2.7.

Table 2.10 Air pollutant emission limit values for the facilities that use biomass as a fuel for RAPCIS

Pollutants	CO (mg/Nm^3)	NO (mg/Nm^3)	SO_x (mg/Nm^3)	TOC (mg/Nm^3)
500kW-15 MW	460	-	200	-
15MW-50 MW	460	-	200	30
>50 MW	460	400	200	30

The biomass is explicitly defined in the related item of the regulation mentioned above. The olive oil production facilities and other burning facilities (energy production facilities, cement and lime factories, etc.) which use biomass (olive cake, sunflower shell, cotton seed and etc.) as a fuel and which have the nominal heat power capacity higher than 500 kW must have burning system with a secondary air feed. The stack gas emission limit values given in Table 2.7 are relevant. In the regulation, for comparison purposes, stack gas emissions are based on 6 vol% O_2 at a temperature of 0 ^oC and a pressure of 1 atm on dry basis.

Olive oil production facilities using biomass (olive cake, sunflower shell, cotton seed and etc.) as a fuel, some additional criteria are given by the regulation. Facilities which use olive cake as fuel should obey the criteria given below:

- The moisture content of olive cake used as a fuel can not exceed 15% and the oil content can be maximum 1.5% on dry basis. Lower heating value of olive cake is limited to 3700 kcal/kg. Sodium (Na) content can not exceed 300 ppm and the ash residue should be less than 4%. The biomass, especially olive cake, can be used in the facilities which have the nominal heating power of 500 kW or less, and having a combustion system with fuel feeding and secondary air. Moreover, the olive cake can be used in the olive oil production facilities which operate maximum 120 days per year. These facilities are exempt from the emission limit values given in Table 2.7. However, these facilities have to meet the soot scale of the regulation that is maximum 4 according to the Bacharach scale.

CHAPTER 3

LITERATURE SURVEY

There are many investigations and research about the combustion of biomass in fluidized bed combustors. Burning biomass is very beneficial way to dispose the biomass waste. Because of its high energy content, combustion of biomass is also a good way to obtain clean energy by minimizing environmental pollution, especially air pollution. The co-combustion of biomass with coal is also another application to generate cleaner energy. In the literature, the research trend is on the co-combustion of coal with several biomass types. Co-combustion of coal and biomass has an advantage for disposal of waste products. Besides, using biomass instead of coal for energy production is another advantage reducing the cost of fuel. Therefore, co-combustion seems to be the most cost effective method of biomass utilization.

The use of any fossil fuel in an energy production system should be considered with its adverse effects on the environment. While the energy consumption in the world increases gradually, pollutant gases in the atmosphere such as CO_2, SO_2 and NO_x also increase. It is expected that CO_2 and other greenhouse gas emissions which cause global warming, and also SO_2 and NO_x emissions which cause acid rains, can be decreased by using biomass in the production of energy. Because of that reason, there are many studies in the literature using biomass in energy production to supply increasing energy demand as well as to minimize environmental pollution.

Recently, new environmental regulations on using fossil fuels for energy production have further increased the interest in the biomass for energy production.

In this section, the studies conducted previously to obtain energy from biomass (especially from olive cake) in fluidized bed combustion systems are summarized.

Abu-Quadis, 1996, carried out an experimental combustion study of olive cake in a fluidized bed combustor. Sand of d_p = 0.53 mm was used as a bed material. Olive cake nearly the same diameter of sand was used as a type of fuel. Temperature distribution in the combustor as a function of distance from the plate for different air/fuel ratios was observed. It was demonstrated that the temperature profile of the combustor reached to uniformity at 12 cm above the distributor plate. Good uniformity was explained by well-mixing of bed solids with fuel particles. It was also indicated that combustion intensity increased with increased air-flow rate. For the same flow rates, it increased by an average of 20% using 15 cm bed height instead of 10 cm. The combustion efficiency ranged from 86 to 95% and increased with air flow rate.

Desroches-Ducarne et al., 1998, investigated the emissions of NO, N_2O, HCl, SO_2 and CO during the combustion of coal and municipal refuse mixtures in a circulating fluidized bed boiler. As the ratio of municipal solid waste (MSW) increased, N_2O and SO_2 emissions decreased. On the other hand, hydrogen chloride and nitric oxide concentrations increased with the amount of waste added. CO emissions slightly decreased when the MSW proportion was low, but when the chlorine supply was significant, inhibition of CO oxidation by HCl provoked the opposite trend: a growth in CO concentration. They also noticed that higher MSW portion leaded to an improvement on the combustion efficiency because of the high volatile matter content.

Alkhamis and Kablan, 1999a, investigated the potential of olive cake as a source of energy and catalyst for oil shale production of energy and its impact on the

environment. In the study, the calorific value of olive cake as a function of its grain size was determined. The average colorific value was calculated to be 31.2 kJ/kg. When it was compared to that of wood (17 kJ/kg), and that soft coal (23 kJ/kg), it was declared that olive cake can be a good fuel and a potential source of energy. It was concluded that direct mixing of olive cake with oil shale was not suitable for direct combustion. **Alkhamis and Kablan, 1999b,** also studied a process for producing carbonaceous matter from tar sand, oil shale and olive cake. A carbonization system was constructed to produce a carbonaceous matter from combinations of tar sand, oil shale and olive cake. It was demonstrated that this system was convenient for complete carbonization. This was proved by the decrease of calorific value of carbonized material compared to that of non-carbonized material. It was stated that the minimum temperature to achieve complete production of carbonaceous matter from sample mixtures was 500 ^{o}C for a minimum heating time of 1.5 hrs.

Cliffe and Patumsawad, 2001, studied the co-combustion of olive cake with coal. They used fluidized bed combustor to research the feasibility of using olive cake as an energy source. The combustion efficiencies were compared. They determined that the combustion efficiency of 20% olive cake+coal mixture was less than that of the coal combustion by own by 5% but it was higher than that of 10% olive cake+coal mixture. A 20% olive oil waste mixture gave a higher CO emission than both 100% coal ®ring and 10% olive oil waste mixture, but the combustion efficiency was higher than the 10% olive oil waste mixture due to lower elutriation from the bed.

Suksankraisorn et al., 2003, investigated the combustion of three high moisture content wastes (olive oil waste, municipal solid waste and potato waste) in a fluidized bed. A comparison with co-firing of these materials with coal in the same bed has been investigated. Water was used up to 20% by weight in mixtures. 20% water content was determined as a limit value to achieve combustion of waste. Above that range, the combustion could not sustain without adding coal. Co-firing with coal resulted in higher combustion efficiency than the simulated

municipal solid waste. But, it was less than the coal combustion efficiency of 93% by own. It was also less than the efficiency (average 90%) of co-firing potato and olive oil waste with coal. It was found that there was not much more difference in the combustion efficiency between the two types of biomass and increasing moisture content. It was declared that the high ash content of simulated municipal solid waste with the value of 26% when compared with the 5% ash content of both wastes resulted in slower burning. This caused char particles to be elutriated from the bed without being completely burnt. Gaseous emissions were investigated. It was found that CO emissions did not changed much more with respect to waste fraction. SO_2 emissions reduced as the waste fraction in the mixture increased because of fuel's low S-content. Emissions of NO and N_2O increased slightly with municipal solid waste fraction.

Armesto et al., 2003, investigated the co-combustion of coal and olive oil industry residues in fluidized bed. Two different Spanish coals, lignite and anthracite were used for the study. The CIEMAT bubbling fluidized bed pilot plant was used for combustion experiments. Furnace temperature, share of foot cake in the mixture and coal types were selected as operating parameters in order to observe the effect on the emissions and combustion efficiency. Foot cake is quite difficult material to use in combustion process due to its high moisture content and alkaline content in ash. Test results showed that the combustion of foot cake/lignite and anthracite mixtures in bubbling fluidized bed is one way to utilize this biomass residue in energy generation. Foot cake mixture ratio did not have any significant effect on the combustion efficiency but the type of the coal had great influence on it. SO_2 and NO_x emissions decreased as the ratio of foot cake in mixture increased. The N_2O emissions increase as the share of the foot cake in the mixtures increases.

Topal et al., 2003, investigated the olive cake (OC) combustion in a circulating fluidized bed (CFB). They used a small scale circulating fluidized bed of 125 mm diameter and 1800 mm height. The results obtained from that combustor were used to compare them with the coal combustion. The freeboard temperature in the

bed with OC combustion is 20-30 ^{o}C higher than with coal combustion. This was explained with the higher volatile matter (VM) content of OC than the coal. The VM content of the OC and the coal were 68.82 and 27.5 wt%, respectively. The effect of excess air ratio on the combustion efficiency and emissions was studied. Online concentrations of O_2, SO_2, CO_2, CO, NO_x and total hydrocarbons were measured in the flue gas. It was found that if the excess air ratio (λ) was less than 30%, appreciable amounts of CO and unburned hydrocarbons were formed and the combustion efficiency drops to 94-95%. CO and C_mH_n emissions were lower for coal than the emissions for OC at the same λ and temperature. The minimum emissions were observed at λ = 1.35. It was suggested that OC was a potential fuel that can be used for clean energy production in a small scale industries by using CFB.

Permchart and Kouprianov, 2004, made an experimental study about the combustion of three different biomass sources in a single fluidized bed combustor (FBC). Sawdust, rice husk and per-dried sugar cane bagasse were used as a biomass fuel. Silica sand was used as an inert material in the combustor. By means of emissions, CO emissions for rice husk were measured much greater than those for sawdust and bagasse for similar operating conditions. This was explained by the coarser char particles and higher ash concentration for rice husk: up to 200 μm, against 5 μm for sawdust and 10 μm for bagasse. The rate of NO reduction for rice husk was found much greater than the others. The heterogeneous reactions on the char surface in the freeboard and cyclone were given as a cause for that reduction. It was concluded that sawdust was the most environmentally friendly biomass fuel whereas the firing of rice husk is accompanied by a noticeable environmental impact.

Gayan et al., 2004, analyzed the circulating fluidized bed combustion performance burning coal and biomass together. Two kinds of coal and a forestry residue (pine bark) were used in experimental studies. Two CFB pilot plants with the power 0.1 and 0.3 MWth, respectively were used. A mathematical model was developed which can predict the different gas concentrations (O_2, CO, CH_4, etc.)

and the carbon combustion efficiency along the bed column. The results of the experiments were compared with the model predictions and a good correlation was found for all the conditions used.

Atımtay and Topal, 2004, studied the co-combustion of olive cake (OC) with lignite coal in a circulating fluidized bed (CFB). Experiments were conducted in the same bed used in the previous work by **Topal et al., 2003**. Various runs were conducted with mixtures of OC and lignite, namely 25, 50 and 75 wt% OC mixed with lignite. These mixtures were burned with various excess air ratios. It was found that if the excess air ratio (λ) was less than 40-50%, appreciable amounts of CO and unburned hydrocarbons were formed and the combustion efficiency drops to 84-87%. CO and C_mH_n emissions were lower for coal than the emissions for OC+coal mixtures at the same λ and temperature. The minimum emissions were observed at about λ = 1.5. A secondary air addition in the freeboard was suggested to increase the combustion efficiency. It was also suggested that OC was a good fuel that can be mixed with lignite for clean energy production in a small scale industries by using CFB. In order to meet the EU emission limits, less than 50 wt% OC mixture was suggested.

As it can be seen from the literature survey, the fluidized bed combustion technology is very effective to burn biomass and it was stated that fluid bed systems had flexibility on fuel selection. The usage of these systems has also an advantage for NO_x formation.

CHAPTER 4

MATERIALS AND METHODS

4.1. Experimental Setup

A bubbling fluidized bed combustor (BFBC) is used in this study for the combustion of olive cake (a waste of olive oil industry). Co-combustion of olive cake with the lignite coal (Tunçbilek) at different mixing ratios is also tested in the same combustor. The experimental setup consisted of a bubbling fluidized bed column, an ash hopper, a fuel feeding system, and a cyclone. The schematic diagram of the setup is shown in Figure 4.1 and a photograph of the setup is given in Figure 4.2. The fluidized bed column is made of Inconel steel. It has an inside diameter of 102 mm and a height of 900 mm. A distributor plate made of stainless steel is located at the lower part of the column above the air box. The diameter of the holes on the distributor plate is 1.5 mm. One fuel feeding pipe and two overflow pipes are also located on the column. There are six thermocouples at certain heights along the column in order to measure the temperature along the column height continuously. Thermocouples are Type K (chromel-alumel) thermocouples. They are located at 40 mm (TC#1), 110 mm (TC#2), 190 mm (TC#3), 330 mm (TC#4), 490 mm (TC#5) and 660 mm (TC#6) above the distributor plate. The data collected with thermocouples are continuously recorded by the Agilent Model-3970A, Data Acquisition Switch Unit with Agilent Benchlink Data Logger software.

The pressure drops in the distributor plate and in the bed are measured with monometers. Air is supplied from a blower and distributed homogenously into the

column with the distributor plate. This air supplied to the column is used as the fluidization air as well as the combustion air.

The combustor column is completely isolated from outside with kaowool having a thickness of about 30 mm.

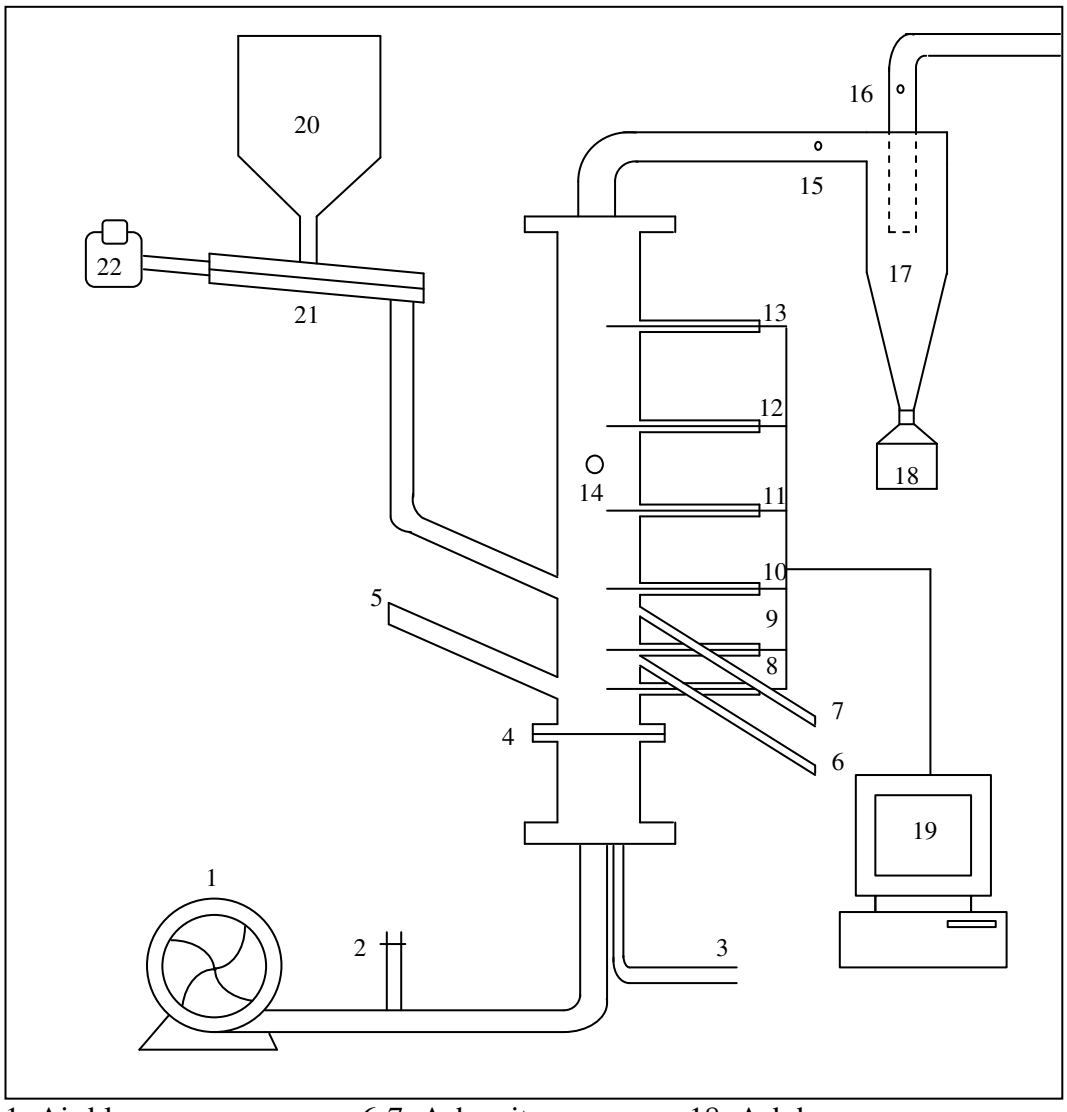

1: Air blower
2: Natural gas feed point
3: Manometer
4: Distributor plate
5: Bed Material feed point
6-7: Ash exit
8-13: Thermocouples
14: Igniter
15-16: Gas sampling ports
17: Cyclone
18: Ash hopper
19: Data Acquisition Unit
20: Fuel hopper
21: Screw feeder
22: Motor for screw feeder

Figure 4.1 Schematic diagram of the experimental setup

Sand is used as the bed material in the column. The average particle diameter is 0.51 mm. The bed height is kept at 10 cm in all experiments by feeding 1420 g of sand into the column in every experiment.

In the experiments, coal and olive cake are used as solid fuels. Coal or a mixture of coal and olive cake at predetermined ratios are stored in a fuel hopper which is a component of a fuel feeding system (number 20 in Figure 4.1). The fuel is fed to the combustor column by means of a screw feeder which is installed just below the fuel hopper (number 21 in Figure 4.1). Fuels used in the experiments are given to the combustor column at the upper surface of the bed material. A cyclone is set at the outlet of the fluidized bed combustor column. There is an ash hopper at the bottom of the cyclone and this hopper is used to collect particles from the flue gas.

Figure 4.2 Photograph of the experimental setup

The fluidized bed combustion system is pre-heated with LPG (liquefied petroleum gas). The LPG is fed to the combustor column by mixing it with the ambient air. A rotameter is used in order to measure the flow rate of the LPG fuel. The distributor plate guarantees to distribute the fuel laden air along the combustor column homogenously. The air and fuel mixture which is passed through the distributor plate and distributed homogenously along the combustor column is ignited by an igniter. Experimental procedure for a combustion test is described in detail in Section 4.2.

Emission measurements are performed from two sampling ports. The first sampling port is located before the cyclone and the other is just located after the cyclone. The sampling probe of BERNATH Atomic-Model 3006 Hydrocarbon Analyzer is located at the sampling port before the cyclone (number 15 in Figure 4.1) and a portable gas analyzer (MRU 95/3 CD) is located at the other sampling port (number 16 in Figure 4.1). The analyzers continuously measure the flue gas composition. Detailed explanation about the gas analyzers is given in Section 4.6.

4.2. Experimental Procedure for a Combustion Test

There are several important points to be checked before a combustion experiment is started. Firstly, the fuel feeding valve is controlled if it functions properly. Secondly, the igniter is checked whether it produces a spark or not. Finally, gas leakage is checked on the LPG feeding lines. An experiment can not be performed unless all controls have been completed and all security precautions have been taken.

1420 g of sand is weighed and fed into the combustor column. The fuel prepared in advance is stored in the fuel hopper. The fuel to be used is olive cake, coal or a mixture of both at a specific mixing ratio.
The air blower is turned on. Air flow rate is adjusted to the required value. Then, the valve of the LPG tube is turned on. LPG fuel is mixed with air and

homogenously distributed along the combustor column. The igniter is located into the place where it is shown with number 14 in Figure 4.1. A spark is generated with the igniter. The spark ignites the air+fuel mixture and combustion starts. The flow rate of LPG fuel is controlled with a rotameter. After ignition, the igniter is taken out of the ignition port and the port is tightly closed.

The temperatures along the column are observed with six thermocouples located at specific heights. In about one-hour the bed material in the column heats up and when the temperature of the bed material reaches a temperature of 700 ^{o}C, the feeding of the solid fuel is started.

The fuel from the hopper is fed to the combustor column by a screw feeder. The calibration curves of the screw feeder and also the calculations used to obtain these calibration curves are given in Appendix A. The experiments are conducted with 10 g/min fuel feeding rate. For a specific experiment, the fuel feeding rate is determined and the on-off mode which is equivalent to the fuel feeding rate is selected from the Table A.1 in Appendix A. The selected value is adjusted on the screw feeder so that the selected amount of fuel can be fed to the combustor column.

After feeding of the solid fuel is started, LPG fuel supply is gradually decreased by observing the temperature profile in the combustor column and LPG flow is stopped after the combustion is self-sustained.

The temperature profile along the column is continuously measured every five seconds and the data obtained is recorded by the software of Agilent Bench Link Data Logger. When the system reaches steady-state condition, the probes of the analyzers are placed at the sampling ports. Here, the steady-state condition refers to no change observed at the bed temperature and the pressure difference measured at the orifice. After the self-calibration of the analyzers is completed, the emission measurements are made. Flue gas composition is measured with MRU Stack gas analyzer and the total hydrocarbons in the flue gas are analyzed

with BERNATH Atomic analyzer. The measurements are stored in the memory of the analyzers with the aid of a special software. For all concentrations of pollutants in the flue gas given in Chapter 5, the results are the average of at least 12 measurements obtained every five seconds during one minute period. Each measurement lasts between three to five minutes. Therefore, statistical analysis of data is conducted for 36-60 measurements for each point.

The number of measurements should be noted for an experiment in order to make sure that emission measurements and the temperature profile of the combustor column are synchronous and match each other. This operation is quite important for the evaluation of emission and temperature data. After a combustion test is completed, the ash collected in the bed and the cyclone are weighted and analyzed in order to find the amount of unburnt carbon content in the ash. The unburnt-C analysis is done by burning the ash samples at 950 ^{o}C until constant weight was reached. The difference in weight gives the unburnt carbon in the ash sample.

4.3. Characteristics of Fuels and Bed Material

4.3.1. Physical Properties

Two types of fuels were used for the experiments. The coal was Tunçbilek lignite coal which is widely used in Turkey. The olive cake was the dry biomass which was provided by the GİRGİN Company. Before the experiments were conducted, the sieve analyses of coal and olive cake were done. In all experiments conducted, the size of the fuel particles used was in the range of 1.0 - 2.0 mm. The weighed average particle sizes (d_p) of coal and olive cake are 1.57 mm and 1.52 mm, respectively. The density of coal is 1,374 kg/m^3 and that of olive cake is 591 kg/m^3. Sand is used as bed material. Sand is the beach sand of Black Sea and it is brought from the Kocaali county of Sakarya. The weighed average particle size of the sand used as the bed material is 0.51 mm. The density of sand is measured as

1,730 kg/m^3. The cumulative size distributions of the coal, olive cake and sand are shown in Figure 4.3.

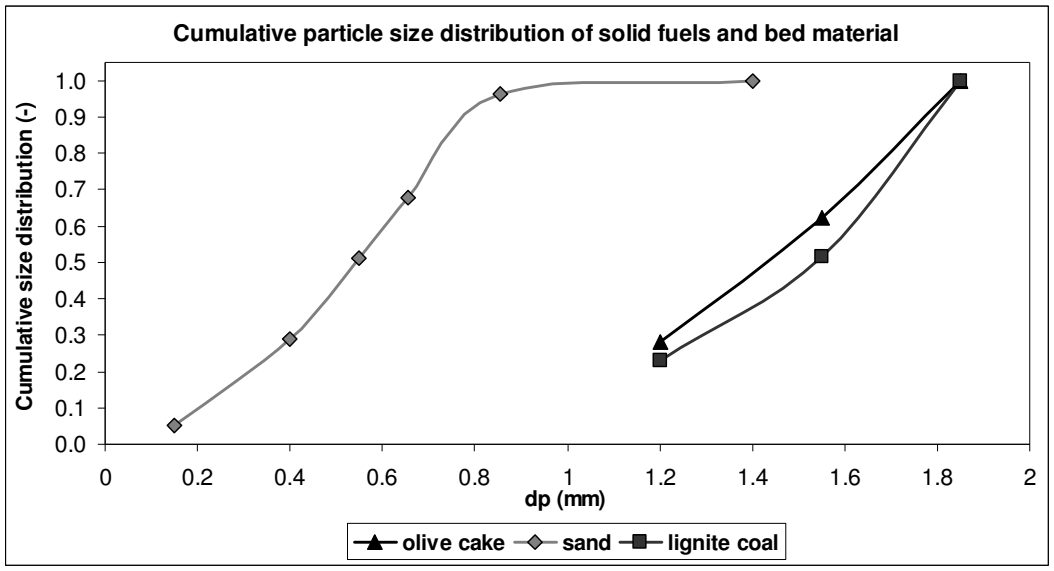

Figure 4.3 Cumulative particle size distribution of olive cake (d_p =1.52 mm), coal (d_p =1.57 mm) and sand (d_p = 0.51 mm).

Olive cake is a solid waste remaining after the olive oil production process. Olive cake contains about 6-9 wt% of oil, 42-54 wt% of seed, 10-11 wt% of peel, and 21-33 wt% of pulp (IOR, 2005). In raw form, olive cake contains about 50 wt% moisture. Since it is difficult to burn the raw olive cake with high amount of moisture, it is dried usually in rotary kilns by supplying heat down to a moisture of 6-7 wt% and put in 50-kg bags. In this study, dried olive cake was used supplied by Girgin Company located in İzmir.

4.3.2. Proximate and Ultimate Analysis

The proximate and ultimate analyses of both coal and olive cake were performed by the Chemical Analysis Laboratories of the General Directorate of Mineral

Research and Exploration (MTA). The proximate and ultimate analyses of coal and olive cake are given in Table 4.1.

4.3.3. Calorific Values of Fuels

Calorific values of coal and olive cake were determined by the Chemical Analysis Laboratories of the MTA. The results are given as higher and lower heating values of coal and olive cake in Table 4.1. The calorific values of olive cake and coal are very close to each other.

Table 4.1 Proximate and ultimate analyses of coal and olive cake

Proximate analysis	**FC**	**VM**	**Ash**	**Moisture**	**HHV**	**LHV**
	%, by weight				**kJ/kg (dry basis)**	
Olive cake (OC)	17.91	71.17	4.21	6.71	20,729	19,445
Coal (Tunçbilek Lignite)	31.91	37.5	19.91	10.68	20,026	19,195

Ultimate analysis	**C**	**H**	**N**	**O**	**S**	**Ash**
	%, by weight (dry basis)					
Olive cake (OC)	51.38	5.85	1.276	36.90	0.086	4.51
Coal (Tunçbilek Lignite)	51.82	3.77	1.276	18.75	2.094	22.29

FC: Fixed Carbon, VM: Volatile Matter
HHV: Higher Heating Value, LHV: Lower Heating Value

4.3.4. Ash Characteristics of Fuels

The characterization of ashes of olive cake and coal was done by the Chemical Analysis Laboratories of the MTA. The results are given as weight % of oxides of elements on dry basis and they are shown in Table 4.2.

Table 4.2 Ash analysis of coal and olive cake

	Olive cake	Lignite coal
	% by weight (dry basis)	
SiO_2	22.0	40.0
K_2O	19.5	1.3
CaO	14.0	10.3
Fe_2O_3	8.0	10.6
Al_2O_3	5.2	14.6
P_2O_5	5.2	0.3
MgO	2.9	4.3
Na_2O	2.4	1.5

When raw olive cake is used as fuel in the combustor, it is possible that there may be some operational problems because of the high moisture content (if it is used in the raw form) and high alkaline content of olive cake. As can be seen from Table 4.2, the alkali metal content (K_2O, CaO, and Na_2O) of olive cake is higher than that of the lignite coal. This characteristic of olive cake brings the risk of bed agglomeration in a fluidized bed combustor. It can cause fouling, slagging and corrosion of combustor surfaces causing a decrease in combustion efficiency. However, the lower ash content of olive cake as compared to coal prevents the bed from agglomeration. No agglomeration was observed throughout the combustion experiments.

4.4. Calibration of the Fuel Feeding System

Calibration curves of the feeding system for olive cake and coal are given in Appendix A, Figure A.1 and Figure A.2, respectively. The feeding rates for each on-off mode were calculated with the formula developed for the calibration curves. For the desired feeding rate, the position of the on-off mode was determined from Table A.1 in Appendix A.

4.5. Determination of Fluidization Velocity

Fluidization velocity for the bed was determined at room temperature and pressure before the hot experiments were started. Hence, this part of the experiment can be called as "cold experiments". Fluidization velocity measurements were performed in order to determine the minimum fluidization velocity (u_{mf}) for the bed. Two distinct experiments were done. The first one was to determine the superficial gas velocity (u_o) through the combustor column while the column was empty. The second one was to determine u_o through the combustor column while the column was loaded with bed material. Sand was used as a bed material with the amount of about 1420 g. As it is indicated in Section 4.1, it corresponds to 10 cm-bed height. ALMEMO 2290-4 multifunctional anemometer was used to measure the air velocity at the top of the combustor column at nine points on a cross sectional area which was perpendicular to the air flow. The average air velocities were calculated for both experiments. While measuring the superficial air velocity, the pressure drop at the orifice and the distributor was also measured at the same time with two manometers. One of the manometers was connected to the air feeding pipe to measure the pressure drop across the orifice. The other one was used to measure the pressure drop across the distributor plate. The superficial air velocity versus pressure drops through the bed and the distributor plate were plotted. The minimum fluidization velocity was determined as 0.50 m/sec at room temperature. The calculations to determine the minimum fluidization velocity are given in details in Appendix B.

4.6. Flue Gas Analysis

Flue gas analyses were conducted with two gas analyzers:

- BERNATH Atomic- Model 3006 Hydrocarbon Analyzer was used for measurement of the total hydrocarbons in the flue gas,
- MRU 95/3 CD Portable Gas Analyzer for measurement of O_2, CO, SO_2, and NO_x emissions in the flue gas.

BERNATH Hydrocarbon Analyzer is placed in the sampling port which is before the cyclone. The analyzer has a heated sample line in order to prevent the condensation of hydrocarbons. The heated line is kept at a temperature of 200 ^{o}C. The analyzer measures the hydrocarbon emissions with a Flame Ionization Detector (FID) and the results of measurements are given as C_3H_8. The analyzer is calibrated with propane gas before each experiment.

The sampling probe of the MRU Portable Gas Analyzer is located at the sampling port after the cyclone. The gas sample first passes through a heated line in order to prevent the condensation of water vapor. Then it is cooled down to 10^{o}C by a peltier cooler for the removal of moisture of the sample. Thus, the emissions are measured and reported on dry basis. The analyzer is calibrated with the certified calibration gases before the experiments. The measured parameters, measurement methods and the sensitivity of measurements are summarized in Table 4.3.

Table 4.3 Measurement methods used for analysis of flue gas

Parameter	**Measurement Method**	**Measurement Resolution**	**Measurement Ranges**
O_2	Electrochemical sensor	± 0.1 vol%	0-20.9 vol%
CO	Electrochemical sensor	± 1 ppmv	0-10 000 ppmv
SO_2	Electrochemical sensor	± 1 ppmv	0-4 000 ppmv
NO	Electrochemical sensor	± 1 ppmv	0-4 000 ppmv
C_mH_n(as C_3H_8)	NDIR: Non-dispersive infrared	± 0.01 vol%	0-10 vol %

CHAPTER 5

RESULTS AND DISCUSSION

The experimental results of this study are presented in this chapter. The effects of excess air ratio and change of olive cake amount in the fuel mixture on the combustion efficiency and the flue gas emissions (CO, NO_x, SO_2 and C_mH_n) are discussed. Additionally, the effect of feeding secondary air on the flue gas emissions and on the combustion efficiency is explained. Test runs conducted for the combustion experiments are listed in Table 5.1. For each experiment, feeding rate for fuel was 10 g/min.

Table 5.1 Test runs conducted for the combustion experiments

Without Secondary Air		**With Secondary Air**	
Run #	**Solid Fuel**	**Run #**	**Solid Fuel**
r-1	Olive Cake (O.C.)	r-6	Olive Cake (O.C.)
r-2	Coal (C)	r-7	Coal (C)
r-3	Olive Cake 25 wt% + Coal 75 wt%	r-8	Olive Cake 25 wt% + Coal 75 wt%
r-4	Olive Cake 50 wt% + Coal 50 wt%	r-9	Olive Cake 50 wt% + Coal 50 wt%
r-5	Olive Cake 75 wt% + Coal 25 wt%	r-10	Olive Cake 75 wt% + Coal 25 wt%

5.1. Combustion of Olive Cake and Coal

5.1.1. Temperature profiles

During combustion tests, the temperature along the combustor column was continuously measured by six thermocouples which are placed along the column at several heights. The change of temperature profile along the column is shown in Figure 5.1 for the combustion of olive cake and coal. Generally, the first thermocouple (TC1) gave the lowest temperature due to cooling effect of the fluidization air. The temperature has increased along the bed height and then decreased along the freeboard after reaching a maximum value. For the combustion of **olive cake** the lowest temperature was observed at TC1 as 162 ^{o}C. This thermocouple is located at 40 mm above the distributor plate. Since TC1 is in the bed, it gives the temperature of the bed material. Lower temperature at TC1 indicates that olive cake particles can not penetrate to the lower parts of the bed. Since the density of olive cake particles is smaller than the density of sand particles, segregation occurs. Therefore, a good mixing of sand and olive cake particles can not be obtained in the bed and olive cake particles mostly burn at the top of the bed.

As soon as the olive cake particles are fed to the bed, they are heated up and the volatile matter is released. The volatile matter content of olive cake (71.17 wt%) is quite high. Combustion of volatile matter continues in the freeboard and the temperature reaches to about 850 ^{o}C at TC4. Therefore, this is a good indication that olive cake combustion mostly takes place in the freeboard.

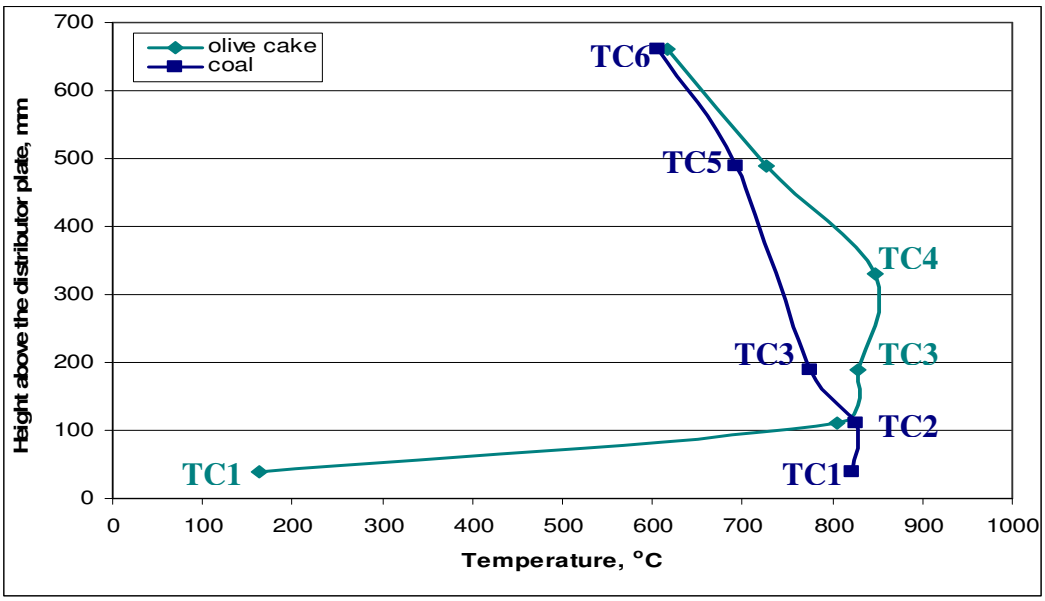

Figure 5.1 Comparison of temperature profiles along the column for the combustion of olive cake and coal

For the combustion of coal, the thermocouple (TC2) located at about 110 mm above the distributor plate gives approximately the temperature of the bed surface at expanded condition. The maximum temperature found at about 110 mm above the distributor plate for the thermocouple TC2 is 825 ^{o}C. After the temperature reaches to a maximum value, it gradually decreases to 607 ^{o}C at about 660 mm above the distributor plate at thermocouple TC6.

As can be seen from Figure 5.1, the average temperature for the first two thermocouples (TC1 and TC2) for the combustion of coal is higher than the average temperature for the combustion of olive cake. However, after the second thermocouple temperatures obtained from the last four thermocouples (TC3, TC4, TC5, and TC6) for the combustion of olive cake are higher than that of coal combustion. Because of the high volatile matter content, olive cake mostly burns in the freeboard region causing the temperature of the region to be high. Moreover, the coal particles (1,374 kg/m^3) are denser than the olive cake particles (591 kg/m^3). Therefore, chars remaining after the devolatilization of coal particles

continue their combustion within the bed. Consequently, the bed temperature for the combustion of coal is higher than the bed temperature for olive cake combustion. This phenomenon was also observed by Atimtay (1987) during the investigation of combustion of lignite particles with high volatile matter content in a bubbling fluidized bed.

5.1.2. Flue gas emissions

Flue gas emissions for the combustion of olive cake and coal are given in Table 5.2. Concentrations of pollutants in the flue gas are presented in mg/Nm^3 at normal temperature (273 ^oK) and pressure (1 atm) to be consistent with the regulations and they are based on 6 vol% O_2 in the flue gas as required in the Turkish Regulation for Air Pollution Control from Industrial Sources (RAPCIS, 2004). Excess air ratio (λ) ranges 1.12-2.30 for olive cake combustion and 1.28-2.24 for coal combustion. The average temperature (TC2-TC6) of the combustor is 700 ^oC for olive cake combustion and 725 ^oC for coal combustion. While superficial gas velocity (u_o) at TC2 temperature is found to be 0.80-1.12 m/sec for olive cake combustion, it is found to be 0.86-1.16 m/sec for coal combustion.

Table 5.2 Flue gas emissions for the combustion of olive cake and coal ($T \cong 710\ ^oC$)

Run #	**Solid fuel**	**CO**	**C_mH_n (as C_3H_8)**	**NO_x (as NO_2)**	**SO_2**
		(mg/Nm^3 based on 6% O_2)			
r-1	Olive Cake (O.C.)	**16 995**	**2171**	**737**	**0**
r-2	Coal (C)	**1178**	**62**	**1068**	**2917**

As can be seen from Table 5.2, for the combustion of olive cake, SO_2 emissions are zero because of very low sulfur content (0.086 wt% on dry basis) of olive

cake. For the combustion of coal, SO_2 emissions are measured as 2,917 mg/Nm^3 which is much higher than the SO_2 emissions for olive cake combustion due to high sulfur content (2.1 wt% on dry basis) of coal.

NO_x, C_mH_n and CO emissions are measured as 737, 2171 and 16995 mg/Nm^3, respectively, for olive cake combustion. CO emissions for olive cake combustion have been found to be about 15 times more than coal, because of higher VM content and the escape of the unburnt volatile matter from the combustor in the case of olive cake.

Effect of excess air ratio on flue gas emissions

The results of the effect of excess air ratio on flue gas emissions for olive cake and coal combustion have been given in this section. The change of CO, C_mH_n, SO_2, and NO_x concentrations with respect to excess air ratio for combustion of olive cake and coal are shown in Figure 5.2, Figure 5.3, Figure 5.4, and Figure 5.5, respectively. The excess air ratio (λ) was changed between 1.12 and 2.30. TC2 temperature is 710 ± 15°C for the combustion tests.

Figure 5.2 shows the effect of excess air ratio on **CO emissions** for the combustion of olive cake and coal. For the combustion of **olive cake,** CO concentration decreases as the excess air ratio increases from 1.12 to 1.58. While the CO emission is 22,959 mg/Nm^3 at λ = 1.12, it becomes 14,844 mg/Nm^3 at λ = 1.58 due to a better combustion. As the excess air ratio is increased further, a slight increase is seen in CO emissions. The reason for this increase can be explained with insufficient residence time of CO in the combustor to burn completely.

As can be seen from the figure, CO emission for the **coal** combustion increases as the excess air ratio increases. While CO emission is 250 mg/Nm^3 at λ = 1.28, it reaches to 2,450 mg/Nm^3 at λ = 2.24 with the increase in the excess air ratio. This can be explained by the insufficient residence time for the CO to be completely

burnt in the freeboard region. Increasing excess air ratio means increasing the air and oxygen supplied to the bed and the fluidization velocity. As a result of this increase gases or particulates leave the combustor column in a short period of time, that means the residence time decreases.

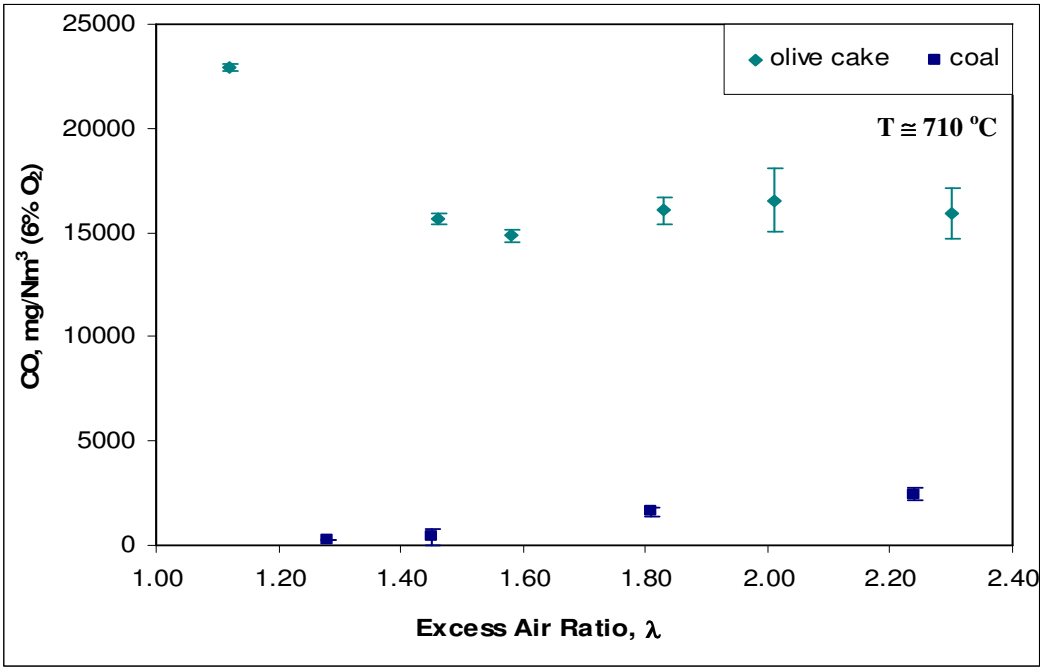

Figure 5.2 Effect of excess air ratio on CO emissions for the combustion of olive cake and coal

When CO emissions from two types of fuels are compared, it is seen that the emissions from coal combustion are much lower than for olive cake combustion. This can be possibly due to the higher density of coal particles than olive cake particles and burning of coal particles in the bed. After the volatiles leave the coal particle, the char formed can sink in the bed material and burn completely. This was observed by Atimtay (1987), too and the reason was explained in a similar way. The other reason could be the higher VM content of the olive cake than coal (about 2 times as much). Therefore, higher amount of volatiles are released from

olive cake per unit weight of fuel. If these volatiles can not find enough oxygen to burn in the freeboard then, they leave the combustor as partially oxidized.

The change of C_mH_n emissions with excess air ratio is shown in Figure 5.3. For the combustion of **olive cake**, **C_mH_n emission** decreases from 2,975 mg/Nm^3 to 1,713 mg/Nm^3 as the excess air ratio increases from 1.12 to 1.58. Then, with the further increase of excess air ratio C_mH_n emission shows an increase up to 2,500 mg/Nm^3 for λ = 2.30. In the case of **coal**, C_mH_n emission increases as the excess air ratio increases. The reason for the increase can be due to the insufficient residence time of the volatiles in the column as in the case of CO. Therefore, some volatiles leave the column unburnt. C_mH_n emissions increase from 22.5 mg/Nm^3 to 146 mg/Nm^3 as the excess air ratio increases from 1.28 to 2.24.

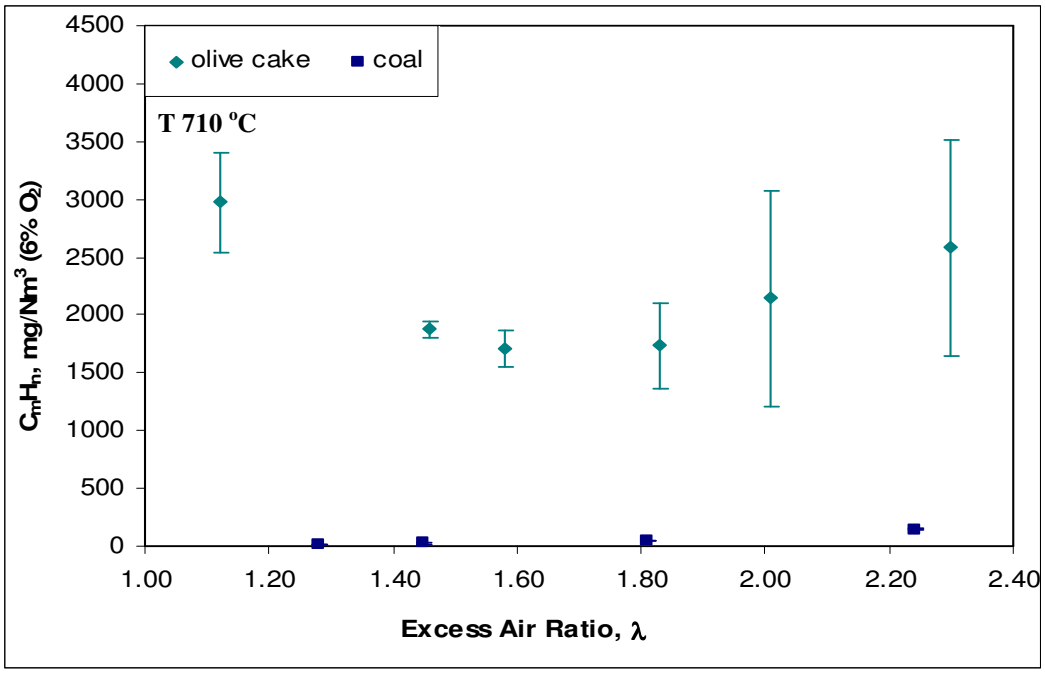

Figure 5.3 Effect of excess air ratio on hydrocarbon (C_mH_n) emissions for the combustion of olive cake and coal

As can be seen from the figure, C_mH_n emission from olive cake is about 35 times higher than coal due to higher volatile matter content of olive cake (71.17 wt%) than coal (37.5 wt%). Some portion of volatiles leave the column unburnt. This problem can be solved by supplying secondary air to the freeboard. The secondary air to be given to the combustor in the freeboard region can provide additional oxygen for combustion reactions in the freeboard and this may lead to lower C_mH_n emissions. Another solution might be to increase the residence time of CO and hydrocarbons in the column by making the column much higher than used in this study. At the present conditions and configurations, the superficial gas velocity used in the bed (u_o) changes between 0.75 m/sec and 1.0 m/sec (corresponding to 1.5-2 u_{mf}) for the combustion of olive cake and coal. The corresponding residence times of gases in the entire column changes between 0.9 sec and 1.2 sec. Therefore, this residence time may be low for volatiles to burn completely. Lower residence time causes the volatiles to leave the system unburnt.

NO_x emissions for the combustion of coal and olive cake are shown in Figure 5.4. For the combustion of **olive cake**, NO_x emission increases as the excess air ratio increases. While the NO_x emission is 553 mg/Nm^3 at λ =1.12, it increases up to 1,029 mg/Nm^3 with excess air ratio increasing to 2.30. This increase may show that a better combustion of fuel-N has been obtained especially in the freeboard due to higher amount of O_2 supplied and this leads to higher combustion temperature and higher formation of NO_x. For the combustion of **coal**, NO_x emissions have been found to increase from 1,425 mg/Nm^3 to 1,700 mg/Nm^3 as the excess air ratio increases from 1.28 to 1.45. Again this might be due to higher temperature obtained in the combustor with the supply of extra O_2 with increasing excess air ratio. Further increase in the excess air ratio causes the combustor column to cool and lead to decrease in NO_x emissions. NO_x emission is about 560 mg/Nm^3 for the excess air ratios of 1.81 and higher.

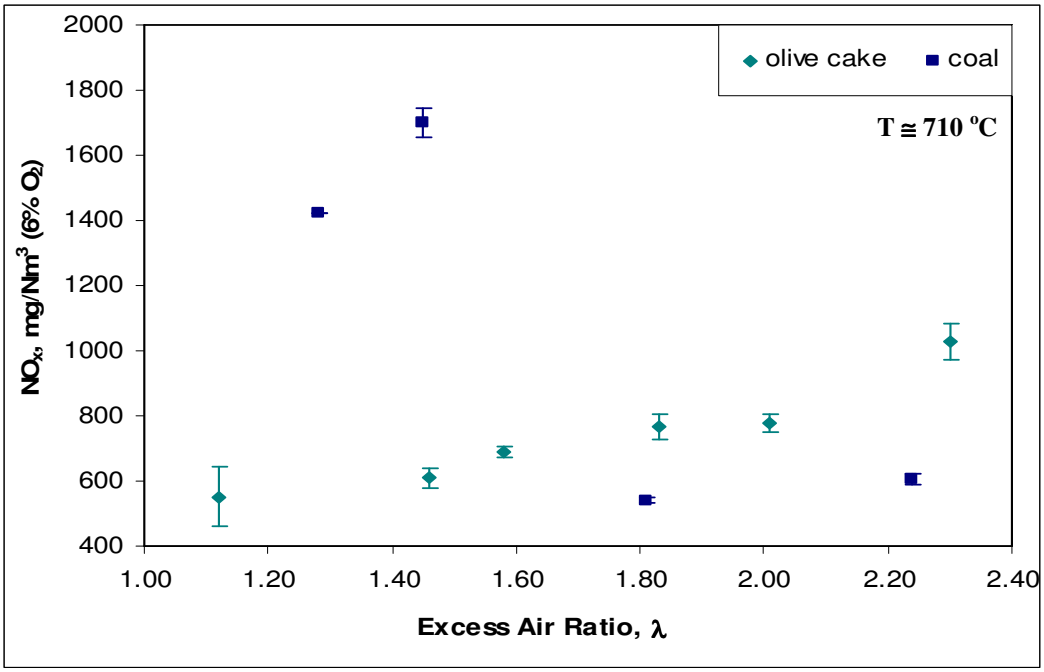

Figure 5.4 Effect of excess air ratio on NO_x emissions for the combustion of olive cake and coal

If the NO_x emissions for the combustion of olive cake and coal are compared, the emissions are higher in the case of coal combustion than in the case of olive cake combustion up to a λ value of about 1.7. The fuel-N contents of both fuels are very close to each other (1.27 wt% on dry basis). The reason that olive cake gives lower NO_x concentration than coal can be explained by relatively fast release of volatiles which causes high levels of hydrocarbon radicals or a reducing atmosphere in the freeboard. This may give a rise to a reduction in the amount of NO_x. This explanation is also given by Armesto, et al. (2003). After the release of the volatiles, char is remained from coal and olive cake. However, the char generated from coal has a higher density and higher fixed carbon content (twice as much as the olive cake). Char particles have the potential to reduce NO_x to N_2 in the combustor. Therefore this might be the reason to have a lower NO_x concentration after certain λ.

The effect of excess air ratio on **SO_2 emissions** for the combustion of olive cake and coal is shown in Figure 5.5. As can be seen from the figure, for the **olive cake** combustion, SO_2 emissions are practically zero because of a very low S content of the olive cake. SO_2 emission for **coal** combustion increases slightly as the excess air ratio increases from 1.28 to 2.24 probably due to a better combustion. SO_2 emissions are on the average between 2,555 to 3,308 mg/Nm^3.

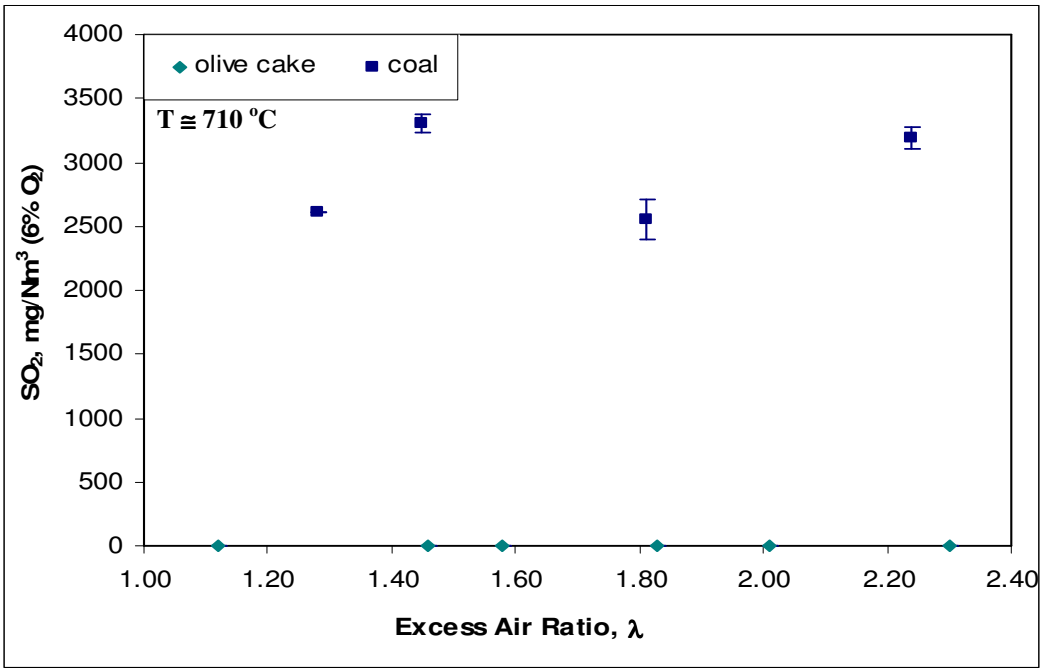

Figure 5.5 Effect of excess air ratio on SO_2 emissions for the combustion of olive cake and coal

SO_2 emissions for the combustion of coal are fairly higher than those for olive cake combustion. This is absolutely due to the higher sulfur content of coal than olive cake. No additive materials were used in the bed during the experiments to absorb SO_2.

5.1.3. Combustion efficiencies

Combustion losses and efficiencies for the coal and olive cake combustion at the feeding rate of 10 g/min are given in Table 5.3. The average **combustion efficiency** for **olive cake** is calculated to be 88.3±2.4% at T = 710±15 ^{o}C for λ values of 1.12-2.30. The combustion losses are mainly due to the formation of CO (L_{CO}) and due to the formation of C_mH_n (L_{CH}). The combustion loss due to the formation of CO is 7.3 % by weight and due to the formation of C_mH_n is 4.3% by weight of the total loss.

The combustion efficiency for **coal** is calculated as 99.1±0.6% at T = 710±15 ^{o}C for λ values of 1.28-2.24. The combustion losses for coal are mainly due to the formation of CO (L_{CO}) and due to unburnt carbon collected in the ash hopper at the bottom of the cyclone ($L_{C,\ cyclone}$). They are 0.5% by wt. and 0.21% by wt., respectively. The contribution of unburnt carbon in the bed to the total combustion losses is almost the same for both the combustion of olive cake and coal. The combustion losses due to the unburnt carbon in bed ($L_{C,\ bed}$) are 0.05% and 0.04% for olive cake and coal combustion, respectively. As can be seen from the table, the overall combustion efficiency for olive cake is lower than that for coal. This is mainly due to the high CO and C_mH_n emissions during the combustion of olive cake. The heating value of olive cake is lost as CO and C_mH_n emissions which are incomplete combustion products.

Table 5.3 Combustion losses and efficiencies for the combustion of olive cake and coal (T ≅ 710 ^{o}C)

Run #	Solid fuel	L_{CO} (%)	L_{CH} (%)	$L_{C,\ bed}$ (%)	$L_{C,\ cyclone}$ (%)	Combustion Efficiency, η (%)
r-1	Olive Cake (O.C.)	**7.3**	**4.3**	**0.05**	**0.04**	**88.3**
r-2	Coal (C)	**0.5**	**0.1**	**0.04**	**0.21**	**99.1**

The combustion efficiencies calculated for the combustion of olive cake and coal are plotted with respect to excess air ratio in Figure 5.6. For the combustion of **coal**, the combustion efficiency decreases from 99.8% to 98.4% as the excess air ratio increases from 1.28 to 2.24. This can be explained by the increase of CO and C_mH_n emissions in the flue gas. For the combustion of **olive cake**, combustion efficiency changes between 83.6% and 90.1%. Combustion losses due to the unburnt carbon in the bed ($L_{C,\ bed}$) and combustion losses due to the unburnt carbon in the cyclone ($L_{C,\ cyclone}$) do not exceed 0.07% by wt. and 0.06% by wt., respectively. The main contributor for the combustion losses is the CO and C_mH_n emissions. As the CO emissions and C_mH_n emissions increase, L_{CO} and L_{CH} also increase resulting in low overall combustion efficiency. The reason for the decrease in combustion efficiency after λ=1.58 is the increase of both CO and C_mH_n emissions, as shown in Figure 5.2 and Figure 5.3, respectively, as the excess air ratio is changed between 1.58 and 2.24.

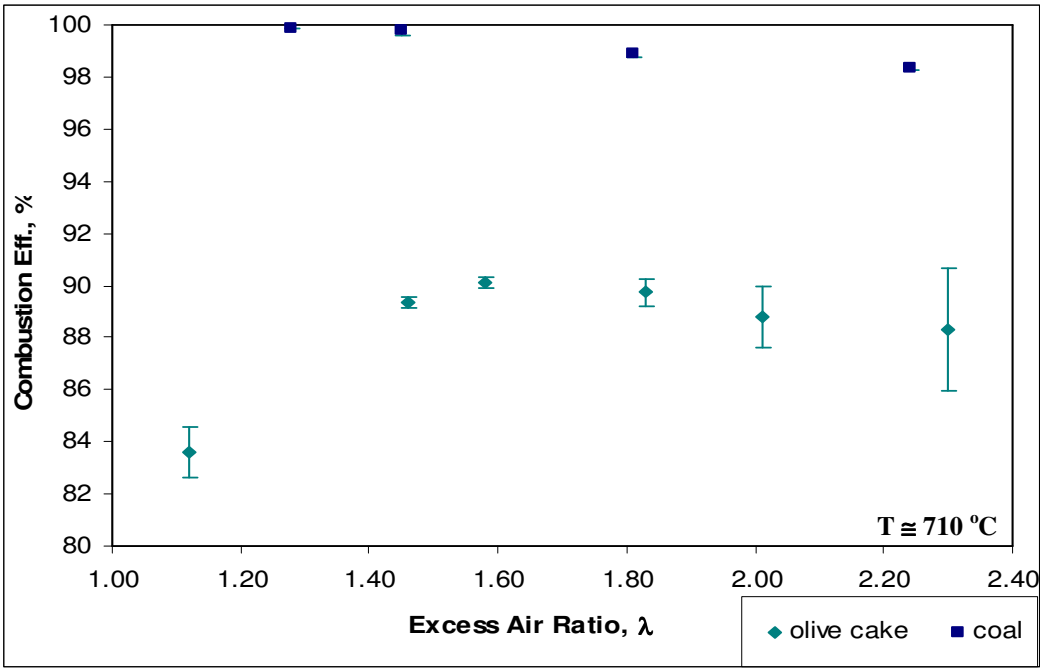

Figure 5.6 Effect of excess air ratio on combustion efficiency for the combustion of olive cake and coal

5.2. Co-combustion of Olive cake with Coal

5.2.1. Temperature profiles

Three co-combustion tests of coal with olive cake are conducted with mixing ratios of 25%, 50%, and 75% of olive cake by weight in the mixture. For co-combustion tests, fuel feeding rate was kept at 10 g/min like in the combustion tests for olive cake and coal. The temperature profiles in the combustor column for the co-combustion of olive cake with coal at three different mixing ratios are shown in Figure 5.7.

For the co-combustion of coal-olive cake mixture containing 25 wt% olive cake, the temperature profile of the combustor column shows that TC2 and TC3 have the highest temperatures of 803 ^{o}C and 790 ^{o}C, respectively. The temperature at TC1 is 765 ^{o}C which indicates that a good mixing of bed material with fuel has occurred. This can be explained as before with the higher density of coal particles than olive cake particles. The coal-rich fuel mostly burns in the lower part of the combustor column where the bed is located. This causes the temperature of bed material to be higher than that of freeboard region. Then, the temperature goes down gradually as the height along the combustor column increases.

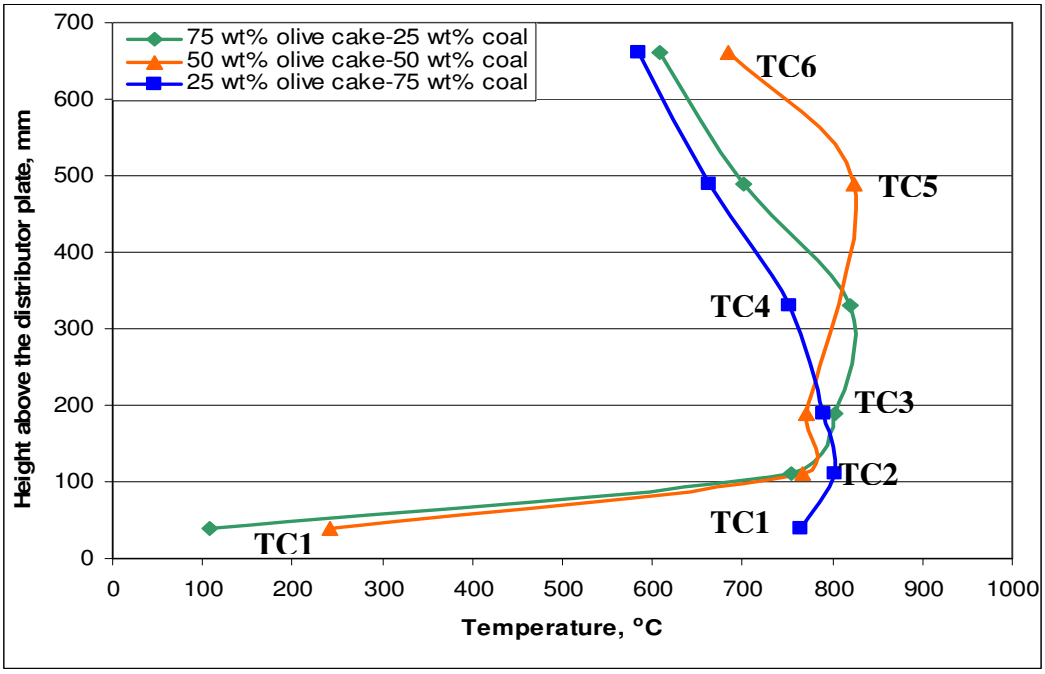

Figure 5.7 Comparison of temperature profiles along the column for the combustion of olive cake and coal for different mixing ratios

The temperature profile along the combustor column for the co-combustion of coal and olive cake mixture of 50 wt% olive cake-50 wt% coal shows the highest temperature at TC5 (825 ^{o}C). TC1 has the lowest temperature (241 ^{o}C) along the combustor column. The highest temperature around TC5 is an indication that most of the VM combustion takes place in the freeboard region at about 500 mm above the distributor plate, therefore causing low CO and C_mH_n emissions in the flue gas. Thus, combustion efficiency is expected to be high.

The temperature profile along the combustor column for the co-combustion of coal and olive cake mixture containing 75 wt% olive cake is again shown in Figure 5.7. For this mixture the highest temperature is obtained at TC4 as 810 ^{o}C. As the olive cake fraction increases in the fuel mixture, the temperature measured at TC1 becomes lower. TC1 has the lowest temperature (108 ^{o}C) along the combustor column. The lowest temperature at TC1 indicates that the mixture of

fuel can not penetrate to the lower parts of the bed material and segregation occurs because of the density difference between the fuel particles and sand.

When the temperature profiles obtained along the combustor column for different fuel mixtures are compared, it can be easily seen that the average of the temperatures measured with the first two thermocouples are 780 ^{o}C, 445 ^{o}C, and 425 ^{o}C for the fuel mixtures containing 25% by wt, 50% by wt and 75% by wt olive cake, respectively. Therefore, this result shows that as the olive cake fraction in the fuel mixture decreases (or as the coal fraction increases), the combustion occurs more at the lower part of the combustor column.

5.2.2. Flue gas emissions

Flue gas emissions for the co-combustion of olive cake with coal mixtures for different mixing ratios are given in Table 5.4. Concentrations are presented in mg/Nm^3 at normal temperature (273 K) and pressure (1 atm) to be consistent with the regulations and they are based on 6 vol% O_2 as required in the Turkish Regulation for Air Pollution Control from Industrial Sources (RAPCIS, 2004). λ varies 1.30-2.04 for combustion of the mixture containing 75 wt% olive cake, 1.32-2.09 for combustion of the mixture containing 50 wt% olive cake, and 1.38-1.99 for combustion of the mixture containing 25 wt% olive cake. Average temperature is 750 ^{o}C for the mixture containing 75 wt% olive cake, 762 ^{o}C for the mixture containing 50 wt% olive cake, and 718 ^{o}C for the mixture containing 25 wt% olive cake. U_o at TC2 is found to be 0.83-0.99, 0.79-1.34, 0.94-1.36 m/sec for the mixture containing 75 wt% olive cake, 50 wt% olive cake, and 25 wt% olive cake, respectively.

Table 5.4 Flue gas emissions for the co-combustion of olive cake with coal mixtures for different mixing ratios (T ≅ 740 ^{o}C)

Run #	Solid fuel	CO	C_mH_n (as C_3H_8)	NO_x (as NO_2)	SO_2
		(mg/Nm^3 based on 6% O_2)			
r-3	Olive Cake 25 wt% + Coal 75 wt%	**3336**	**361.3**	**838.1**	**2518**
r-4	Olive Cake 50 wt% + Coal 50 wt%	**2792**	**103.6**	**1036**	**1642**
r-5	Olive Cake 75 wt% + Coal 25 wt%	**12031**	**2036**	**606.2**	**63.4**

Effect of excess air ratio on flue gas emissions

The results on the effect of excess air ratio on flue gas emissions for the co-combustion of coal and olive cake mixtures at predetermined ratios for the feeding rate of 10 g/min have been given in this section. The changes in CO, C_mH_n, SO_2, NO_x emissions originated from the co-combustion of olive cake with coal mixture with change in the excess air ratio are shown in Figure 5.8, Figure 5.9, Figure 5.10, and Figure 5.11, respectively. During these combustions the average temperature (TC2-TC6) of the column was tried to be kept at about constant values of 740± 20 ^{o}C.

The effect of excess air ratio on **CO emissions** for the co-combustion of coal with olive cake at predetermined mixing ratios is shown in Figure 5.8. For 25 wt% olive cake in the mixture, CO emissions decrease as the excess air ratio increases. While at λ = 1.38, CO emission is 7,367 mg/Nm^3, it decreases to 821 mg/Nm^3 at λ = 1.99. A decreasing trend in CO emission with excess air ratio is also valid for combustion of the fuel mixture with 50 wt% olive cake and 75 wt% olive cake as well. CO emission decreases from 10,760 mg/Nm^3 at λ = 1.32 to 569 mg/Nm^3 at

λ = 2.09 for the case of 50 wt%-50 wt% mixture. However, when the fuel mixture with 75 wt% olive cake is burned, CO emissions were observed to be higher than the cases of 25 wt% and 50 wt% olive cake. The CO emissions change from 14,690 mg/Nm^3 at λ = 1.30 to 8,375 mg/Nm^3 at λ = 2.04. Minimum CO emission has been measured for the case of 50-50 wt% mixture. This can be explained with the temperature profile shown in Figure 5.7. The temperature measured in the freeboard region for the 50-50 wt% olive cake and coal mixture is the highest among the other three mixtures tested. Therefore, CO emissions are minimum.

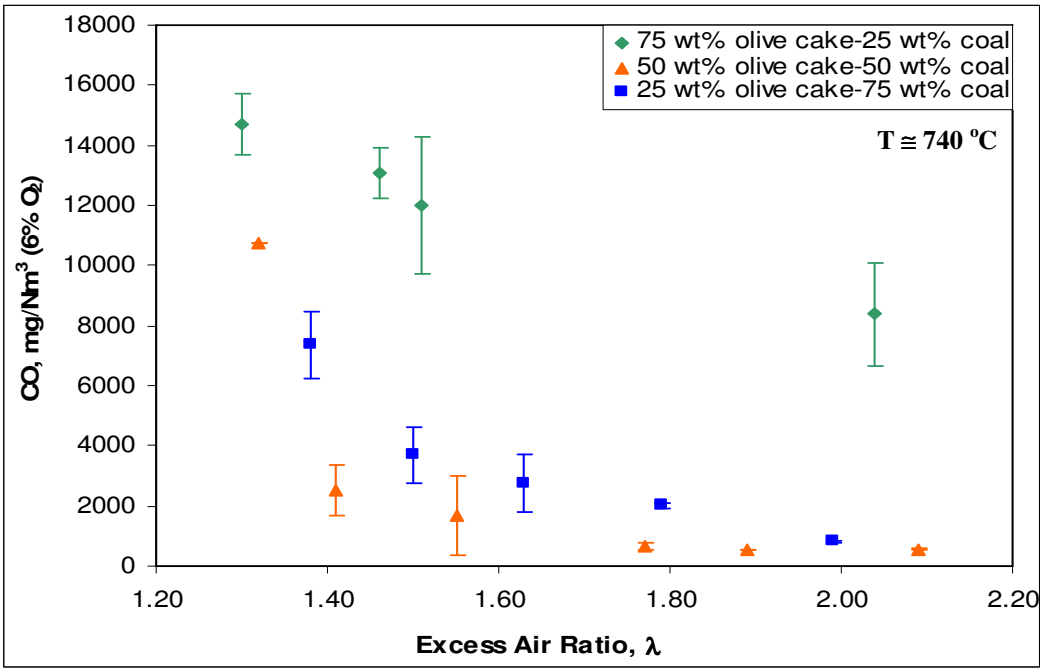

Figure 5.8 Effect of excess air ratio on CO emissions for the co-combustion of olive cake with coal for different mixing ratios

The emissions of C_mH_n for various excess air ratios for the co-combustion of coal and olive cake mixture are shown in Figure 5.9. **C_mH_n emissions** decrease for the co-combustion of coal with olive cake at three different mixing ratios as the excess air ratio increases. For the combustion of mixture with 25% olive cake, C_mH_n emissions decrease from 735 mg/Nm^3 to 178 mg/Nm^3 as the excess air ratio

changes from 1.38 to 2.0. For the combustion of the mixture with 50% olive cake, there is a sharp decrease on C_mH_n emissions for the λ values between 1.32-1.41. C_mH_n emission is 414 mg/Nm^3 at λ = 1.32 and 70 mg/Nm^3 at λ = 1.41. C_mH_n emissions do not change much with a further increase in excess air ratio. For the combustion of the mixture with 75% olive cake, C_mH_n emission decreases from 2,850 mg/Nm^3 to 969 mg/Nm^3 as the excess air ratio changes from 1.30 to 2.04.

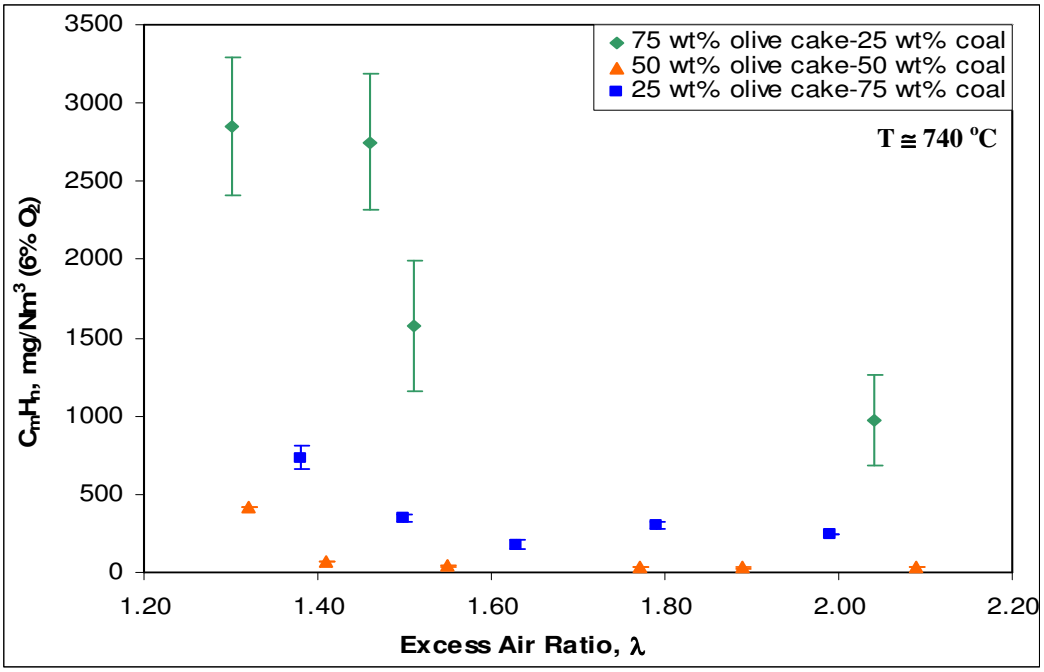

Figure 5.9 Effect of excess air ratio on hydrocarbon (C_mH_n) emissions for the co-combustion of olive cake with coal for different mixing ratios

As the olive cake percent increases in the fuel mixture, the average C_mH_n emission is expected to increase because the volatile matter content of olive cake is higher than in the coal. However, C_mH_n emissions for the combustion of the mixture with 50% olive cake are found to be the lowest among the other fuel mixtures. This is due the high temperature of the freeboard region for the 50 wt% olive cake combustion. The 50-50 wt% mixture burns most effectively probably due to the good balance between the coal and olive cake.

The effect of excess air ratio on **NO_x emissions** for the co-combustion of coal with olive cake is shown in Figure 5.10. For the fuel mixture with 25 wt% olive cake, after a slight decrease in NO_x emissions for λ values of 1.38-1.50, NO_x emissions increase as the excess air ratio increases. The NO_x emissions are found to be at a minimum (623 mg/Nm^3) at λ=1.50. They increase from 623 mg/Nm^3 at λ = 1.50 to 1,153 mg/Nm^3 at λ = 1.99. For the mixture containing 50 wt% olive cake, a similar decrease on NO_x emissions is observed, then, NO_x emissions increase as the excess air ratio increases. They are 918 mg/Nm^3 at λ = 1.41 and 1,148 mg/Nm^3 at λ = 2.09. For the mixture containing 75 wt% olive cake, NO_x emissions increase as the excess air ratio increases like in the other cases. But the emissions values are lower than that for the other two cases. NO_x emission is 517 mg/Nm^3 at λ = 1.30, it increases to 800 mg/Nm^3 at λ = 2.04.

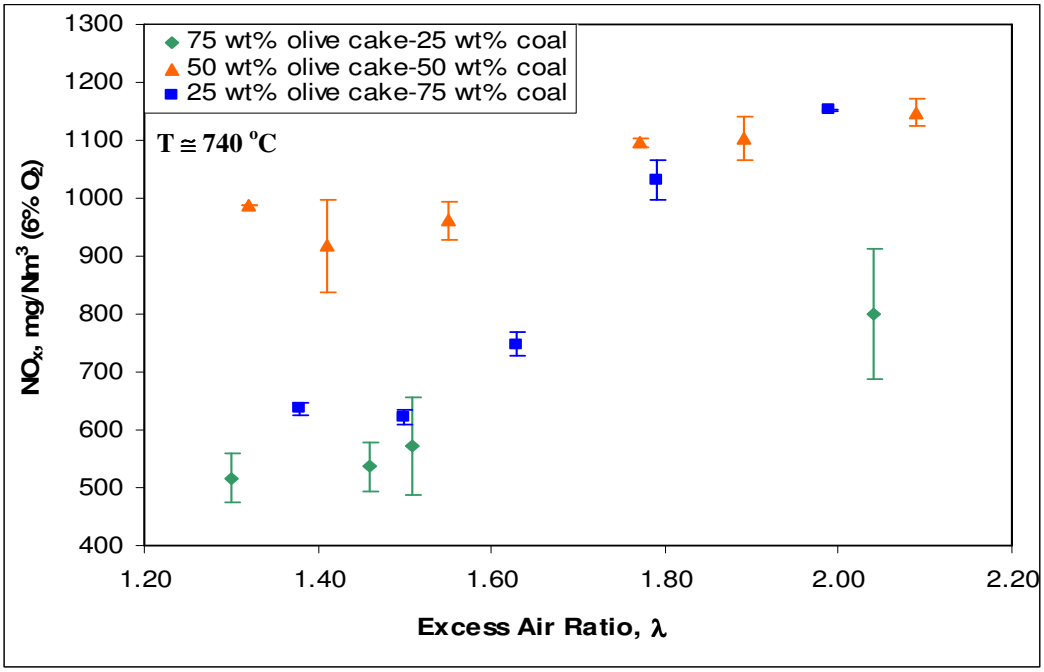

Figure 5.10 Effect of excess air ratio on NO_x emissions for the co-combustion of olive cake with coal for different mixing ratios

Because of high temperatures measured in the freeboard region for 50 wt% coal-50 wt% olive cake mixture, NO_x emissions are also higher than the other two cases most probably due to formation of thermal NO_x. The average temperature measured at TC5 is 824.5 ^oC which is higher than both that for mixture containing 25 wt% olive cake (752.4 ^oC) and that for mixture containing 75 wt% olive cake (819.7 ^oC).

The effect of excess air ratio on **SO_2 emissions** for the co-combustion of coal with olive cake is shown in Figure 5.11. For the mixture with 25 wt% olive cake, the SO_2 emissions increases from 2,350 mg/Nm^3 to 2,650 mg/Nm^3 as the excess air ratio increases from 1.38 to 1.50 probably due to a better combustion. Then, as the excess air ratio increases, SO_2 emissions start to decrease. For the combustion of the mixture with 50 wt% olive cake, SO_2 emissions increase within the interval of λ between 1.32-1.55, then, they start to decrease with a further increase of the excess air ratio most probably due to dilution of the flue gases. For the mixture with 75 wt% olive cake, SO_2 emissions are very low because olive cake contains very small amount of sulfur.

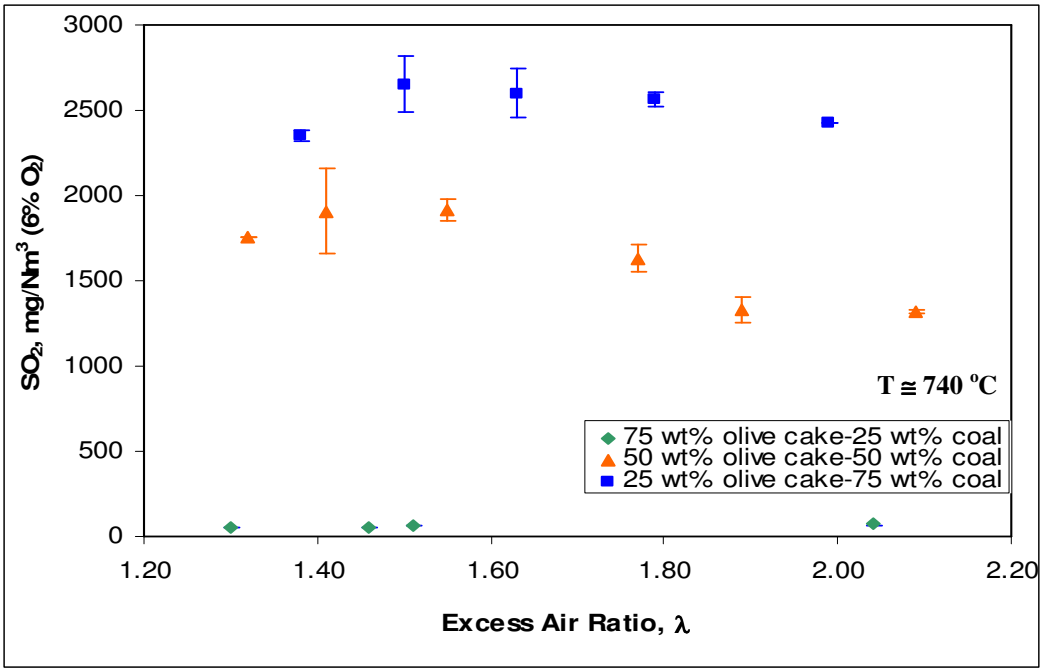

Figure 5.11 Effect of excess air ratio on SO_2 emissions for the co-combustion of olive cake with coal for different mixing ratios

SO_2 emissions for the combustion of fuel mixtures containing 25 wt% and 50 wt% olive cake are fairly higher than those for the combustion of the fuel mixture with 75 wt% olive cake. As the coal fraction increases in the fuel mixture, the SO_2 emissions increase. This is due to the higher sulfur content of coal than olive cake.

5.2.3. Combustion efficiencies

The average **combustion efficiency** for **olive cake** is calculated to be 88.3±2.4% at T = 710±15 °C for λ values of 1.12-2.30. The combustion losses are mainly due to the formation of CO (L_{CO}) and due to the formation of C_mH_n (L_{CH}). The combustion loss due to the formation of CO is 7.3% and due to the formation of C_mH_n is 4.3% of the total loss.

Combustion losses and combustion efficiencies calculated for the co-combustion of olive cake with coal at the feeding rate of 10 g/min are given in Table 5.5. The

combustion efficiency for the mixture containing 25 wt% olive cake is found to be 97.8±1.5% at T = 740±20 ^{o}C for λ values of 1.38-1.99%. The combustion losses are mainly due to the formation of CO and hydrocarbons in the flue gas. For the mixture with 25 wt% olive cake, L_{CO} is 1.4% and L_{CH} is 0.7%. The combustion efficiency for the fuel mixture containing 50 wt% olive cake is found to be 98.6±2.0% at T = 740±20 ^{o}C for λ values of 1.32-2.09%. The combustion losses are mainly due to the formation of CO and hydrocarbons and they are 1.2% and 0.2% of the total loss, respectively. The combustion efficiency for the fuel mixture containing 75 wt% olive cake is 90.7±3.0% at T = 740±20 ^{o}C for λ values of 1.30-2.04%. The combustion losses are mainly due to the formation of CO and hydrocarbons and they are 5.1% and 4% of the total loss, respectively. As can be seen from the table, the overall combustion efficiency for a mixture of 50 wt% olive cake and 50 wt% coal is the highest. This is mainly due to the low CO and C_mH_n emissions for this mixture. However, a solution should be found to decrease emissions in order to be able to use more biomass in the mixture. Therefore, a secondary air addition to the freeboard region can be beneficial to obtain less CO and hydrocarbon emissions.

Table 5.5 Combustion losses and efficiencies for the combustion and co-combustion of olive cake and coal for different mixing ratios (T ≅ 740 ^{o}C)

Run	Solid fuel	L_{CO}	L_{CH}	$L_{C, bed}$	$L_{C, cyclone}$	Combustion Efficiency, η
#		(%)	(%)	(%)	(%)	(%)
r-1	Olive Cake (O.C.)	**7.3**	**4.3**	**0.05**	**0.04**	**88.3**
r-2	Coal (C)	**0.5**	**0.1**	**0.04**	**0.21**	**99.1**
r-3	Olive Cake 25 wt% + Coal 75 wt%	**1.4**	**0.7**	**0.02**	**0.07**	**97.8**
r-4	Olive Cake 50 wt% + Coal 50 wt%	**1.2**	**0.2**	**0.03**	**0.01**	**98.6**
r-5	Olive Cake 75 wt% + Coal 25 wt%	**5.1**	**4.0**	**0.09**	**0.05**	**90.7**

Combustion efficiencies for the combustion of coal with olive cake are plotted with respect to excess air ratio in Figure 5.12. For the combustion of the mixture with 25 wt% olive cake, combustion efficiency is found to be 95.4% for the excess air ratio of 1.38 and it slightly increases as the excess air ratio increases. It reaches to its maximum value (99.1%) at λ=1.99. For the mixture with 50 wt% olive cake, the combustion efficiency increases as the excess air ratio increases. For the 75 wt% olive cake, combustion efficiency changes from 87.9% to 94.5% as the excess air ratio increases. For the combustion of all three fuel mixtures, combustion losses due to the unburnt carbon in the bed ($L_{C,\ bed}$) and combustion losses due to the unburnt carbon in the cyclone ($L_{C,\ cyclone}$) do not exceed 0.1% by wt. The main contributor to the combustion losses is the CO and hydrocarbon emissions. As the CO emissions and also C_mH_n emissions increase, L_{CO} and L_{CH} also increase resulting on low overall combustion efficiency. Therefore, decreasing CO and hydrocarbon emissions is necessary in order to increase the combustion efficiencies.

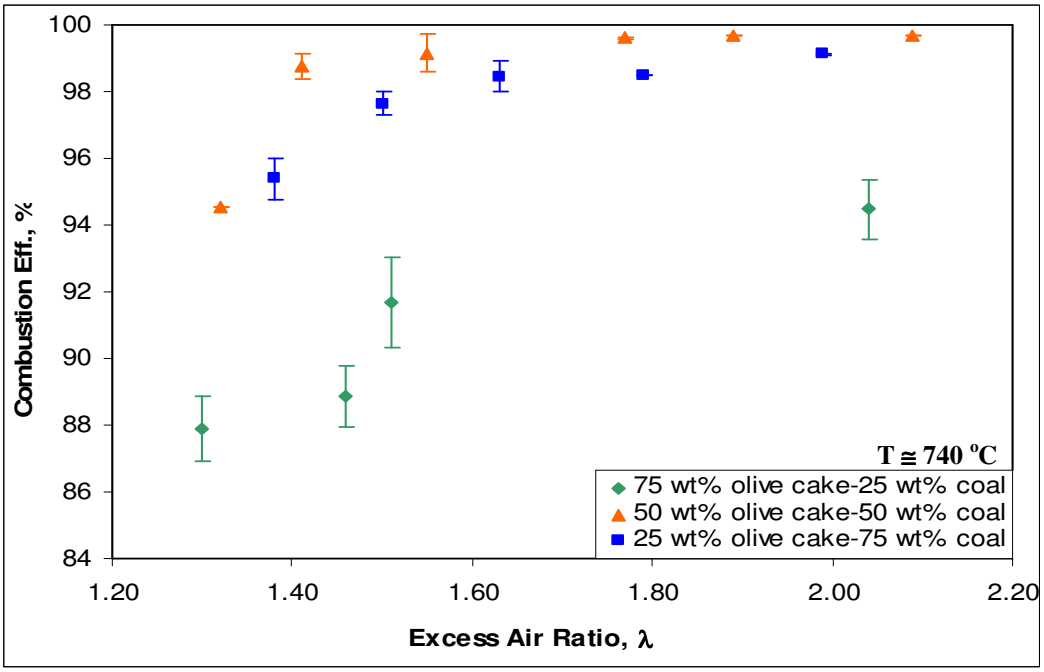

Figure 5.12 Effect of excess air ratio on combustion efficiency for the co-combustion of olive cake with coal for different mixing ratios

5.3. Combustion and Co-combustion of Olive Cake and Coal with Secondary Air

In order to investigate the effect of the secondary air on the combustion efficiency and emissions, secondary air was given to the freeboard of the combustor column from the place where thermocouple (TC4) was located. Secondary air flowrate was controlled with a rotameter and given to the system at 330 mm above the distributor plate. Therefore, the temperature at 330 mm could not be obtained for the combustion tests conducted with secondary air. Combustion and also co-combustion tests were done with secondary air flowrates of 30, 40, 50, 60, and 70 L/min. The results of these five tests were compared with the results of combustion tests which were conducted without secondary air. The ratio of secondary air to the total air supplied to the system was 0.11 for 30 L/min and 0.23 for 70 L/min.

5.3.1. Temperature profiles

The temperature profiles for the combustion of olive cake with various secondary air flowrates are given in Figure 5.13. For the olive cake combustion where secondary air is not used, the highest temperature (848 ^{o}C) is obtained at about 330 mm above the distributor plate. With the addition of secondary air at a rate of 30 L/min, the temperature decreases at all points along the column. While there is a slight decrease at the upper part of the combustor column, this decrease becomes larger at the lower part of the column. For the secondary air flowrate of 40 L/min, temperature in the freeboard region increases. The highest freeboard temperatures are obtained for the secondary air flowrate of 50 L/min. This case indicates that CO and especially hydrocarbons burn better in the freeboard as the secondary air flowrate increases. With a further increase in the secondary air flowrate, the temperature in the freeboard starts to decrease due to cooling effect.

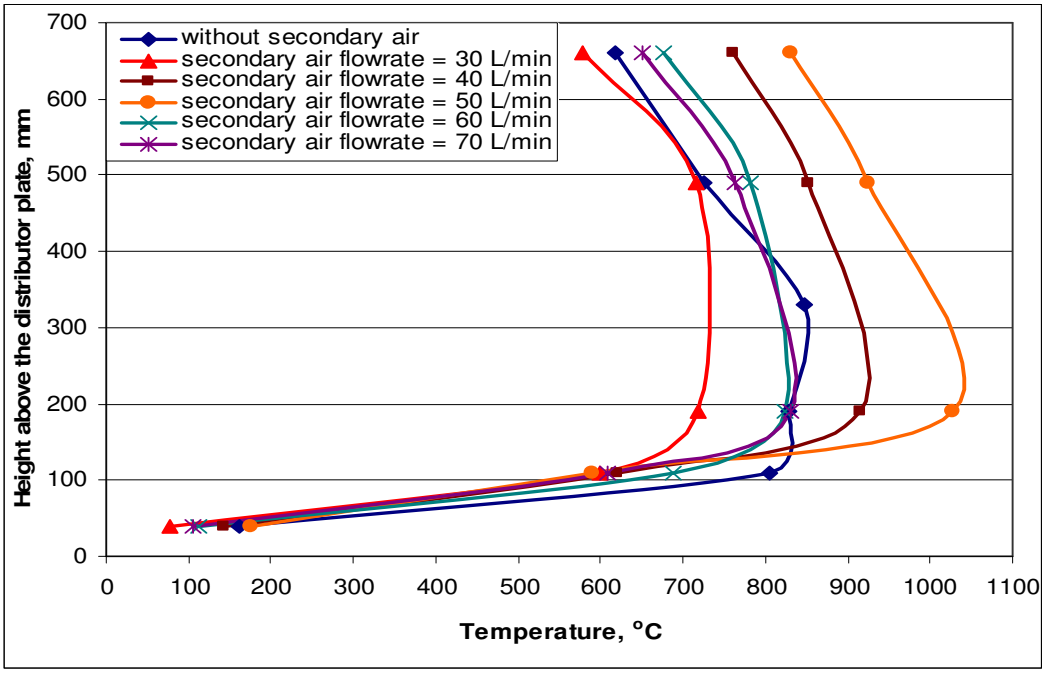

Figure 5.13 Temperature profile along the column for the combustion of olive cake with various secondary air flowrates

The temperature profiles for the combustion of the fuel mixture containing 75 wt% olive cake with various secondary air flowrates are seen in Figure 5.14. The highest temperature for the combustion of fuel mixture without secondary air is measured as 846.5 ^{o}C at 110 mm above the distributor plate. With the secondary air fed to the system, the temperature in the freeboard increases with increase in the secondary flowrate. The highest temperatures are obtained at TC3 (190 mm above distributor plate). The temperature at the freeboard reaches its highest value (910-920 ^{o}C) in the case of secondary air flowrates of 50 L/min and 60 L/min. In all cases, the temperatures at the freeboard are still higher than the temperatures obtained when fuel mixtures are burned without secondary air.

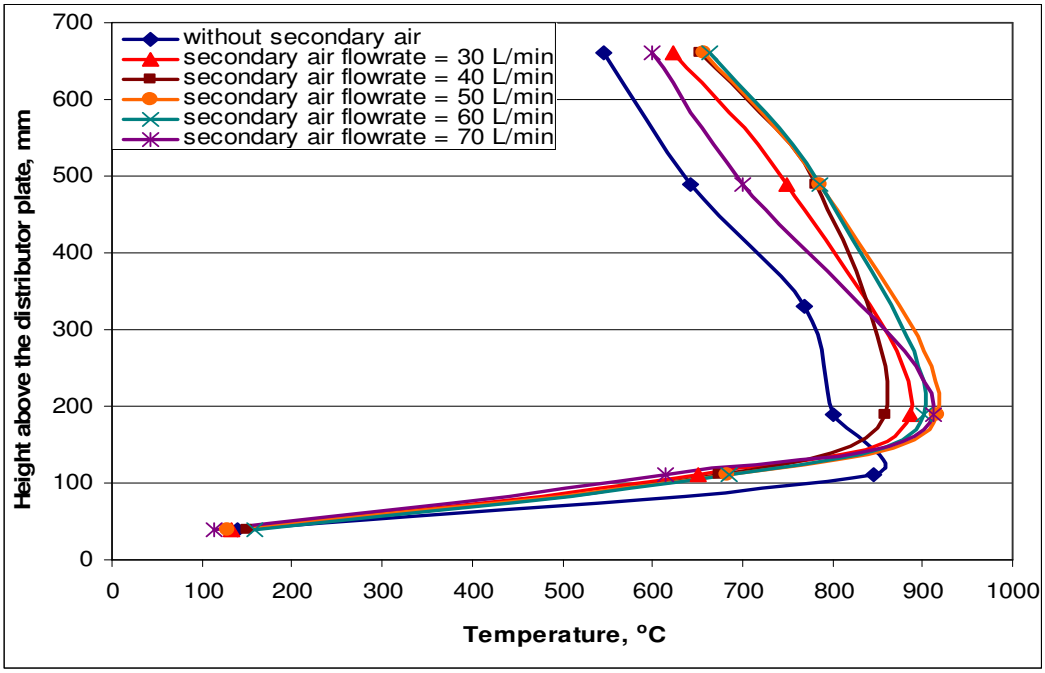

Figure 5.14 Temperature profile along the column for the co-combustion of the fuel mixture containing 75 wt% olive cake with various secondary air flowrates

The temperature profiles for the combustion of the fuel mixture with 50 wt% olive cake with various secondary air flowrates are given in Figure 5.15. As can be seen from the figure, the highest temperatures are measured again at TC3. The temperatures measured at TC3 increase with increase in the secondary air flowrate. At the same time, the temperatures at the upper part of the column decrease. As the amount of coal in the fuel mixture increases, because of the high density of coal, the fuel mixture burns particularly more at the lower part of the combustor column.

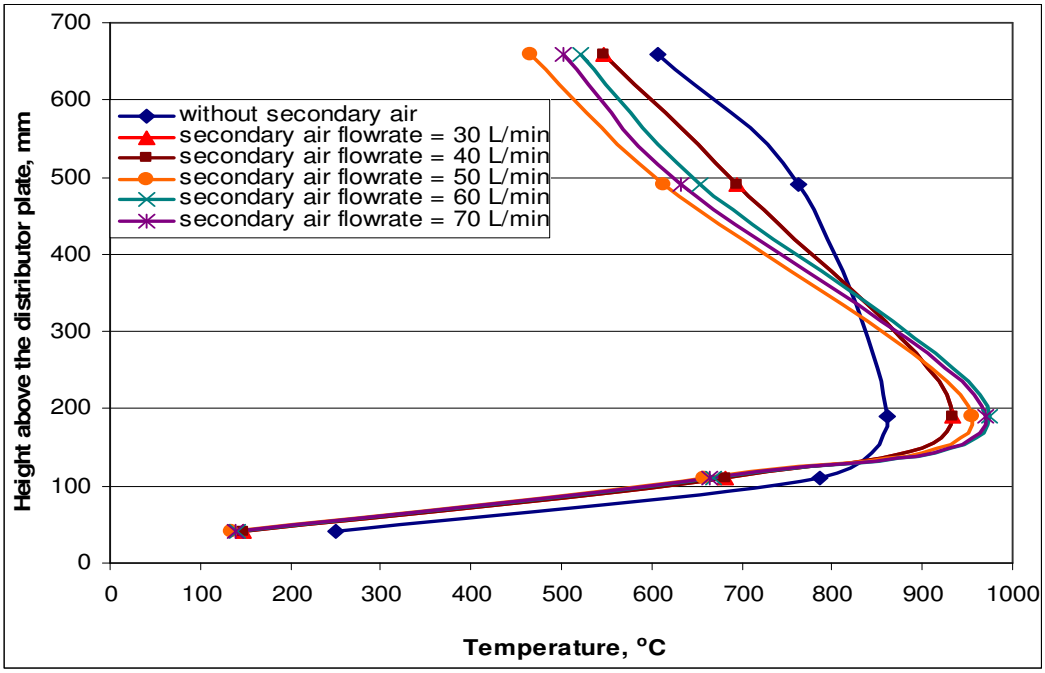

Figure 5.15 Temperature profile along the column for the co-combustion of the fuel mixture containing 50 wt% olive cake with various secondary air flowrates

The temperature profiles for the combustion of the fuel mixture containing 25 wt% olive cake with various secondary air flowrates are given in Figure 5.16. A similar trend in the temperature profile is seen as in the other cases. As the amount of the olive cake in the fuel mixture decreases, the volatile matter content of the fuel mixture decreases, too. Consequently, the volatiles leaving the system unburnt also decrease. When the highest temperatures along the combustor column without secondary air are measured at TC2, the highest temperatures measured with the addition of secondary air are at TC3. The temperatures measured at TC3 increase with increase in the secondary air flowrate.

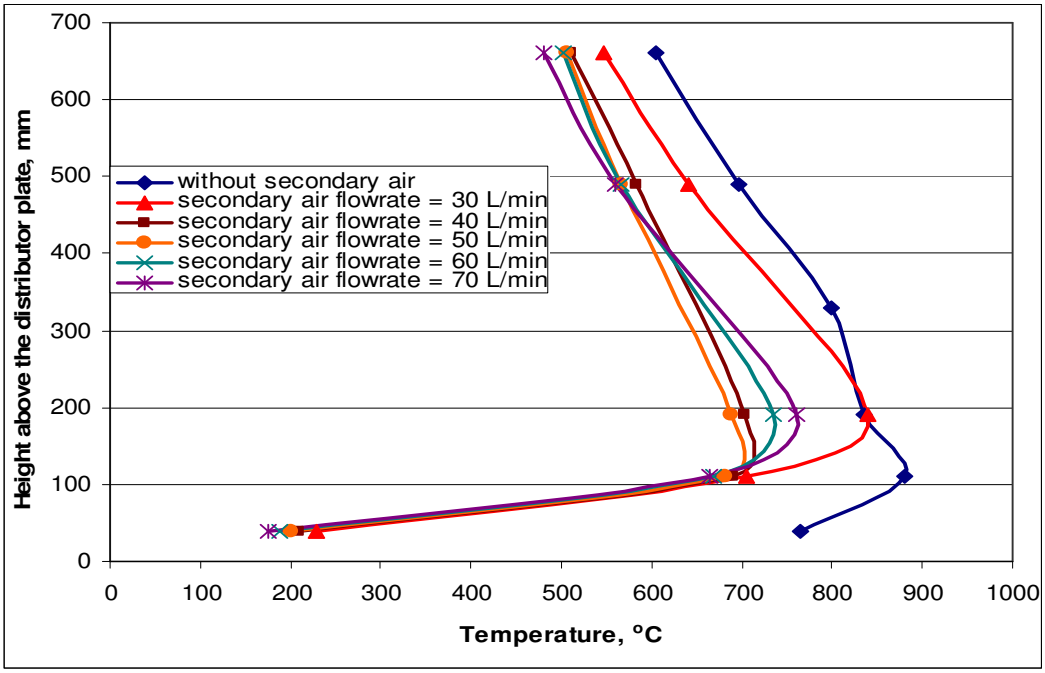

Figure 5.16 Temperature profile along the column for the co-combustion of the fuel mixture containing 25 wt% olive cake with various secondary air flowrates

In Figure 5.17, the temperature profiles for the combustion of coal only with various secondary air flowrates are given. The secondary air given to the system causes a cooling effect on the column. As the flowrate of the secondary air increases, the temperature along the column decreases and gives a receding temperature profile with respect to the case with no secondary air. As a result of this decrease in temperature, CO and C_mH_n emissions increase.

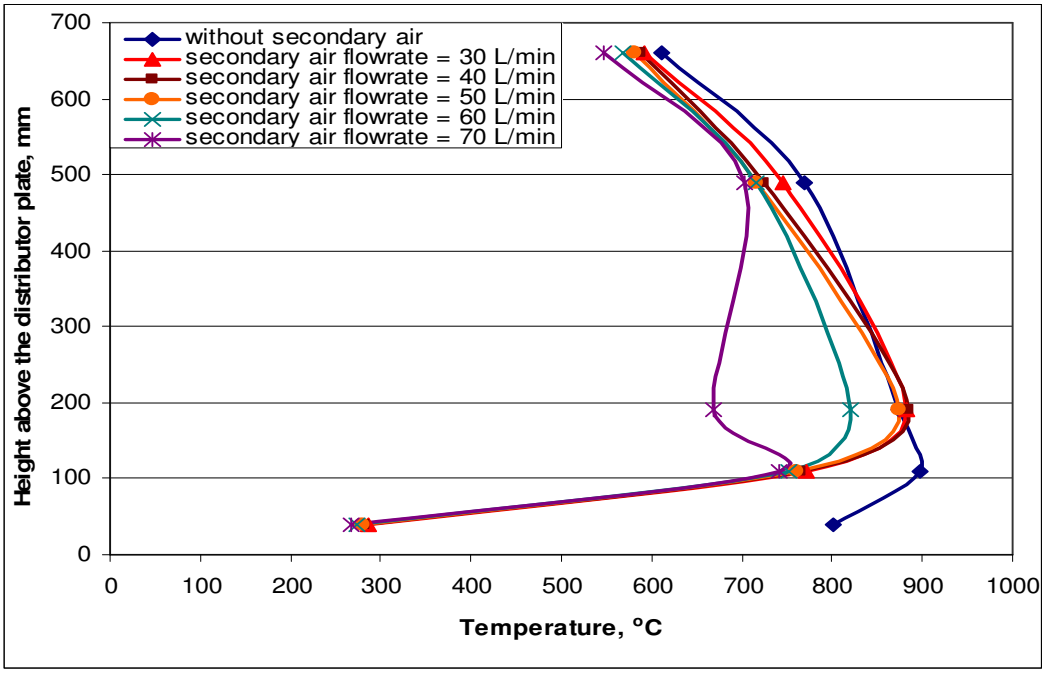

Figure 5.17 Temperature profile along the column for the combustion of coal with various secondary air flowrates

In all combustion tests, with the addition of secondary air to the system, the temperatures measured at TC2 start to decrease and the highest temperatures measured shift to TC3 from TC2. In the combustion tests with secondary air, temperatures measured at TC3 increase as the amount of olive cake in the fuel mixture increases. The highest temperature at TC3 is measured as 953 ^{o}C for the combustion of fuel mixture containing 50 wt% olive cake.

5.3.2. Flue gas emissions

The flue gas emissions for the combustion of olive cake and coal are given in Table 5.6. Concentrations are presented in mg/Nm^3 at normal temperature (273 K) and pressure (1 atm) to be consistent with the regulations and they are based on 6 vol% O_2 as required in the Turkish Regulation for Air Pollution Control from Industrial Sources (RAPCIS, 2004).

Table 5.6 Flue gas emissions for the combustion of olive cake and coal with secondary air (T = 730 ^{o}C)

Run #	S.A. Flowrate L/min	λ -	CO	C_mH_n (as C_3H_8)	NO_x (as NO_2)	SO_2
			(mg/Nm^3 based on 6% O_2)			
r-6	0	**1.05**	**22,959**	**2,975.10**	**552.6**	**0.00**
	30	**1.08**	**11,559**	**1,372**	**342.2**	**0.00**
	40	**1.09**	**10,771**	**512.5**	**261.9**	**0.00**
	50	**1.14**	**10,225**	**338.7**	**237.4**	**0.00**
	60	**1.50**	**8,461**	**143.0**	**421.6**	**0.00**
	70	**1.67**	**7,809**	**197.7**	**534.8**	**0.00**
r-7	0	**1.28**	**250.2**	**22.50**	**1,425**	**2,614**
	30	**1.35**	**101.4**	**22.06**	**1,345**	**3,023**
	40	**1.50**	**109.9**	**26.78**	**1,336**	**3,111**
	50	**1.57**	**112.0**	**30.24**	**1,357**	**3,185**
	60	**1.76**	**117.9**	**34.71**	**1,300**	**3,406**
	70	**1.88**	**125.8**	**37.18**	**1,296**	**4,123**

S.A.= Secondary Air

Effect of secondary air flowrate on flue gas emissions

A. Combustion of olive cake and coal

The results on the effect of secondary air flowrate on flue gas emissions for olive cake and coal combustion for the fuel feeding rate of 10 g/min have been given in this section. The change in CO, C_mH_n, SO_2, and NO_x concentrations due to the combustion of olive cake and coal, with respect to secondary air flowrate are shown in Figure 5.18, Figure 5.19, Figure 5.20, and Figure 5.21, respectively. The secondary air flowrate was changed between 30 and 70 L/min which corresponded to secondary air to total air ratio (SAR) of 0.11 and 0.23, respectively. During these combustions the average temperature of combustor was 730≅20 ^{o}C. U_o at TC2 is found to be 0.64-0.71 m/sec for olive cake combustion and 0.75-0.77 m/sec for coal combustion.

The effect of the secondary air flowrate on **CO emissions** for the combustion of olive cake and coal is given in Figure 5.18. For the combustion of **olive cake** without secondary air, CO emissions are at about 23,000 mg/Nm^3. However, CO emissions significantly decrease with the addition of secondary air. While CO emission is 12,000 mg/Nm^3 for the secondary air flowrate of 30 L/min, it becomes 7,800 mg/Nm^3 when the secondary air flowrate increases to 70 L/min.

For the combustion of **coal** without secondary air, CO emission is 250 mg/Nm^3. However, with the addition of the secondary air, CO emission is measured below 125 mg/Nm^3. With the addition of secondary air to the system, the excess oxygen which is needed for the complete combustion of CO is supplied in the freeboard of the combustor. Thus, some of CO in the flue gas finds a chance to be oxidized in the freeboard. As can be seen from the figure, CO emission for the combustion of coal is much less than that for the combustion of olive cake because of twice as much as VM content of the olive cake than coal.

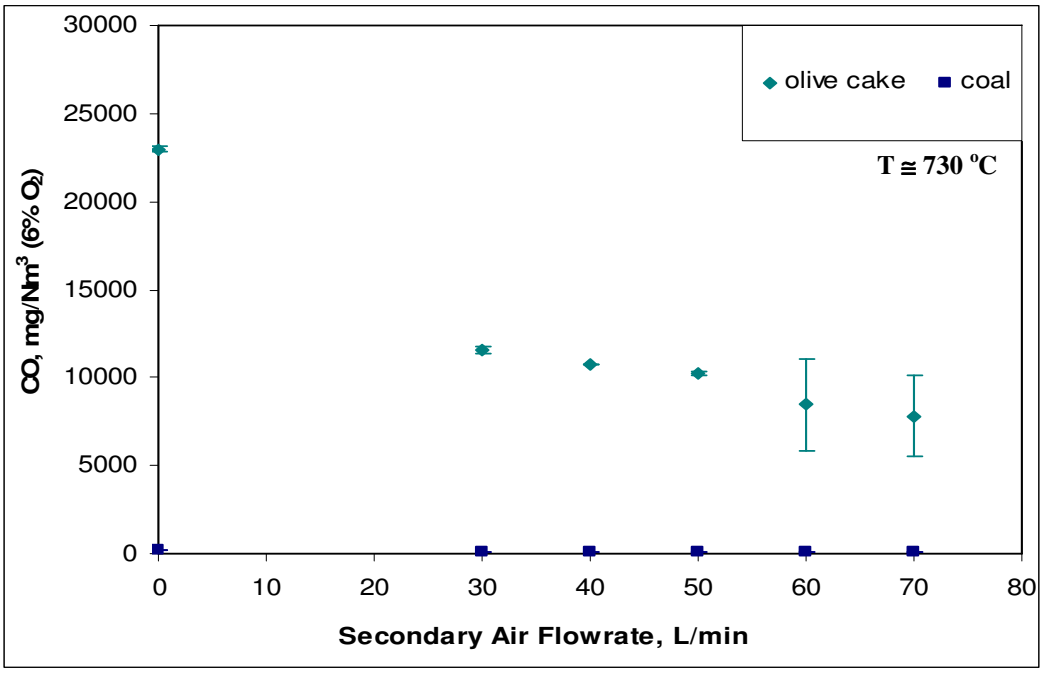

Figure 5.18 Effect of secondary air flowrate on CO emissions for the combustion of olive cake and coal

The effect of the secondary air flowrate on **C_mH_n emissions** for the combustion of olive cake and coal is given in Figure 5.19. For the combustion of **olive cake** without secondary air, C_mH_n emissions are at about 3,000 mg/Nm^3. However, C_mH_n emissions decrease with the addition of secondary air in the freeboard. While C_mH_n emission is at about 1,372 mg/Nm^3 for the secondary air flowrate of 30 L/min, it becomes 143 mg/Nm^3 when secondary air flowrate increases to 60 L/min. The decrease in C_mH_n emissions is more than the decrease in CO emissions at the same flowrate of the secondary air, simply because of the higher reactivity of volatile hydrocarbons with oxygen than CO.

For the combustion of **coal** without secondary air, C_mH_n emission is 22.5 mg/Nm^3 and it increases slightly to 37 mg/Nm^3 for the secondary air of 70 L/min. C_mH_n emissions for the combustion of olive cake are higher than those for the combustion of coal. This is because of the higher volatile matter content of olive cake than coal (about 2 times as much).

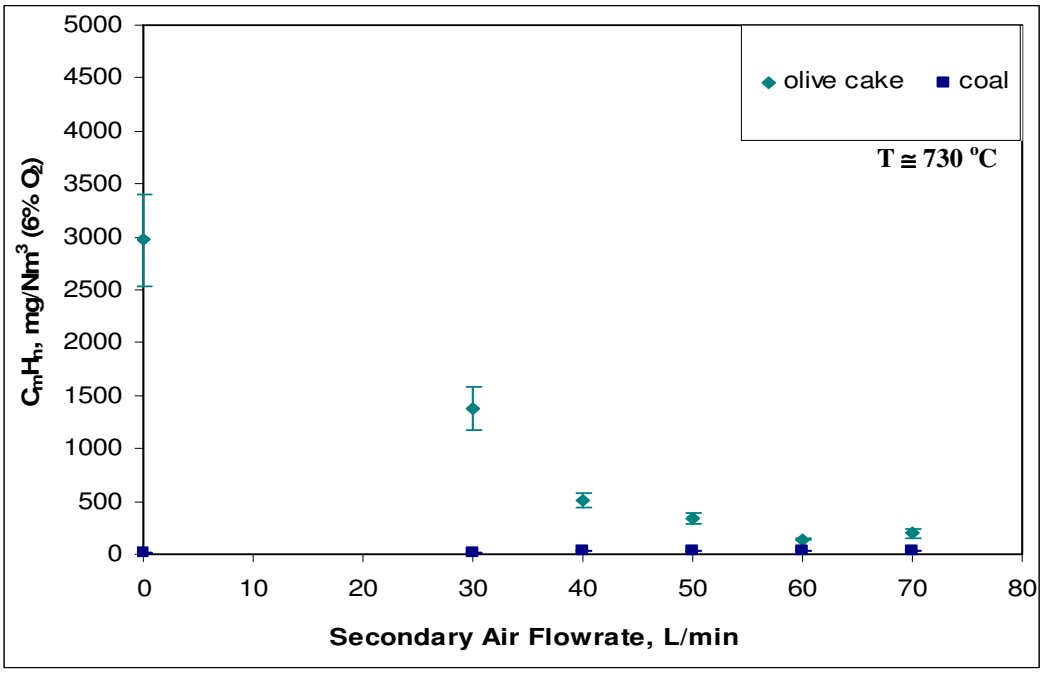

Figure 5.19 Effect of secondary air flowrate on hydrocarbon (C_mH_n) emissions for the combustion of olive cake and coal

The change of **NO_x emissions** with respect to secondary air flowrate is shown in Figure 5.20. For the combustion of **olive cake**, addition of secondary air to the combustor causes NO_x emissions to decrease for the secondary air flowrate of 30-50 L/min. Giving a part of the combustion air to the upper part of the combustor column instead of supplying the entire combustion air through the bottom of the combustor column has a reduction effect on the NO_x emissions, especially for highly volatile fuels. This may be due to the decrease in the temperatures in the bed and freeboard with increasing secondary air flowrates. After 50 L/min, a further increase in NO_x emission is observed. Lowering the temperature and increasing the excess air ratio cause NO_x emissions to increase as shown in Figure 5.20. For the combustion of **coal**, NO_x emissions do not change much with respect to the secondary air flowrate. Addition of secondary air for the coal combustion reduces the NO_x emissions from 1,425 mg/Nm^3 to 1,300 mg/Nm^3. But, this reduction effect is not as significant as that for olive cake combustion.

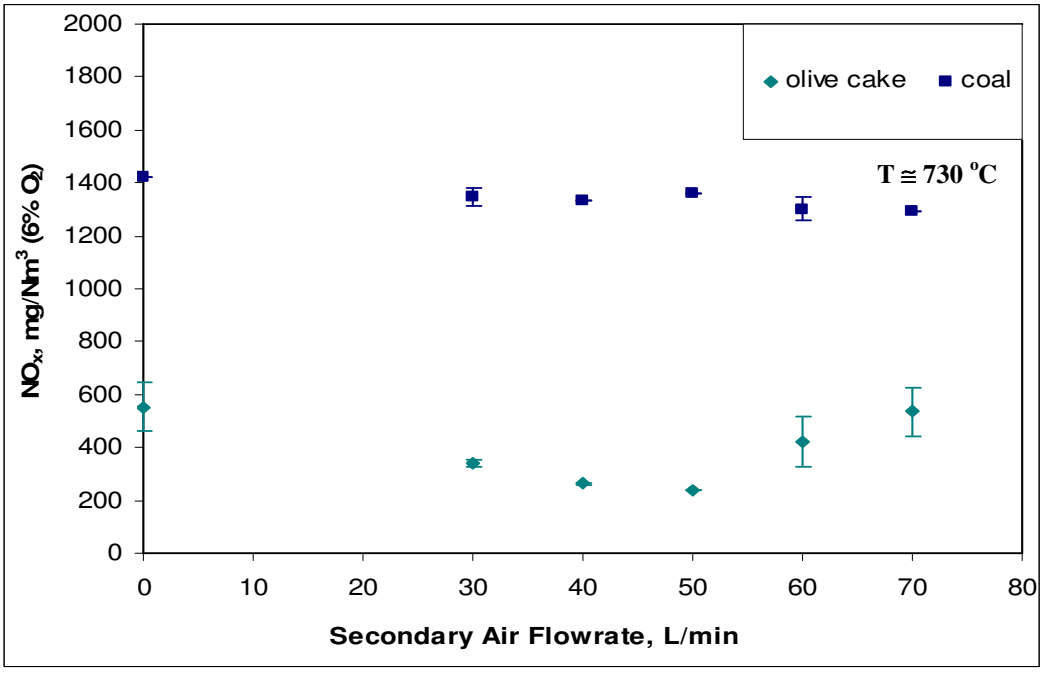

Figure 5.20 Effect of secondary air flowrate on NO_x emissions for the combustion of olive cake and coal

The effect of the secondary air flowrate on **SO_2 emissions** for the combustion of olive cake and coal is given in Figure 5.21. For the combustion of **olive cake**, SO_2 emissions are practically zero because of a very low S content of the olive cake. For the combustion of **coal**, SO_2 emissions increase as the secondary air flowrate increases. SO_2 emissions for the combustion of coal are higher than those for olive cake combustion. This is due to the higher sulfur content of coal than olive cake.

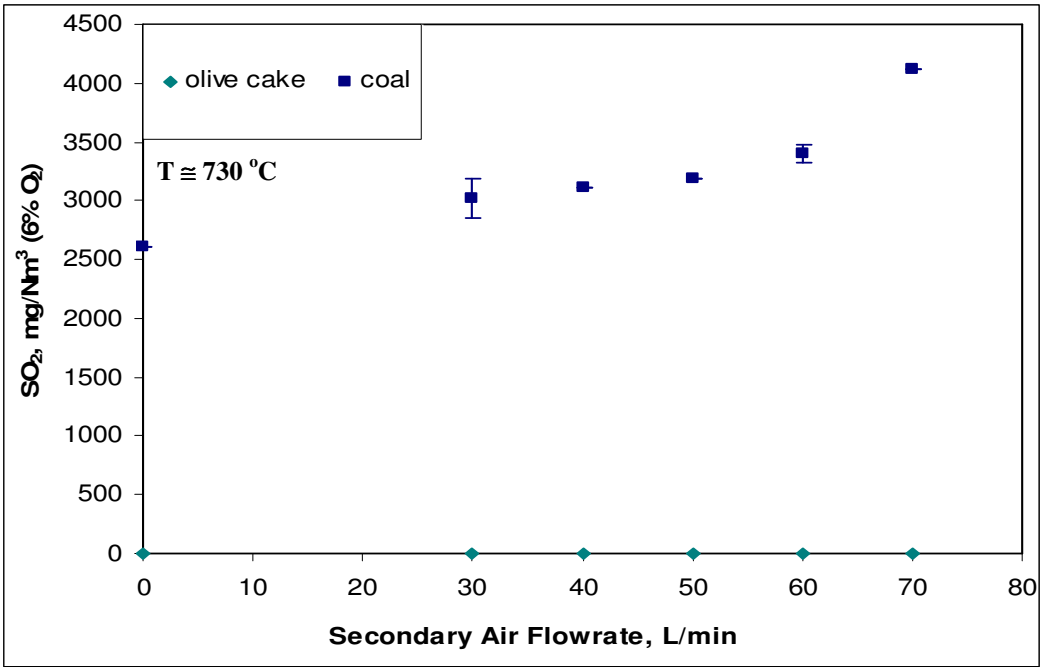

Figure 5.21 Effect of secondary air flowrate on SO_2 emissions for the combustion of olive cake and coal

B. Co-combustion of olive cake with coal

The flue gas emissions for the co-combustion of olive cake with coal for different mixing ratios and secondary air flowrates are given in Table 5.7. Emission values are presented in mg/Nm^3 on the basis of 6% O_2 according to the Turkish Regulation for Air Pollution Control from Industrial Sources (RAPCIS, 2004).

Table 5.7 Flue gas emissions for the co-combustion of olive cake with coal for different mixing ratios with secondary air (T = 730 ^{o}C)

Run #	S.A. Flowrate L/min	λ -	CO	C_mH_n (as C_3H_8)	NO_x (as NO_2)	SO_2
			(mg/Nm^3 based on 6% O_2)			
r-8	0	**1.38**	**7,367**	**734.7**	**636.2**	**2,350**
	30	**1.48**	**931.3**	**19.53**	**1,079**	**1,676**
	40	**1.71**	**303.9**	**9.40**	**1,079**	**1,885**
	50	**1.80**	**614.1**	**11.61**	**1,031**	**2,019**
	60	**1.94**	**357.1**	**16.57**	**1,041**	**2,290**
	70	**2.20**	**442.2**	**17.89**	**1,074**	**2,584**
r-9	0	**1.32**	**10,760**	**413.6**	**988.6**	**1,755**
	30	**1.33**	**6,227**	**148.7**	**836.1**	**1,665**
	40	**1.47**	**1,453**	**28.41**	**939.5**	**1,694**
	50	**1.60**	**425.6**	**5.37**	**1,012**	**1,953**
	60	**1.70**	**602.2**	**5.84**	**1,037**	**1,878**
	70	**1.91**	**375.6**	**4.30**	**1,149**	**1,977**
r-10	0	**1.30**	**14,690**	**2,850**	**516.9**	**56.23**
	30	**1.35**	**6,015**	**469.4**	**460.5**	**165.3**
	40	**1.54**	**3,671**	**399.7**	**474.7**	**223.8**
	50	**1.67**	**1,514**	**134.2**	**516.9**	**256.2**
	60	**1.73**	**930.9**	**115.4**	**568.1**	**300.4**
	70	**1.91**	**771.9**	**65.11**	**577.1**	**325.0**

S.A. = Secondary Air

The change in CO, C_mH_n, SO_2, and NO_x concentrations in the emissions due to co-combustion of olive cake with coal, with respect to secondary air flowrate are shown in Figure 5.22, Figure 5.23, Figure 5.24, and Figure 5.25, respectively. The secondary air flowrate was changed between 30 and 70 L/min which corresponded to the secondary air to total air ratio (SAR) of 0.11 and 0.23, respectively. During these combustions the average temperature of combustor was 690≅50 ^{o}C. U_o at TC2 is found to be 0.66-0.71, 0.69-0.71, and 0.69-0.72 m/sec for the mixture containing 75 wt% olive cake, 50 wt% olive cake, and 25 wt% olive cake, respectively.

The effect of secondary air flowrate on **CO emissions** for the co-combustion of olive cake with coal for predetermined mixing ratios is shown in Figure 5.22. For the combustion of the fuel mixture with 75 wt% olive cake, CO emissions decrease with the addition of secondary air. While the CO emission is at about 14,700 mg/Nm^3 for the combustion of fuel mixture without secondary air, it decreases to 6,000 mg/Nm^3 for the combustion of fuel mixture with secondary air flowrate of 30 L/min. As the secondary air flowrate increases, CO emissions decrease and reach their minimum value of 772 mg/Nm^3 for 70 L/min. The effect of the secondary air flowrate on CO emissions is almost the same as before for the combustion of the fuel mixtures with 50 wt% olive cake and 25 wt% olive cake. For the fuel mixture of 50 wt% olive cake and 50 wt% coal, CO emissions decrease from 10,760 mg/Nm^3 to 376 mg/Nm^3 for 70 L/min; and for the fuel mixture of 25 wt% olive cake and 75 wt% coal, CO emissions decrease from 7,370 mg/Nm^3 to 357 mg/Nm^3 for 60 L/min.

As the amount of olive cake in the fuel mixture increases, the volatile matter content of the mixture also increases. If these volatiles can not find enough oxygen to burn, they leave the combustor as partially oxidized. That is why CO emissions become high in the flue gas. This problem has been solved by supplying secondary air to the freeboard. With this application, CO emissions are drastically reduced due to the combustion of CO with plenty of oxygen in the freeboard.

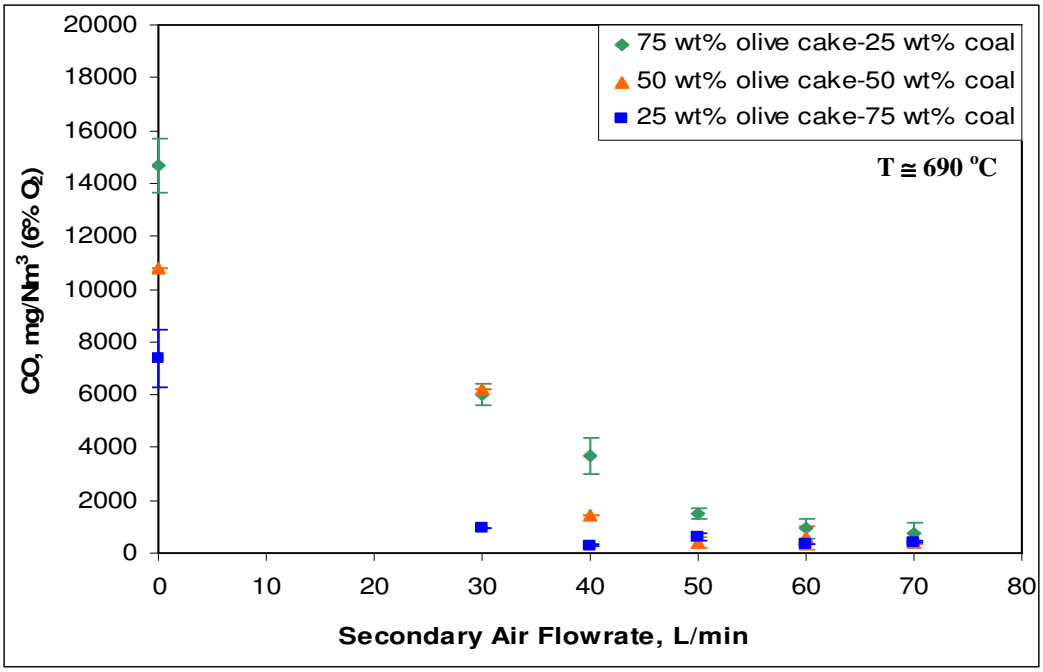

Figure 5.22 Effect of secondary air flowrate on CO emissions for the co-combustion of olive cake with coal for different mixing ratios

The effect of secondary air flowrate on **C_mH_n emissions** for the co-combustion of olive cake with coal for predetermined mixing ratios is shown in Figure 5.23. For the combustion of 75 wt% olive cake-25 wt% coal mixture, C_mH_n emissions decrease from 2,850 mg/Nm^3 to 65 mg/Nm^3 for secondary air flowrate of 70 L/min. This is a drastic reduction. For the combustion of 50 wt% olive cake-50 wt% coal, C_mH_n emissions decrease from 415 mg/Nm^3 down to 5 mg/Nm^3 for the secondary air flowrate of 50-70 L/min. The same explanation given above for CO reduction is relevant here for hydrocarbon reduction in the flue gas.

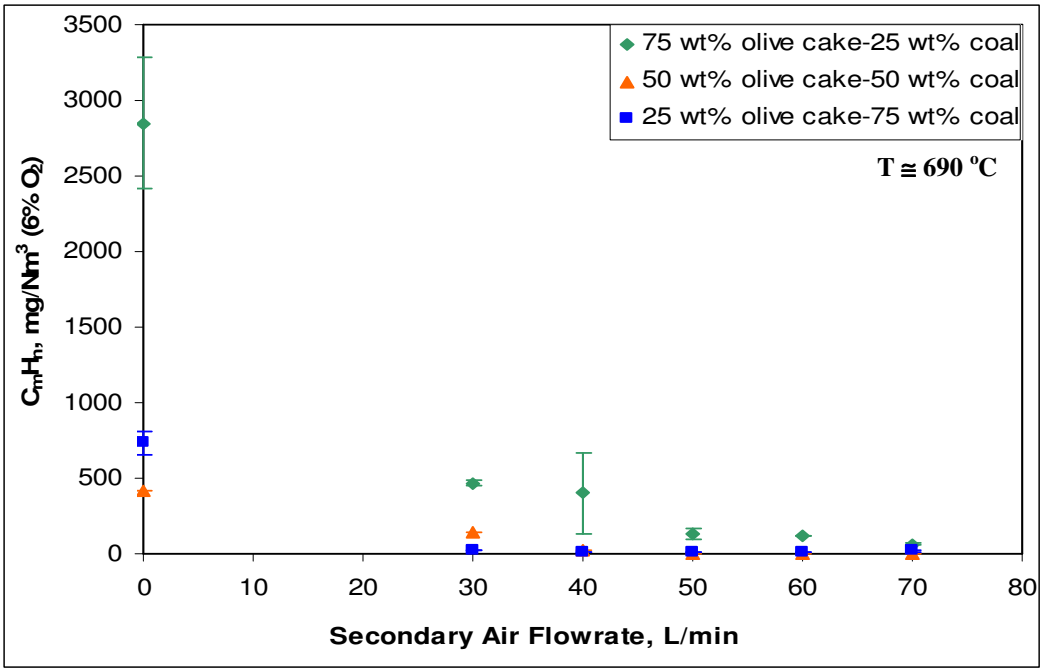

Figure 5.23 Effect of secondary air flowrate on hydrocarbon (C_mH_n) emissions for the co-combustion of olive cake with coal for different mixing ratios

The change of **NO_x emissions** with respect to secondary air flowrate is shown in Figure 5.24. For the combustion of 75 wt% olive cake without secondary air, NO_x emissions are about 520 mg/Nm^3. With the addition of secondary air of 30 L/min, NO_x emissions decrease to 460 mg/Nm^3. A further increase on the secondary air flowrate causes NO_x emissions to increase because of the increasing the temperature of the upper part of the column. Although a decrease on NO_x emissions for the combustion of 50 wt% olive cake with secondary air flowrate of 30 L/min, there is an increase on NO_x emissions for the combustion of 25 wt% olive cake. Secondary air injection has a reduction effect on NO_x emissions for the highly volatile fuels. Thus, giving secondary air to the column does not reduce NO_x emissions for the combustion of 25 wt% olive cake. On the contrary, it causes NO_x emissions to increase. While they are about 635 mg/Nm^3 without secondary air, they change between 1,030 mg/Nm^3 and 1,080 mg/Nm^3 with the various secondary air flowrates.

As the share of the olive cake in the fuel mixture increases, NO_x emissions slightly decrease. NO_x emissions generally result from the nitrogen content of the fuel. In this case, both two fuels have similar nitrogen content. From this point of view, the volatile matter content of the fuel mixture may be responsible for the reduction of NO_x emissions. When the fuel enters the column, the volatiles are rapidly released causing the presence of the hydrocarbon radicals. Hydrocarbon radicals have a reduction effect on NO_x emissions (Armesto et al. 2003).

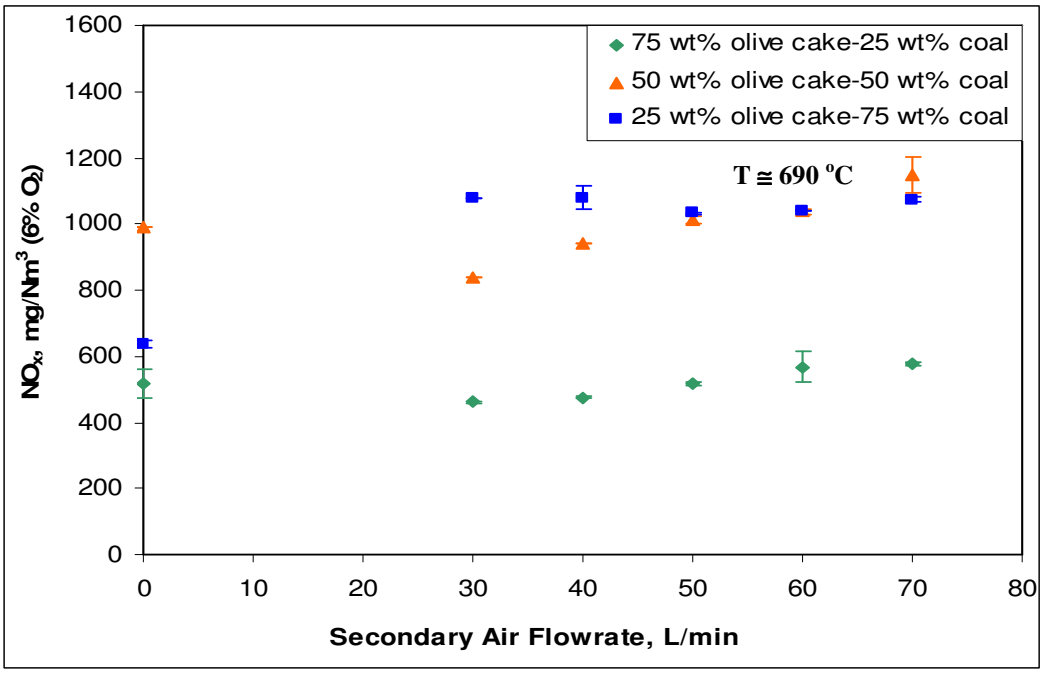

Figure 5.24 Effect of secondary air flowrate on NO_x emissions for the co-combustion of olive cake with coal for different mixing ratios

The effect of the secondary air flowrate on **SO_2 emissions** for the co-combustion of olive cake with coal is given in Figure 5.25. For the combustion of 75 wt% olive cake, SO_2 emissions are about 55 mg/Nm^3 and they increase as the secondary air flowrate increases. For the combustion of 50 wt% olive cake, SO_2 emissions change between 1,665 mg/Nm^3 and 1,975 mg/Nm^3. For the combustion of 25 wt% olive cake, SO_2 emissions increase as the secondary air flowrate

increases. SO_2 emissions increase as the share of coal in the fuel mixture increases. This is due to the higher sulphur content of coal than olive cake.

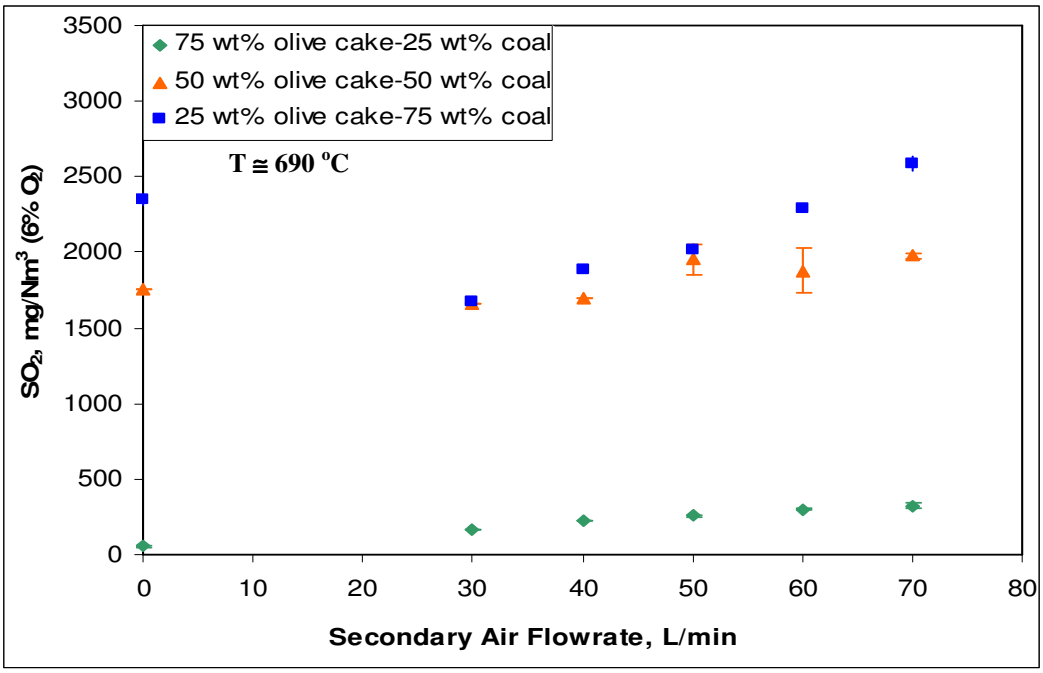

Figure 5.25 Effect of secondary air flowrate on SO_2 emissions for the co-combustion of olive cake with coal for different mixing ratios

Effect of the olive cake share in fuel mixture on emissions

The effect of the share of olive cake in fuel mixture on CO emissions for the co-combustion of olive cake with coal for different mixing ratios with various secondary air flowrates is plotted in Figure 5.26. The share of the olive cake "0" represents the coal combustion and "100" represents the olive cake combustion. As the share of olive cake in fuel mixture increases, CO emissions increase as well for any flowrate of the secondary air. On the other hand as the secondary air flowrate in the freeboard increases, CO emissions decrease as expected. While CO emission is about 150 mg/Nm^3 for the combustion of coal, with the increase in the share of olive cake in the mixture, it becomes about 23,000 mg/Nm^3 without

addition of the secondary air. CO emissions decrease with the addition of secondary air in the freeboard.

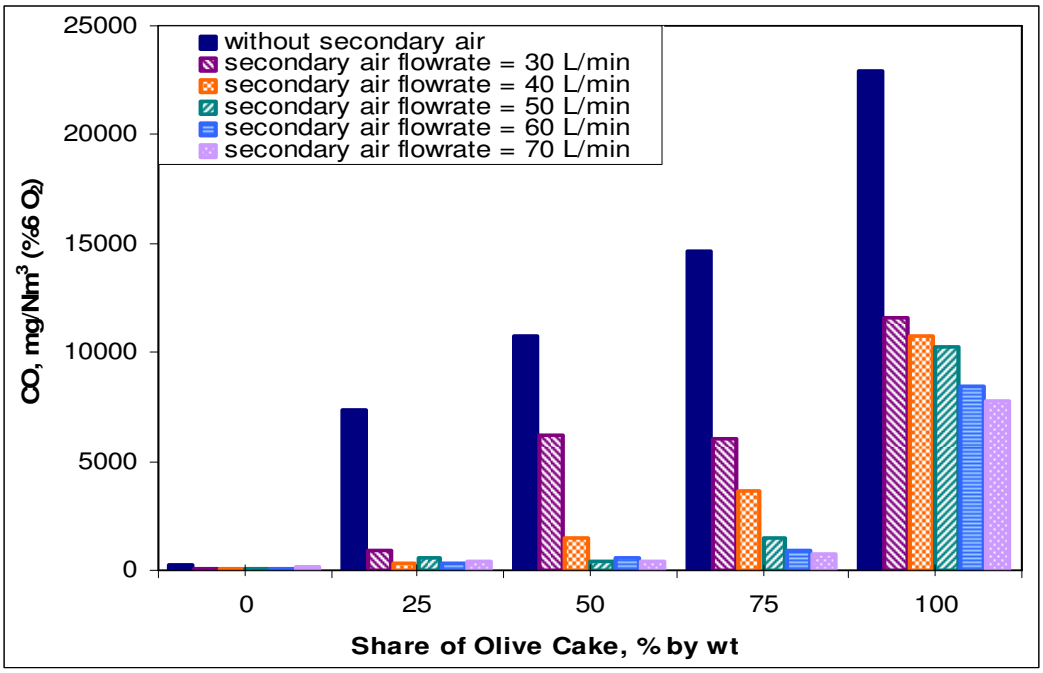

Figure 5.26 Effect of share of olive cake in fuel mixture on CO emissions for the co-combustion of olive cake with coal for different mixing ratios and with various secondary air flowrates

The effect of the share of olive cake in the fuel mixture on C_mH_n emissions is given in Figure 5.27. Like CO emissions, C_mH_n emissions also increase with the increase of the share of olive cake in the fuel mixture. While C_mH_n emission is about 30 mg/Nm^3 for the combustion of coal, with the increase in the share of olive cake in the mixture, it becomes about 2,975 mg/Nm^3 without addition of the secondary air. The increase in C_mH_n emissions is due to the higher volatile matter content of olive cake than that of coal. As the secondary air flowrate in the freeboard increases, C_mH_n emissions decrease as expected due to a better combustion. An unexpected result was obtained for the combustion of the fuel mixture containing 50 wt% olive cake and 50 wt% olive coal and without

secondary air. The hydrocarbon concentration was expected to be higher than 1000 mg/Nm^3, however it was measured as 414 mg/Nm^3. This might be due to an experimental error.

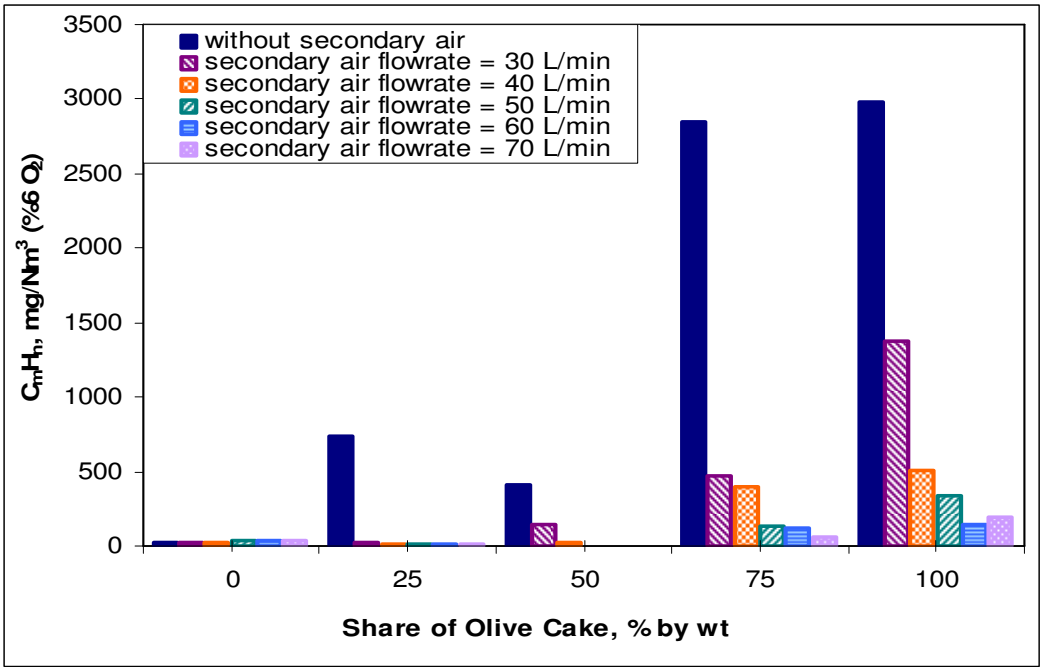

Figure 5.27 Effect of share of olive cake in fuel mixture on C_mH_n emissions for the co-combustion of olive cake with coal for different mixing ratios and with various secondary air flowrates

In the case of NO_x emissions, there is a decreasing trend in NO_x emissions with increase in the share of olive cake in the fuel mixture as can be seen in Figure 5.28. While NO_x emission is about 1,425 mg/Nm^3 for the combustion of coal, it decreases to 552 mg/Nm^3 for the combustion of olive cake. The volatile matter content of olive cake is much higher than coal. Olive cake and coal have similar nitrogen content. Therefore, the increase of volatile matter in the fuel mixture with the increase in the share of the volatile is responsible for the decrease in the NO_x emissions. The fast release of volatiles in the combustor causes the presence of a reducing atmosphere and may be a high level of hydrocarbon radicals. This gives

rise to the reduction of in the amount of NO_x. This result is in agreement with the results found by *Armesto, et al.* (2003). As the secondary air flowrate in the freeboard increases, the reducing atmosphere decreases and this results in increase in NO_x concentration. This is clearly seen in Figure 5.28. An unexpected result was obtained for the combustion of the fuel mixture containing 25 wt% olive cake and 75 wt% coal and without secondary air. The NO_x concentration was expected to be around 1,100 mg/Nm^3. However, it was found to be about 650 mg/Nm^3. This may be due to an experimental error.

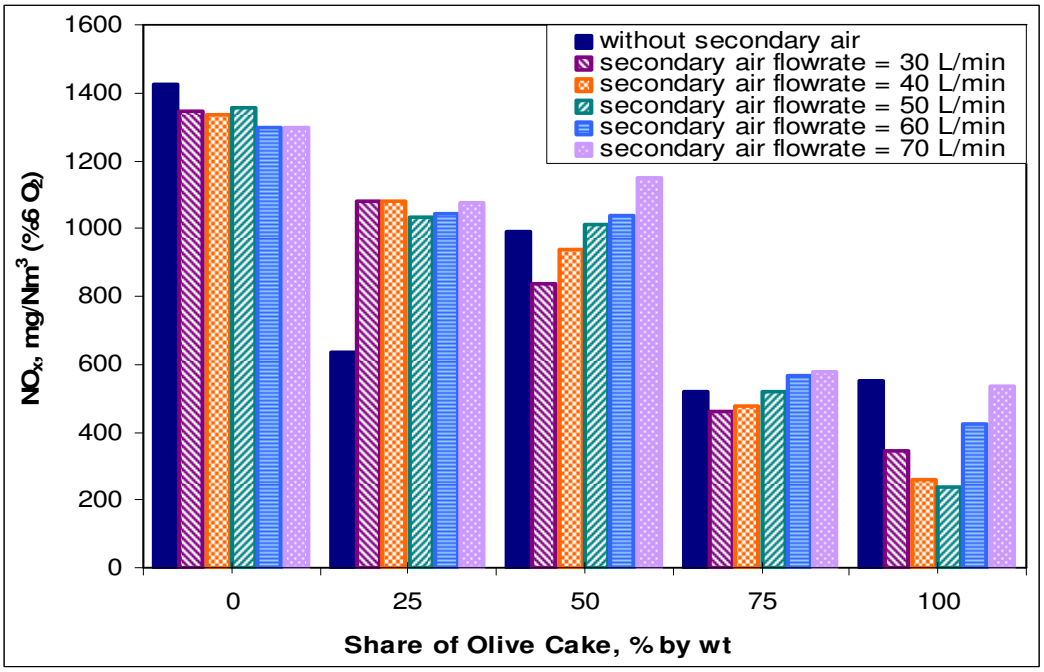

Figure 5.28 Effect of share of olive cake in fuel mixture on NO_x emissions for the co-combustion of olive cake with coal for different mixing ratios and with various secondary air flowrates

While the ratio of fuel-N conversion to NO_x emissions for the combustion of coal-rich mixtures was found to be 0.2-0.33, it was between 0.05 and 0.25 for the combustion of olive cake-rich mixture. As the amount of olive cake in the mixture increases, the ratio of fuel-N conversion to NO_x decreases. This might be

explained that NO_x emissions may be reduced to N_2 because of the high CO concentration in the freeboard region. High concentration of CO may create a reducing environment.

The effect of the share of olive cake in the fuel mixture on SO_2 emissions is given in Figure 5.29. SO_2 emissions decrease with the increase of the share of olive cake in fuel mixture. While SO_2 emission is about 4,123 mg/Nm^3 for the combustion of coal, with the increase in the share of olive cake in the mixture, it becomes practically zero for the combustion of olive cake. This is of course due to the negligible S content of olive cake as compared to coal. As the flowrate of secondary air increases, SO_2 emissions slightly increase. This can be explained with better combustion achieved in the freeboard region.

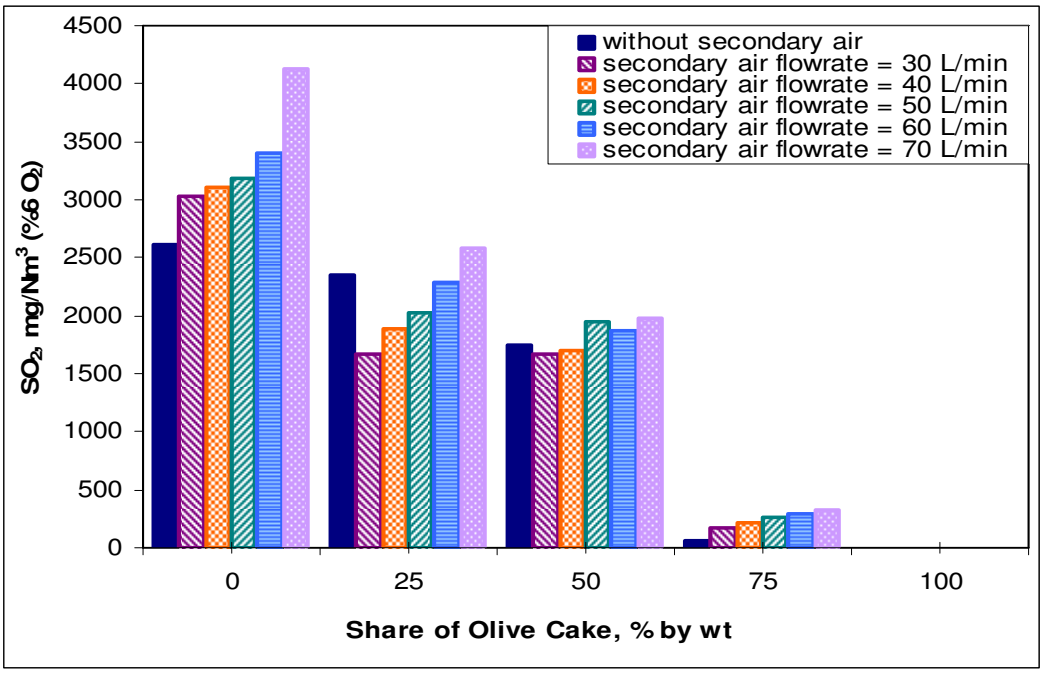

Figure 5.29 Effect of share of olive cake in fuel mixture on SO_2 emissions for the co-combustion of olive cake with coal for different mixing ratios and with various secondary air flowrates

5.3.3. Combustion efficiencies

Combustion efficiencies for the co-combustion of olive cake with coal for different mixing ratios are given in Table 5.8. The average combustion efficiency for olive cake has been found to be 83.6% without secondary air and 96.0% with secondary air of 70 L/min. For the combustion of coal alone, the efficiencies are 99.7% and 99.8% without and with secondary air, respectively.

As it is observed from the table, the combustion efficiency decreases as the share of olive cake in the fuel mixture increases which is due to the escape of unburnt CO and C_mH_n in the combustion gases. On the other hand, as the secondary air flowrate increases, there is a considerable improvement in the overall combustion efficiency simply because of oxygen supply to the freeboard to oxide the incomplete combustion products.

Table 5.8 Combustion efficiencies for the combustion and co-combustion of olive cake and coal for different mixing ratios with secondary air

Run #	Solid fuel	Combustion Efficiency, η (%)					
		Secondary Air Flowrate, L/min					
		0	30	40	50	60	70
r-6	Olive Cake (O.C.) – secondary air	83.6	91.8	93.9	94.6	95.8	96.1
r-7	Coal (C) - secondary air	99.7	99.8	99.8	99.7	99.7	99.7
r-8	Olive Cake 25 wt% + Coal 75 wt% - secondary air	95.4	99.5	99.7	99.6	99.7	99.7
r-9	Olive Cake 50 wt% + Coal 50 wt% - secondary air	94.5	97.0	99.3	99.8	99.7	99.8
r-10	Olive Cake 75 wt% + Coal 25 wt% - secondary air	87.9	96.4	97.6	99.0	99.3	99.5

The combustion efficiencies calculated for the combustion of olive cake and coal are plotted with respect to secondary air flowrate in Figure 5.30. For the combustion of olive cake, combustion efficiency changes between 83.6% and 96.1%. Combustion losses due to the unburnt carbon in the bed ($L_{C,\ bed}$) and combustion losses due to the unburnt carbon in the cyclone ($L_{C,\ cyclone}$) do not exceed 0.04% and 0.2%, respectively. The main contributor for the combustion losses is the CO and C_mH_n emissions. As the CO and C_mH_n emissions increase, L_{CO} and L_{CH} also increase resulting in low overall combustion efficiency. While L_{CO} is 10.2% for the combustion of olive cake without secondary air, it decreases to 3.3% for the combustion of olive cake with secondary air flowrate of 70 L/min. For the combustion of coal, combustion efficiency changes between 99.7% and 99.8%. Addition of secondary air does not affect the combustion efficiency. The contribution of the L_{CO} to the combustion losses is between 0.05% and 0.1%. The other contributor to the combustion losses is $L_{C,\ cyclone}$ which does not exceed 0.1%. As can be seen from the table, the overall combustion efficiency for olive cake is lower than that for coal. This is mainly due to the high CO and C_mH_n emissions during the combustion of olive cake. The heating value of olive cake is lost as CO and C_mH_n emissions which are incomplete combustion products.

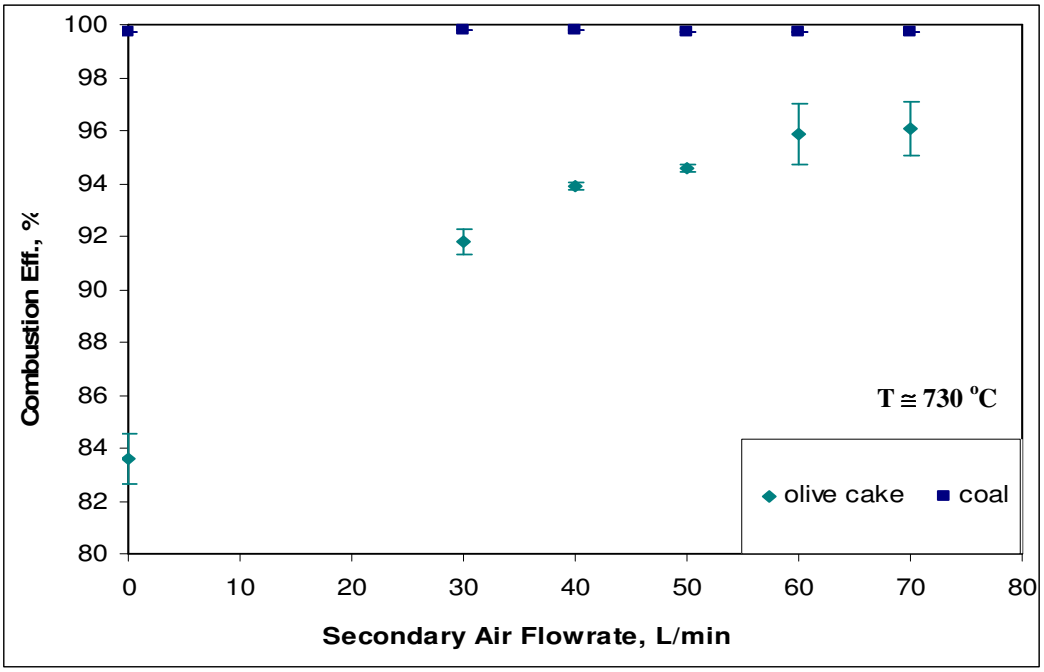

Figure 5.30 Effect of secondary air flowrate on combustion efficiency for the combustion of olive cake and coal

The combustion efficiencies for the combustion of olive cake and coal are plotted with respect to secondary air flowrate in Figure 5.31. For the 75 wt% olive cake, combustion efficiency changes from 87.9% to 99.5% as the secondary air flowrate increases. For the 50 wt% olive cake, combustion efficiency increases as the secondary air flowrate increases. For the combustion of 25 wt% olive cake, combustion efficiency is 95.4% without secondary air. With the addition of secondary air, it rapidly increases to 99.5% for secondary air flowrate of 30 L/min, and it almost stays constant as the secondary air flowrate increases. For the combustion of three fuel mixtures, combustion losses due to the unburnt carbon in the bed ($L_{C,\ bed}$) and combustion losses due to the unburnt carbon in the cyclone ($L_{C,\ cyclone}$) do not exceed 0.1%. The main contributor to the combustion losses is the CO and hydrocarbon emissions. As the CO emissions and C_mH_n emissions increase, L_{CO} and L_{CH} also increase resulting on low overall combustion efficiency. As the share of olive cake in fuel mixture decreases, CO and C_mH_n emissions decrease leading the combustion efficiency to increase.

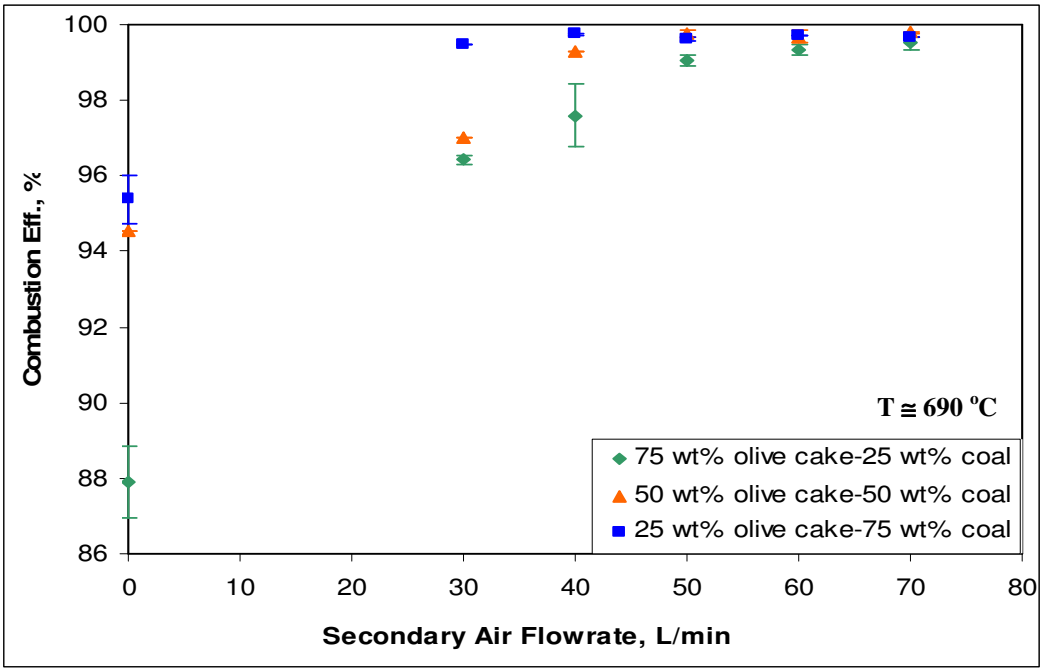

Figure 5.31 Effect of secondary air flowrate on combustion efficiency for the co-combustion of olive cake with coal for different mixing ratios

Effect of the olive cake share in fuel mixture on combustion efficiency

The effect of the share of olive cake in fuel mixture on combustion efficiency for the co-combustion of olive cake with coal for different mixing ratios with various secondary air flowrates is plotted in Figure 5.32. As the share of olive cake in fuel mixture increases, combustion efficiency decreases for any condition of secondary air feeding. While combustion efficiency is around 99.7-99.8% for the combustion of coal, with the increase on share of olive cake in mixture, for the combustion of olive cake, it changes between 96.1% with secondary air flowrate of 70 L/min and 83.6% without secondary air. Minimum CO emissions are achieved at 70 L/min flowrate of secondary air.

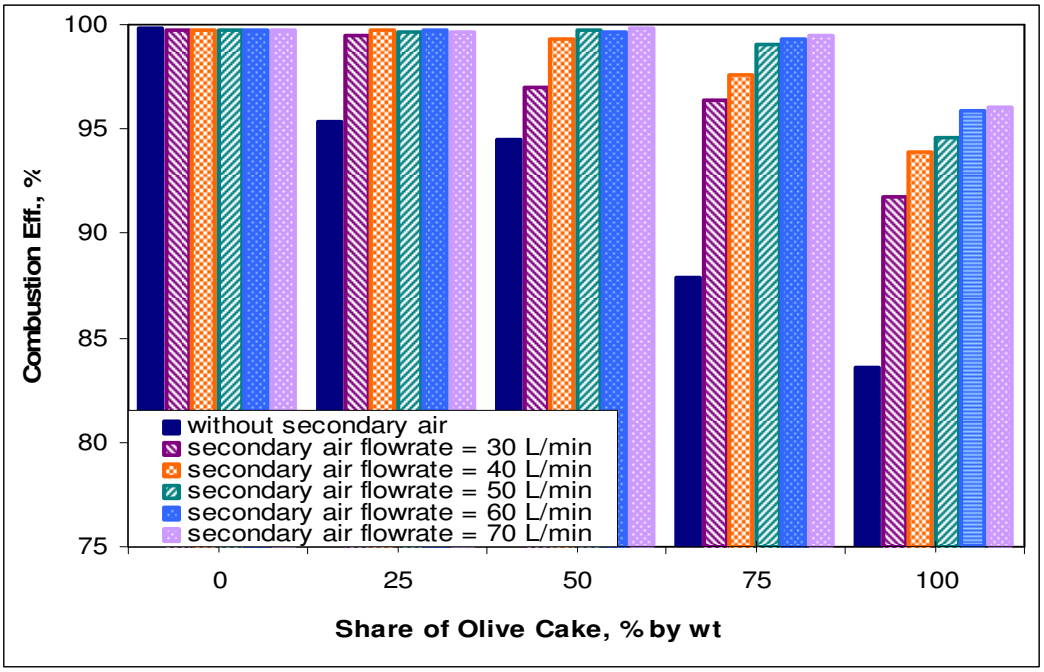

Figure 5.32 Effect of share of olive cake in fuel mixture on combustion efficiency for the co-combustion of olive cake with coal by different mixing ratios with various secondary air flowrates

5.4. Comparison of the Emissions with Standards and Previous Studies

The Turkish Regulation for Air Pollution Control from Industrial Sources (RAPCIS) of 2004 declares that the olive oil production facilities and other burning facilities (energy production facilities, cement and lime factories, etc.) which use biomass (olive cake, sunflower shell, cotton seed and etc.) as a fuel and which have the nominal heat power capacity higher than 500 kW must have burning system with a secondary air feed. From this point of view, the emissions obtained for the combustion tests with secondary air are compared to the emission limits of the Turkish Regulation, EU Directive-2001/80/EC and previous studies.

5.4.1. Comparison of emissions with limit values

The limit values of SO_2 and CO emissions are 200 mg/Nm^3 and 460 mg/Nm^3, respectively, for the combustion facilities using biomass as fuel in RAPCIS. However, there is no limit value for NO_x emissions for the facilities having a nominal power capacity less than 50 MW. The limit value of NO emission is given as 400 mg/Nm^3 for the facilities having nominal power capacity higher than 50 MW. This value corresponds to 645 mg/Nm^3 NO_x expressed as NO_2. According to the EU-Directive/80/EC, the limit values for SO_2 and NO_x emissions for the facilities having a thermal input greater than 50 MW_{th} and less than 100 MW_{th} are given as 200 mg/Nm^3 and 400 mg/Nm^3, respectively. The comparison of the emissions found in this study with the limit values of RAPCIS is given in Table 5.9.

Table 5.9 Comparison of emissions with limit values of Turkish Regulation

Run #	**Solid fuel**	**SO_2**	**NO_x as NO_2**	**CO**
		200 mg/Nm^3	**645 mg/Nm^3**	**460 mg/Nm^3**
Without Secondary Air				
r-1	Olive Cake (O.C.)	√		
r-5	Olive Cake 75 wt% + Coal 25 wt%	√		
r-4	Olive Cake 50 wt% + Coal 50 wt%			
r-3	Olive Cake 25 wt% + Coal 75 wt%			
r-2	Coal (C)			√(λ=1.3-1.45)
With Secondary Air				
r-6	Olive Cake (O.C.)	√	√	
r-10	Olive Cake 75 wt% + Coal 25 wt%		√	
r-9	Olive Cake 50 wt% + Coal 50 wt%			√(SA>40L/min)
r-8	Olive Cake 25 wt% + Coal 75 wt%			√(SA>30L/min)
r-7	Coal (C)			√

When SO_2 emissions in this study are compared with the standards for the combustion of olive cake with or without secondary air, the emissions are below the limit values because sulfur content of the olive cake is very low. Besides, SO_2 emissions obtained from the co-combustion of fuel mixture containing 75 wt% olive cake without secondary air are below the emission limits. But, high SO_2 emission is not a big problem for the other co-combustion tests for different mixing ratios. SO_2 emissions can be easily decreased by addition of limestone to the combustor.

All combustion and co-combustion tests without secondary air have the NO_x emissions above the limits both for the Turkish and EU standards. Although only NO_x emissions for the co-combustion of mixture with 75 wt% olive cake with secondary air are below the limit value of the Turkish Regulation, NO_x emissions for the combustion of olive cake only with secondary air are below the limits of Turkish and EU standards.

All combustion and co-combustion tests without secondary air except the combustion of coal with λ values of 1.3-1.45 have higher CO emissions than the limits stated in the above mentioned regulation. For the tests conducted with secondary air, CO emissions are below the limits when coal is burned. CO emissions are also below the limits for the co-combustion of the mixture containing 25 wt% olive cake with secondary air flowrate greater than 30 L/min and for the co-combustion of the mixture containing 50 wt% olive cake with secondary air flowrate greater than 40 L/min.

5.4.2. Comparison of results with literature

The co-combustion of coal and olive oil industry residues (foot cake) in a bubbling fluidized bed (BFB) was studied by *Armesto et al.* (2003). They investigated the effect of the amount of foot cake in the fuel mixture on NO_x and SO_2 emissions. The share of foot cake in the fuel mixture was 10, 15, 20, and 25% by weight. For comparison purposes, the fuel mixture with 25 wt% foot cake was

selected and the SO_2 emissions were found about 900 mg/Nm^3 for this mixture. SO_2 emissions are found as 2,350-2,650 mg/Nm^3 for the co-combustion of fuel mixture containing 25 wt% olive cake without secondary air. When secondary air is fed, SO_2 decrease a little amount and change between 1,675-2,585 mg/Nm^3. The lower SO_2 emissions in their study can be explained by the lower sulfur content of the fuel mixture used in their study. The sulfur content of the lignite coal (Spanish) used in the study was 0.8 wt% on dry basis. The sulfur content of the lignite coal (Tunçbilek) used in our study is 2.1 wt% on dry basis. The sulfur content of biomass is similar for both studies. Additionally, they also explained that the higher alkalies and alkaline earths (especially calcium and potassium) in biomass ash have a decreasing effect on SO_2 emissions. CaO and K_2O content of the olive cake ash is less than that of foot cake ash. For the fuel mixture containing 25% foot cake, the fuel-N to NO_x conversion was about 10 %. However, the fuel-N to NO_x conversion is calculated as 12-30% for combustion of fuel mixtures both with or without secondary air in this study. The nitrogen content (1.1 wt%) of the foot cake used in *Armesto et al.* (2003) is less than the nitrogen content of olive cake (1.3 wt%). This can be a reason for the higher conversion ratio between fuel-N and NO_x obtained in this study.

The combustion characteristics of olive cake and also comparison of these characteristics with coal combustion was studied by *Topal et al.* (2003) in a circulating fluidized bed (CFB). The olive cake and coal used in both studies have the same physical and chemical characteristics. When only coal was burned with the excess air ratio of 1.25-2.12, the SO_2 emissions changed between 2,800 and 2,977 mg/Nm^3. However, for the coal combustion conducted without secondary air in this study for λ of 1.28-2.24, SO_2 emissions change between 2,614 and 3,308 mg/Nm^3. The results are close. SO_2 emissions obtained in this study are higher than their results. However, when olive cake was burned alone, SO_2 emission is practically zero for both studies because of very low sulfur content of olive cake.

NO_x emissions were found as 204-292 mg/Nm^3 for the combustion of coal in their study. Both NO_x emissions (541-1,700 mg/Nm^3) without secondary air and NO_x emissions (1,295-1,345 mg/Nm^3) with secondary air are higher than the results obtained in their study. When NO_x emissions are compared for the combustion of olive cake, the results obtained in their study are lower than the results obtained in this study. While NO_x emissions are found as 553-1,029 for the olive cake combustion without secondary air, the emissions decrease to the range of 237-534 mg/Nm^3 with the additional of secondary air.

When C_mH_n emissions are compared for the combustion of coal, C_mH_n emissions (53-428 mg/Nm^3) found in *Topal et al.* (2003) are higher than the emissions found in this study both for the coal combustion with and without secondary air. This may be due to the circulation regime of the CFB (more escape of the hydrocarbons). In this study, C_mH_n emissions are found as 22.5-145 mg/Nm^3 for the coal combustion without secondary air and they are found as 22-37 mg/Nm^3 for the coal combustion with secondary air. When olive cake is burned without secondary air, C_mH_n emissions are found as 1,713-2,975 mg/Nm^3. When secondary air is used, C_mH_n emissions significantly decrease and are found as 143-1,372 mg/Nm^3. The decrease is explained by the better combustion of hydrocarbons in freeboard with the additional of extra oxygen to the freeboard. C_mH_n emissions (62-3,376 mg/Nm^3) found in *Topal et al.* (2003) study are higher than the results found in this study. A decrease in C_mH_n emissions is observed when the secondary air is used in this study. This decrease is relevant for CO emissions both for coal and olive cake combustion. When coal is burned without secondary air, CO emissions change between 250-2450 mg/Nm^3. With the addition of secondary air, CO concentration decreases down to 110-125 mg/Nm^3. Although CO emissions obtained without secondary air is higher than those (197-929 mg/Nm^3) in Topal's study, a decrease in CO emissions can be obtained by the process of addition of secondary air. For the combustion of olive cake, while CO emission is 23,000 mg/Nm^3 without secondary air, emissions decrease to 7,810-11,560 mg/Nm^3 by secondary air injection. Both CO emissions found in this study are higher than those (91-6,253 mg/Nm^3) in Topal's. CO emissions found in CFB

are lower than those found in bubbling fluidized bed because of the circulation of char and higher residence time of the char particles in CFB.

CHAPTER 6

CONCLUSIONS

The results of this study have shown that it is possible to burn olive cake in a bubbling fluidized bed combustor with a combustion efficiency of 83.6-90.1%. It is seen that the major indicators responsible for the decrease in the combustion efficiency are combustion losses due to the formation of CO and hydrocarbons, leaving the system unburnt. Also a combustion loss due to the unburnt carbon escaping from the system and collected in the cyclone as fly ash is another indicator to decrease combustion efficiency. The efficiency of coal combustion under the same conditions has been found to be 98.4-99.7%. Co-combustion of olive cake with coal at different mixing ratios from 25 wt% olive cake to 75 wt% olive cake is also possible with efficiencies in a range of 83.6% and 99.7%. As the olive cake content in the fuel mixture increases, a decrease in the overall combustion efficiency is observed.

The temperature profiles measured along the combustor column have shown that the olive cake particles release their volatile matter due to the rapid heating after they enter the combustor. Volatiles mostly burn in the freeboard of the combustor. Therefore, the maximum temperatures are seen in the freeboard rather than in the bed. Since the density of olive cake particles is smaller than the bed material, segregation occurs in the bed. The location of the maximum temperature in the freeboard shifts to the upper part of the column, as the volatile matter content in the fuel mixture increases, except in the case of 50 wt% olive cake-50 wt% coal mixture.

During the combustion of olive cake and coal, the excess air ratio is important for the concentrations of pollutants in the flue gas. As the excess air ratio increases, CO and hydrocarbon emissions first decrease and after a certain ratio (λ about 1.6), emissions start to increase. For the case of co-combustion of olive cake with coal, CO and hydrocarbon emissions decrease with excess air ratio and the best combination where CO and hydrocarbon emissions are minimized have been found to be a 50 wt% olive cake-50 wt% coal mixture.

Since the major indicators showing the decrease in the combustion efficiency have been found to be CO and hydrocarbons in the flue gas, secondary air injection into the freeboard has been a useful solution to decrease the CO and hydrocarbon emissions and to increase the combustion efficiency.

As the amount of olive cake in the fuel mixture increases, SO_2 emissions decrease because of the very low sulfur content of olive cake. SO_2 emission for the combustion of coal is as high as 2,500-4,100 mg/Nm^3, whereas it is practically zero for olive cake combustion with or without secondary air, and almost zero for the co-combustion of coal with 75 wt% olive cake. SO_2 emissions for the other combustion and co-combustion tests are above the SO_2 limits (200 mg/Nm^3) determined by the RAPCIS.

Emissions of NO_x for the combustion of olive cake, coal and olive cake-coal mixtures are found to increase with increase in the excess air ratio. However, when olive cake and coal mixture is co-combusted, lower NO_x emissions are obtained as the olive cake content of the mixture increases. Addition of secondary air during the combustion of olive cake-coal mixtures is found to increase the NO_x emissions slightly. It can be seen that only the combustion of olive cake and co-combustion of the mixture containing 75 wt% olive cake with secondary air injection have NO_x emissions below the limits of the regulation (645 mg/Nm^3 NO_x as NO_2).

In order to achieve high combustion efficiency, coal combustion with superficial gas velocity of 0.75-0.77 m/sec and secondary air flowrate of 30-70 L/min seems best solution because of the low CO and hydrocarbon emissions obtained in the flue gas. For the setup used in this study, the optimum operating conditions with respect to NO_x and SO_2 emissions were found as 1.2 for excess air ratio, 50 L/min for secondary air flowrate, and 0.64 m/sec for superficial gas velocity during the combustion of olive cake. Furthermore, co-combustion of olive cake with 25 wt% coal for excess air ratio of 1.7-1.9, secondary air flowrate of 50-70 L/min, and superficial gas velocity of 0.66-0.71 m/sec can be an alternative solution both to obtain combustion efficiency higher than 99%, and to obtain NO_x and SO_2 emissions which are below the limits.

Olive cake is an agricultural waste and a fuel which has an energy potential. The results of this study suggests that olive cake can be used as a fuel in a bubbling fluidized bed combustor system due to both its high heating value and its low sulfur content. Olive cake has a potential to be utilized to obtain cleaner energy for the small and medium scale industries (SMEs) using fluidized bed combustor systems instead of conventional systems.

CHAPTER 7

RECOMMENDATIONS FOR FURTHER STUDIES

In order to achieve more efficient combustion and less pollutant concentrations, some recommendations can be done for further studies. These recommendations can be listed as follows:

- In order to decrease CO and hydrocarbon emissions and increase combustion efficiency;
    - A circulating fluidized bed combustor can be used instead of a bubbling fluidized bed combustor.
    - Diameter of the column can be increased.
    - The system can be operated at lower superficial gas velocity (u_o).

  The following two modifications of the experimental setup will be helpful to increase the residence time of the CO and hydrocarbon emissions in the combustor column.
    - The position of the fuel feeding can be changed. The fuel can be fed to the combustor from the bottom of the column. This modification can be helpful for the good mixing of the fuel particles with bed material, increasing the temperature of the bed material as well as the temperature of entire column.
    - The fluidization air can be given to the combustor column as pre-heated. This can be helpful in order to minimize the cooling effect of the fluidization air on bed material.

- Because of the density difference between the olive cake and sand particles, segregation occurs during the combustion of olive cake. In order to eliminate this problem, different materials having lower density than sand can be used as bed materials. These materials can be pumice stone or the ash remained after the combustion of coal.

REFERENCES

Abu-Quadis M., 1996. Fluidized bed combustion for energy production from olive cake, *Energy*, 21, 173-178.

Alkhamis T.M., Kablan M.M., 1999a. Olive cake as an energy source and catalyst for oil shale production of energy and its impact on the environment, *Energy Conversion & Management*, 40, 1863-1870.

Alkhamis T.M., Kablan M.M., 1999b. A process for producing carbonaceous matter from tar sand, oil shale and olive cake, *Energy*, 24, 873-881.

Armesto L., et. al, 2003. Co-combustion of coal and olive oil industry residues in fluidized bed, *Fuel*, 82, 993-1000.

Atımtay T. A., 1987. "Combustion of volatile matter in fluidized beds", *Industrial and Engineering Chemistry Research*, 26, 452-456,

Atımtay T. A., Topal H., 2004. Co-combustion of olive cake with lignite coal in a circulating fluidized bed, *Fuel*, 83, 859-867.

Balat M., 2005. Use of biomass sources for energy in Turkey and a view to biomass potential, *Biomass and Bioenergy*, 29, 32-41.

Basu P., Fraser A.S., 1991. Circulating Fluidized Bed Boilers, Design and Operation, Butterworths-Heinemann-Reed Publishing.

Chem 347 (Chemical Engineering 347), 1999. Lecture notes: Hydrodynamics of Fluidized Beds. Department of Chemical Engineering, Princeton University.

Cliffe K.R., Patumsawad S., 2001. Co-combustion of waste from olive oil production with coal in a fluidised bed, *Waste Management*, 21, 49-53.

Crane Company, 1988. Flow of fluids through valves, fittings, and pipes. Technical Paper, No 410 (TP410).

Chemical Rubber Company (CRC), 1984. CRC Handbook of Chemistry and Physics. Weast, Robert C., editor. 65th edition. CRC Press, Inc., Florida, USA.

Desroches-Ducarne E., Eric M., Gerard M., Lucien D., 1998. Co-combustion of coal and municipal solid waste in a circulating fluidized bed, *Fuel*, 77, 1311-1315.

Directive 2001/80/EC of the European Parliament and of the Council of 23 October 2001 on the limitation of emissions of certain pollutants into the air from large combustion plants.

Exploitation of Agricultural Residues in Turkey-Life Training Course Technical Notes, 2005. Ankara, Turkey.

Food and Agriculture Organization of the United Nations (FAO), 2005. Agricultural Data, http://faostat.fao.org/faostat/collections?subset=agriculture, accessed on December, 2005.

Gayan P., et. al., 2004. Circulating fluidised bed co-combustion of coal and biomass, *Fuel*, 83, 277-286.

Howard J.R., 1989. Fluidized Bed Technology: Principles and Applications, Adam Hilger, England.

IOR (Institute of Olive Researches), 2005. Zeytinyağı Teknolojisi (in Turkish), http://www.zae.gov.tr/zeytinyagi/7.asp, accessed on December, 2005.

Kaygusuz K., 2002. Sustainable development of hydropower and biomass energy in Turkey, *Energy Conversion and Management*, 43, 1099-1120.

Kaygusuz K., Türker M.F, 2002. Biomass energy potential in Turkey, *Renewable Energy*, 26, 661-678.

Klass D.L., 1998. Biomass for Renewable Energy, Fuels, and Chemicals, Academic Press, USA.

Kunii D., Levenspiel O., 1991. Fluidization Engineering, 2nd Edition, Butterworth-Heinemann, USA.

Kutkan F., 2002. Olive and Olive Oil Report, T.C. The Ministry of Agriculture and Rural Affairs, the Presidency of Research, Planning and Coordination Committee.

LMNO Engineering, Research, and Software, Ltd., 2006. Gas Viscosity Calculator, http://www.lmnoeng.com/Flow/GasViscosity.htm, accessed on April, 2006.

Lutgens F. K., Tarbuck E.J., Tasa D.,1997. The atmosphere: An Introduction to Meteorology, 7th edition, Prentice Hall College Div., USA.

McKendry P., 2002a. Energy production from biomass (part 1): overview of biomass, *Bioresource Technology*, 83, 37-46.

McKendry P., 2002b. Energy production from biomass (part 2): conversion technologies, *Bioresource Technology*, 83, 47-54.

Oregon, 2006. Biomass Energy and the Environment, http://egov.oregon.gov/ENERGY/RENEW/Biomass/Environment.shtml, accessed on April, 2006.

Özkaya M. T., 2006. Olive and Olive Oil (in Turkish), Department of Garden Plants - Faculty of Agriculture, University of Ankara, http://www.agri.ankara.edu.tr/bahce/pratikbilgiler/meyve/zeytin/genel.htm, accessed on April, 2006.

Permchart W., Kouprianov V.I., 2004. Emission performance and combustion efficiency of a conical fluidized bed combustor firing various biomass fuels, *Bioresource Technology*, 92, 83-91.

Perry R. H., Chilton H. C., 1973. Chemical Engineers' Handbook, 5th edition, McGraw Hill Chemical Engineering Series.

RAPCIS, 2004. Turkish Regulation for Air Pollution Control from Industrial Sources.

Suksankraisorn K., Patumsawad S., Fungtammasan B., 2003. Combustion studies of high moisture content waste in a fluidized bed, *Waste Management*, 23, 433-439.

Task 29: International Association for the Evaluation of Educational Achievement (IEA), 2006. Bioenergy Network on Social-economics, IEA Bioenergy, http://www.aboutbioenergy.info/index.html, accessed on April, 2006.

Task 32: International Association for the Evaluation of Educational Achievement (IEA), 2006. Biomass Combustion and Co-firing, IEA Biomass Combustion and Co-firing, http://www.ieabcc.nl, accessed on April, 2006.

Topal H., Atımtay T.A., Durmaz A., 2003. Olive cake combustion in a circulating fluidized bed, *Fuel*, 82, 1049-1056.

UNFCCC (United Nations Framework Convention on Climate Change), 2006. Parties to the Convention, http://unfccc.int/parties_and_observers/parties/items/2218.php, accessed on April, 2006.

WEC/TNC (Turkish National Committee of World Energy Council), 2006. General Energy Balances in 2003 for Turkey, http://www.dektmk.org.tr/turkish/Rapor/2003istatistik/2003istindex.htm, accessed on April, 2006.

APPENDIX A

CALIBRATION CURVES FOR THE FUEL FEEDING SYSTEM

The feeding system was calibrated for olive cake and coal. The feeding rate calibration curves for olive cake and coal are given in Figure A.1 and Figure A.2, respectively. The screw feeder conveys the fuel to the combustor column with the "on mode" and it stops to feed with the "off mode". There are ten control steps for both on and off modes. For the control of the feeding rate, a minute is divided into ten equal segments. Each segment has six seconds of time interval. For instance; if the feeding rate of the screw feeder is adjusted to 1-1 mode, the feeder works for six seconds and it stops for a period of six seconds and then it works six seconds again.

The calibration was done for 10 (on) – 10 (off) mode. That means that the screw feeder works for a minute and stops to feed for a minute. In Table A.1, the feeding rates for both olive cake and coal were calculated using the formula of the calibration curves. For the other three mixtures, the feeding rates were obtained by multiplying separately the feeding rates of olive cake and coal with the weight fraction of each fuel in the mixture for the same on-off mode and summing them up. In order to make it clear, an example for a 5-4 mode is presented below.

5-4 mode means that the screw feeder operates (5*6) 30 seconds and stops to feed for (4*6) 24 seconds. Total time for a cycle to be completed is 54 sec. In this time interval, the screw feeder operates for 30 sec. It gives the operation ratio as follows;

Operation ratio = 30 / 54 = 0.556

In order to find the feeding rate per minute, the operation ratio is multiplied by one minute. The physical meaning of this multiplication is just a proportion. If operation time is 30 sec within the 54 sec, it is (0.556*60) 33.33 sec within a minute.

From the calibration calculations, the equations of the curve for solid fuels are found as follows.

$y = 18.706\ x - 0.0972$ for olive cake (O.C.)

$y = 28.672\ x - 0.2350$ for coal (C)

where,

x: time, min

y: fuel feeding rate, g/min

$x = 0.556 * 1\ min = 0.556\ min$

$y_{O.C} = 18.706\ (0.556) - 0.0972 = 10.30\ g/min$ for O.C.

$y_C = 28.672\ (0.556) - 0.2350 = 15.71\ g/min$ for C

By the weight fraction of the solid fuel in mixture, feeding rates are calculated for different mixtures.

$$y = y_{O.C} * wf_{O.C.} + y_C * wf_C$$

where,

$wf_{O.C.}$ = weight fraction of olive cake in mixture

wf_C = weight fraction of coal in mixture

For the mixture of 25% olive cake and 75% coal;

$y = 10.30\ g/min * 0.25 + 15.71\ g/min * 0.75 = 14.36\ g/min$

The feeding rates of the other two mixtures can be calculated by the same way.

Table A.1 Feeding rates for different feeding types of solid fuel

on	off	Feeding Rate, g/min				
		Olive Cake (OC)	Coal (C)	%25 OC +%75 C	%50 OC +%50 C	%75 OC +%25 C
1	1	9.256	14.101	12.890	11.678	10.467
1	3	4.579	6.933	6.345	5.756	5.168
1	4	3.644	5.499	5.036	4.572	4.108
1	5	3.020	4.544	4.163	3.782	3.401
2	6	4.579	6.933	6.345	5.756	5.168
2	8	3.644	5.499	5.036	4.572	4.108
2	9	3.304	4.978	4.560	4.141	3.722
3	2	11.126	16.968	15.508	14.047	12.587
3	3	9.256	14.101	12.890	11.678	10.467
3	5	6.918	10.517	9.617	8.717	7.817
3	6	6.138	9.322	8.526	7.730	6.934
4	5	8.217	12.508	11.435	10.362	9.289
4	7	6.705	10.191	9.320	8.448	7.577
4	9	5.658	8.587	7.855	7.123	6.391
5	3	11.594	17.685	16.162	14.640	13.117
5	4	10.295	15.694	14.344	12.994	11.645
5	7	7.697	11.712	10.708	9.704	8.701
6	3	12.373	18.880	17.253	15.627	14.000
6	8	7.920	12.053	11.020	9.986	8.953
6	9	7.385	11.234	10.272	9.310	8.347
6	10	6.918	10.517	9.617	8.717	7.817
7	4	11.807	18.011	16.460	14.909	13.358
7	6	9.975	15.204	13.897	12.590	11.282
7	7	9.256	14.101	12.890	11.678	10.467
7	8	8.632	13.145	12.017	10.889	9.761
8	2	14.868	22.703	20.744	18.785	16.826
8	3	13.507	20.617	18.840	17.062	15.285
8	5	11.414	17.409	15.911	14.412	12.913
9	7	10.425	15.893	14.526	13.159	11.792
9	8	9.806	14.944	13.660	12.375	11.091
9	9	9.256	14.101	12.890	11.678	10.467
10	1	16.908	25.830	23.600	21.369	19.139
10	3	14.292	21.820	19.938	18.056	16.174
10	5	12.373	18.880	17.253	15.627	14.000

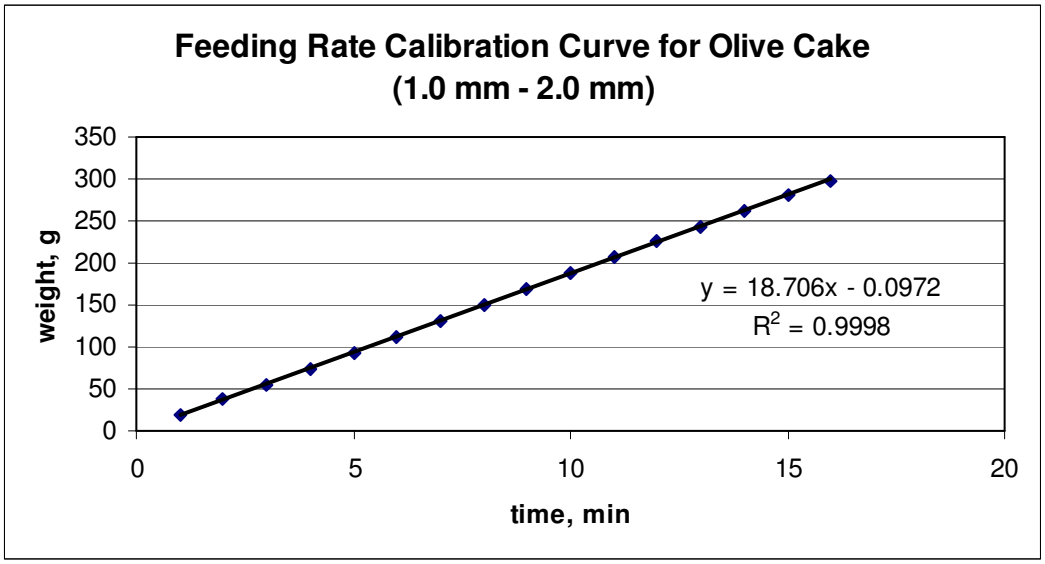

Figure A.1 Feeding rate calibration curve for olive cake

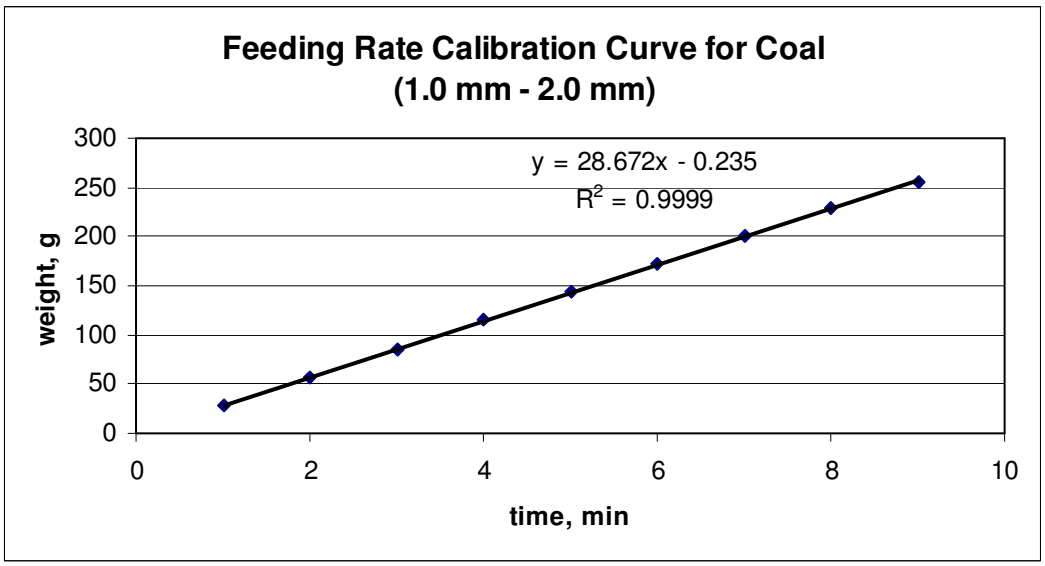

Figure A.2 Feeding rate calibration curve for coal (Tunçbilek lignite)

APPENDIX B

DETERMINATION OF MINIMUM FLUIDIZATION VELOCITY

To understand the behavior of fluidized beds consider a column packed with solid particles through which a fluid (either a liquid or gas) flows. Initially one needs to apply a force to cause the fluid to flow through the solids, and this force results in a pressure drop across the bed of solids. This is a well-known phenomenon and the pressure drop can be found from an appropriate expression, such as the Ergun equation (Chem 347, 1999).

It is assumed that all particles are spherical (ϕ=1).

$$\Delta P_{bed} / L = 150 * (1 - \varepsilon)^2 * \mu * u / \varepsilon^3 / d_p^2 + 1.75 * (1 - \varepsilon) * u^2 * \rho_f / \varepsilon^3 / d_p \quad (B.1)$$

ΔP_{bed}: Pressure drop across the bed
L: height of bed
ε: void fraction of bed
μ: fluid viscosity
u: fluid velocity
d_p: particle diameter
ρ_f: fluid density

The particles in the bed will remain in a packed bed as long as the gravitational forces holding the solid particles down are greater than the force exerted by the

fluid passing up through the bed of particles. At the point where the two forces become equal the solid particles begin to move. The force balance given in equation (B.6) describes this condition known as incipient fluidization (Chem 347, 1999).

$$F_D = \Delta P_{bed} * A \quad (B.2)$$

F_D: Drag force exerted by upward moving fluid

ΔP_{bed}: Pressure drop across the bed

A: Cross sectional area of the reactor

$$G = A * L_{mf} * (1 - \varepsilon_{mf}) * (\rho_s - \rho_f) * g \quad (B.3)$$

G: Weight of particles

A: Cross sectional area of the reactor

L_{mf}: height of bed at minimum fluidization

ε_{mf}: void fraction at minimum fluidization

ρ_s: solid density

ρ_f: fluid density

g: gravitational acceleration

$$F_D = G \quad (B.4)$$

$$\Delta P_{bed} * A = A * L_{mf} * (1 - \varepsilon_{mf}) * (\rho_s - \rho_f) * g \quad (B.5)$$

By rearranging, equation (B.6) is found for minimum fluidization conditions;

$$\Delta P_{bed} / L_{mf} = (1 - \varepsilon_{mf}) * (\rho_s - \rho_f) * g \quad (B.6)$$

The minimum fluidization velocity, u_{mf}, is found by combining the equations (B.1) and (B.6).

$$(1-\varepsilon_{mf})(\rho_s-\rho_f)g = 150(1-\varepsilon_{mf})^2*\mu*u_{mf}/\varepsilon_{mf}^3/d_p^2 + 1.75(1-\varepsilon_{mf})u^2*\rho_f/\varepsilon_{mf}^3/d_p \quad (B.7)$$

Multiplying both side of equation (B.7) by $[\rho_f * d_p^3 / (1 - \varepsilon_{mf}) / \mu^2]$, equation (B.8) is obtained (Kunii and Levenspiel, 1991).

$$[150 * (1-\varepsilon_{mf}) / \varepsilon_{mf}^3] * Re + [1.75 / \varepsilon_{mf}^3] * Re^2 = Ar \qquad (B.8)$$

$$Re \text{ (Reynolds number)} = d_p * u_{mf} * \rho_f / \mu$$

$$Ar \text{ (Archimedes number)} = d_p^3 * \rho_f * (\rho_s - \rho_f) * g / \mu^2$$

When a particle of size d_p fall through a fluid, its terminal free-fall velocity can be estimated from fluid mechanics by the expression

$$u_t = [4 * d_p * (\rho_s - \rho_f) * g / 3 / \rho_f / C_D]^{1/2} \qquad (B.9)$$

where C_D is an experimentally determined drag coefficient (Kunii and Levenspiel, 1991). The drag coefficient for spherical particles is given by equation (B.10),

$$C_D = 24 / Re + 3.3643 * Re^{-0.3471} + 0.4607 * Re / (Re + 2682.5) \qquad (B.10)$$

where Re is the Reynolds number based on the particle. The leading term in the expression for the drag coefficient is for creeping flow past a sphere, where Re<0.1. The second two terms are empirical fits to data at higher Re (Chem 347, 1999).

Calculation of minimum fluidization velocity

If Reynolds number is less than 20, the formula below can be used for the calculation of minimum fluidization velocity (Kunii and Levenspiel, 1991).

$$u_{mf} = [d_p^2 * (\rho_s-\rho_f) * g * \varepsilon_{mf}^3 * \phi_s^2] / [150 * \mu * (1-\varepsilon_{mf})] \quad ; Re<20 \qquad (B.11)$$

where;

d_p: average particle diameter (0.051 cm)

ρ_s: solid (sand) density, experimentally found as 2.57 g/m^3

ρ_f: air density (0.0012 g/m^3)

g: gravitational acceleration (981 cm/s^2)

ε_{mf}: void fraction at minimum fluidization, experimentally found as 0.485

ϕ_s: sphericity of a particle, assumed as 1

μ: viscosity of air (0.00018 g/cm-s)

From the Ideal gas law, density of air at 20^{o}C can be calculated by the formula below.

$$P * V = n * R * T \qquad \text{(B.12)}$$

$V = m / \rho_f$

$\rho_f = (P * m) / (n * R * T) = (P * MW_{air}) / (R * T)$

$P = 1$ atm

$MW_{air} = 0.21 * MW_{O2} + 0.79 * MW_{N2} = 0.21 * 32 + 0.79 * 28 = 28.84$ g/mole

$R = 8.205 * 10^{-5}$ atm-m^3/mole-K

$T = 293$ K

ρ_f @ 20 ^{o}C $= 1.20 * 10^{-3}$ g/cm^3

The viscosity of air (μ) at 20^{o}C can correlated according to the temperature with the Sutherland's formula given below (Crane, 1988). The formula is quoted from the webpage of LMNO Engineering, Research and Software, Ltd (LMNO, 2006).

$$\mu = \mu_o * (a/b) * (T/T_o)^{3/2} \qquad \text{(B.13)}$$

where;

μ_o: reference viscosity @ T_o (0.01827 centipoises)

T_o: reference temperature (524.07 ^{o}R), (CRC, 1984)

$a = 0.555 * T_o + C$

$b = 0.555 * T + C$

C: Sutherland's constant (120)

$T = 20$ ^{o}C $= 527.67$ ^{o}R

The temperature in Celsius can be converted to Rankine by the formula given below.

$$^{o}R = [(^{o}C * 1.8) + 32] + 459.67 \quad \text{(B.14)}$$

The viscosity of air at 20 ^{o}C is calculated as;

μ @ 20 ^{o}C = 0.018 centipoises = 0.00018 g/cm-s

100 centipoises = 1 g/cm-s

After doing all necessary correlations for the temperature variation, minimum fluidization velocity at 20 ^{o}C can be calculated by the formula B.11.

u_{mf} =53.78 cm/sec

Re = 53.78 * 0.051 * 0.0012 / 0.00018 = 18.29 < 20

Since the Reynolds number is less than 20, u_{mf} which is calculated by the formula B.11 is acceptable.

In order to verify the calculated u_{mf} and experimentally determine the minimum fluidization velocity, the experimental study which is done is explained below.

The cyclone part can be separated from the main column. It is screwed off the combustor column. On the cross sectional area of the column nine measurement points are determined. The area is perpendicular to the air flow. The measurement points are shown in Figure B.1. The velocities at nine points are averaged and recorded as the superficial air velocity. While measuring the velocity, the pressure drops at two points are observed. The first one is at the orifice. The other one is at the distributor plate.

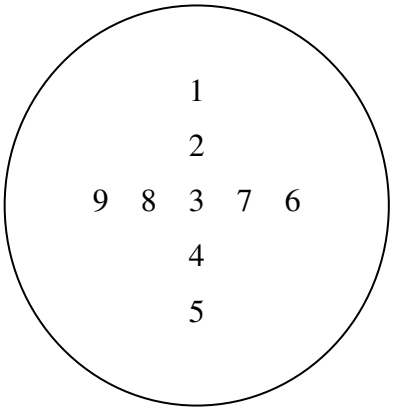

Figure B.1 Cross sectional area of the combustor column and velocity measurement points

While the column is empty, the compressor is operated at minimum flow. The control valve of the compressor is gradually opened. In every velocity measurement, the pressure drops at the orifice and the distributor plate are also recorded. Thus, the pressure drops are determined for each air velocity. Then, sand is loaded into the combustor column. 1420 g of sand equivalent to the 10 cm-bed height is located into the column. Same procedure is applied and the pressure drops are determined for each air velocity. An anemometer was used to measure the air velocity and two manometers were used to determine the pressure drops.

The pressure drop measured while the bed is loaded is the sum of the pressure drops caused by the distributor plate and the bed material. Therefore, the pressure drop across the bed is the difference between the pressure drops when the bed is loaded to the column and when the column is empty. It is given in Table B.1 below.

Table B.1 Pressure drops through the bed corresponding to the air velocities

gas velocity m/sec	Δp @ distributor mmH_2O	Δp @ distributor+bed mmH_2O	Δp @ bed mm H_2O
0.01	0.00	0.20	0.20
0.10	26.00	85.25	59.25
0.26	7.00	95.00	88.00
0.42	11.00	140.00	129.00
0.50	18.00	169.00	151.00
0.54	20.00	172.00	152.00
0.60	26.00	177.00	151.00
0.73	47.00	190.00	143.00
0.84	65.00	204.00	139.00
0.91	83.00	215.00	132.00
0.94	89.00	222.00	133.00
1.00	110.00	242.00	132.00
1.09	121.00	253.00	132.00
1.01	115.00	248.00	133.00
0.92	86.00	218.00	132.00
0.77	48.00	182.00	134.00
0.58	24.00	158.00	134.00
0.44	14.00	142.00	128.00
0.32	11.00	105.00	94.00
0.17	5.00	44.00	39.00
0.09	0.00	15.00	15.00
0.01	0.00	0.10	0.10

The pressure drop versus superficial velocity is plotted in Figure B.2 in order to find the minimum fluidization velocity (u_{mf}). For the fix bed regime at low air flow rates, the pressure drop is approximately proportional with the air velocity. It reaches to the maximum value with a further increase in air velocity. Then, it starts to decrease because of the increase in voidage of the bed material from ε_m to ε_{mf}. ε_m is the void fraction in the fix bed and ε_{mf} is the void fraction of the bed at minimum fluidization. The straight line in Figure B.2 is the static pressure of the

bed and it is slightly less then the maximum pressure drop. The velocity at minimum fluidization is taken as the intersection of the pressure drop versus velocity curve with the horizontal line corresponding to W/A. The minimum fluidization velocity is found as 0.50 m/sec. It is confirmed by the calculated minimum fluidization velocity of 0.54 m/sec.

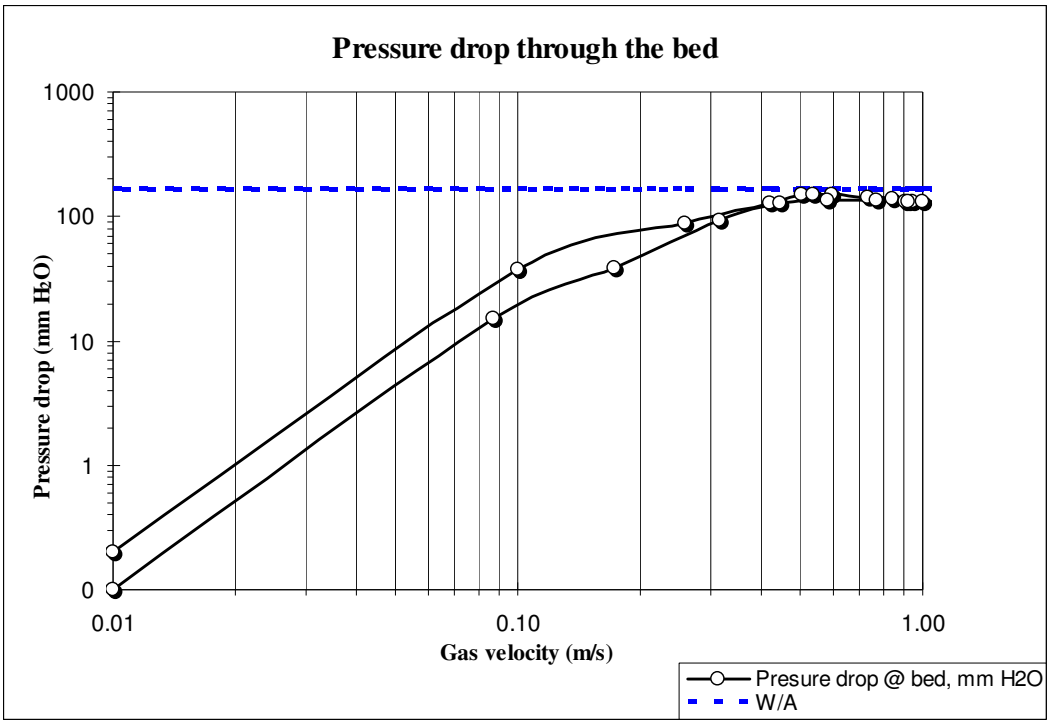

Figure B.2 Pressure drop versus the superficial gas velocity across the bed

The W/A refers to the static pressure of the bed material.

W/A = weight of particles / cross sectional area of the column

APPENDIX C

COMBUSTION AND EFFICIENCY CALCULATIONS

Theoretical oxygen requirement calculations;

a. $\mathbf{C + O_2 \rightarrow CO_2}$ **(C.1)**

In accordance with Eq. (C.1), one mole of oxygen (O_2) is needed to burn one mole of carbon (C).

1 mole C = $12 * 10^{-3}$ kg

From the ideal gas law;

Volume of O_2 (V_{O2}) = n * R * T / P

Number of moles of O_2 required = 1 mole

R = $8.205 * 10^{-5}$ atm-m^3/mole-K

T = 273 K

P = 1 Atm

Volume of O_2 required = $22.4 * 10^{-3}$ Nm^3 @ NTP (Normal Temperature and Pressure)

Required O_2 for one kg of C = $22.4 * 10^{-3}$ Nm^3 / $12 * 10^{-3}$ kg = 1.87 Nm^3/kg C

Volume of CO_2 formed = $22.4 * 10^{-3}$ Nm^3 / $12 * 10^{-3}$ kg = 1.87 Nm^3/kg C

$$\boxed{\mathbf{V_{CO2} = 1.87 * C}} \qquad \textbf{(C.1-1)}$$

where;

V_{CO2}: Volume of CO_2 in flue gas, Nm^3/kg fuel

C: Amount of carbon in fuel, kg C/kg fuel

b. $H_2 + ½\ O_2 \rightarrow H_2O$ **(C.2)**

The same calculation procedure is applied to other reactions;

In accordance with Eq. (C.2), one-half (1/2) mole of oxygen (O_2) is needed to burn one mole of hydrogen (H_2).

1 mole $H_2 = 2 * 10^{-3}$ kg
Number of moles of O_2 required = 0.5 mole
Volume of O_2 required = $11.2 * 10^{-3}$ Nm^3 @ NTP

Required O_2 for one kg of H = $11.2 * 10^{-3}$ Nm^3 / $2 * 10^{-3}$ kg = 5.6 Nm^3/kg H
Volume of H_2O formed = $22.4 * 10^{-3}$ Nm^3 / $2 * 10^{-3}$ kg = 11.2 Nm^3/kg H

$$\boxed{V_{H2O\ in\ flue\ gas} = 11.2 * H} \qquad \textbf{(C.2-2)}$$

where;

$V_{H2O\ in\ flue\ gas}$: Volume of H_2O in flue gas, Nm^3/kg fuel

H: Amount of hydrogen in fuel, kg H/kg fuel

c. $S + O_2 \rightarrow SO_2$ **(C.3)**

In accordance with Eq. (C.3), one mole of oxygen (O_2) is needed to burn one mole of sulphur (S).

1 mole S = $32 * 10^{-3}$ kg
Number of moles of O_2 required = 1 mole
Volume of O_2 required = $22.4 * 10^{-3}$ Nm^3 @ NTP

Required O_2 for one kg of S = $22.4 * 10^{-3}$ Nm^3 / $32 * 10^{-3}$ kg = 0.7 Nm^3/kg S
Volume of SO_2 formed = $22.4 * 10^{-3}$ Nm^3 / $32 * 10^{-3}$ kg = 0.7 Nm^3/kg S

$$\boxed{V_{SO2} = 0.7 * S} \qquad \textbf{(C.3-3)}$$

where;

V_{SO2}: Volume of SO_2 in flue gas, Nm^3/kg fuel

S: Amount of sulphur in fuel, kg S/kg fuel

d. $\mathbf{N_2 + O_2 \rightarrow 2NO}$ **(C.4)**

In accordance with Eq. (C.4), one mole of oxygen (O_2) is needed to burn one mole of nitrogen (N_2).

1 mole $N_2 = 28 * 10^{-3}$ kg

Number of moles of O_2 required = 1.0 mole

Volume of O_2 required = $22.4 * 10^{-3}$ Nm^3 @ NTP

Required O_2 for one kg of N = $22.4 * 10^{-3}$ Nm^3 / $28 * 10^{-3}$ kg = 0.8 Nm^3/kg N

Volume of NO formed = $2 * 22.4 * 10^{-3}$ Nm^3 / $28 * 10^{-3}$ kg = 1.6 Nm^3/kg N

$$\boxed{V_{NO} = 1.6 * N} \qquad \textbf{(C.4-4)}$$

where;

V_{NO}: Volume of NO in flue gas, Nm^3/kg fuel

N: Amount of nitrogen in fuel, kg N/kg fuel

e. **O_2 supplied from fuel;**

1 mole $O_2 = 32 * 10^{-3}$ kg

Number of moles of O_2 = 1 mole

Volume of one mole of O_2 = $22.4 * 10^{-3}$ Nm^3 @ NTP

O_2 supplied from fuel for one kg of fuel = $22.4 * 10^{-3}$ Nm^3 / $32 * 10^{-3}$ kg = 0.7 Nm^3/kg O

Volume of O_2 supplied from fuel:

$$\boxed{V_{O2} = 0.7 * O} \qquad \textbf{(C.5)}$$

where;

V_{O2}: Volume of O_2 in flue gas, Nm^3/kg fuel

O: Amount of oxygen in fuel, kg O/kg fuel

Theoretical oxygen requirement for combustion;

As C, H, S, N and O amounts are given in kg, the theoretical oxygen requirement ($O_{2,th}$) can be obtained in the unit of Nm^3/kg fuel by the following equation:

$$O_{2,th} = 1.87 * C + 5.6 * H + 0.7 * S + 0.8 * N - 0.7\ O \qquad (C.6)$$

Atmospheric oxygen concentration (O_2 atm) is assumed to be 20.90% by volume.

Theoretical air requirement for combustion;

$$V_{air,th} = (O_{2,th} / O_2\ atm) * (100\ \%) \qquad (C.7)$$

where;

$V_{air,th}$: Volume of air theoretically required for the combustion of one kg of fuel, Nm^3/kg fuel

$O_{2,th}$: Theoretical oxygen requirement for the combustion of one kg of fuel, Nm^3/kg fuel

O_2 atm: Atmospheric oxygen concentration (20.90 %).

Actual air requirement for combustion;

$$V_{air,actual} = V_{air,th} * \lambda \quad (C.8)$$

where;

$V_{air,actual}$: Actual volume of air required for the combustion of one kg of fuel, Nm^3/kg fuel

λ : Excess air ratio, (-)

Excess air ratio can be calculated with the following equation assuming that air used for combustion is dry;

$$\lambda = 20.9 / (20.9 - O_2 \text{ measured}) \quad (C.9)$$

The term "excess air ratio" is used to define the amount of excess air required for the fuel to burn completely. If λ =1, there is no excess air supplied to the system. This indicates that combustion takes place on stoichiometric condition. Stoichiometric condition refers to the condition where theoretical oxygen demand of fuel to burn is met. In order to obtain complete combustion of the fuel, some excess air is supplied to the combustion process to ensure that each fuel particle is completely surrounded by sufficient volume of combustion air.

N_2 supply from air to the combustor;

$$V_{N2} = V_{air,th} * [(100 - O_2 \text{ atm}) / (100\ \%)] \quad (C.10)$$

where;

V_{N2}: Volume of nitrogen supplied from air for the combustion of one kg of fuel, Nm^3/kg fuel

Calculation of the amount of flue gases formed at the end of the combustion process on dry basis;

$$V_{fluegas,th(d.b)} = V_{CO2} + V_{SO2} + V_{NO} + V_{N2} \quad (C.11)$$

where;

$V_{fluegas,th(d.b)}$: Volume of flue gas formed on dry basis for the combustion of one kg of fuel, Nm^3/kg fuel

Calculation of the total amount of flue gases formed at the end of the combustion process on wet basis;

$$V_{fluegas,th(w.b)} = V_{fluegas,th(d.b)} + V_{total,\ H2O} \quad (C.12)$$

where;

$V_{fluegas,th(w.b)}$: Volume of flue gas formed on wet basis for the combustion of one kg of fuel, Nm^3/kg fuel

$$V_{total,\ H2O} = V_{H2O\ in\ flue\ gas} + V_{moisture\ in\ fuel} + V_{H2O\ in\ air} \quad (C.13)$$

where;

$V_{total,\ H2O}$: Total volume of water vapor formed for the combustion of one kg of fuel, Nm^3/kg fuel

$V_{moisture\ in\ fuel}$: Volume of water vapor formed by the moisture content of fuel, Nm^3/kg fuel

$V_{H2O\ in\ air}$: Volume of water vapor formed by the moisture content of air, Nm^3/kg fuel

$$V_{moisture\ in\ fuel} = (M.C._{fuel} / M.W._{H2O}) * (R * T / P) \quad (C.14)$$

where;

$M.C._{fuel}$: moisture content of fuel, (g moisture/kg fuel)

$M.W._{H2O}$ = 18 g/mole

R = $8.205 * 10^{-5}$ atm-m^3/mole-K

T = 273 K

P = 1 Atm

Saturation Mixing Ratio (SMR) is the amount of water vapor in a unit mass of dry air. Relative Humidity (RH) is the ratio of actual water vapor in air to the amount of water vapor required for saturation at the same temperature. In order to find the actual amount of water vapor in air, m_{H2O}, SMR is multiplied by RH.

$$m_{H2O} = (SMR * RH) / 100 \quad (C.15)$$

where;

SMR: Saturation Mixing Ratio, g H_2O/kg of air

RH: Relative Humidity, %

Mixing ratio (X) is the ratio of amount of water vapor in dry air by mole.

$$X = (m_{H2O} / 1000) * (M.W._{air} / M.W._{H2O}) * 100 \quad (C.16)$$

where;

$M.W._{air}$ = 28.84 g/mole (20.9% of O_2 and 79.1% of N_2)

$M.W._{H2O}$ = 18 g/mole

$$V_{H2O\ in\ air} = X * (\lambda * V_{air,th}) / 100 \quad (C.17)$$

Actual amount of flue gases formed at the end of the combustion process;

$$V_{fluegas,actual}^{0} = V_{fluegas,th,w.b.} + (\lambda - 1) * V_{air,th} \quad (C.18)$$

where;

$V_{fluegas,actual}^{0}$: Actual amount of flue gas formed, Nm^3/kg fuel

The notation "0" which is used in $V_{fluegas,actual}^{0}$ as superscript represents the volume of flue gas at normal conditions (P =1 Atm, T = 0 ^oC)

Actual amount of flue gas originated from the combustion process should be corrected with respect to temperature variations.

$$V_{fluegas,\ actual} = V_{fluegas,\ actual}^{0} * (T_2 / T_1) \quad (C.19)$$

where,

T_1 = Reference temperature @ normal conditions, 273 ^oK

T_2 = Flue gas temperature, ^oK

CO_2 concentration is not measured by a portable gas analyzer; therefore, it is calculated with a formula given below;

$$X_{CO2} = X_{CO2max} * [1 - (O_2 \text{ measured} / O_2 \text{ atm})] \quad (C.20)$$

where,

X_{CO2}: CO_2 concentration in % by volume

X_{CO2max}: Maximum concentration of CO_2 in combustion gas, characteristic for coal, 19.1 %

O_2 measured: Measured oxygen concentration

O_2 atm: Atmospheric oxygen concentration, 20.9 %

Calculation of Combustion Efficiency;

The combustion efficiency of the system is calculated by using the flue gas analysis and by determining the ash composition generated during the combustion. From these findings, combustion losses are calculated. There are four components of the combustion losses: 1) Combustion losses because of the formation of carbon monoxide (CO) (L_{CO}); 2) Combustion losses because of the formation of hydrocarbons (L_{CH}), 3) Combustion losses due to the ash in the bed (bottom ash) ($L_{C,\ bed}$) and 4) Combustion losses due to the ash in the cyclone (fly ash) ($L_{C,\ cyclone}$).

❖ As a result of the incomplete combustion, CO formed caused the heat loss due to CO in flue gas. The combustion loss due to **the formation of CO** is calculated as follows:

$$L_{CO} = CO * V_{fluegas,\ actual}^{0} * H_{L\_CO} / H_{L\_fuel} / 10{,}000 \qquad (C.21)$$

where,

L_{CO}: Total C loss with CO, %

CO: CO concentration measured in flue gas, ppm

H_{L_CO}: Lower heating value of CO (ΔH_c^0, Heat of combustion), 12.64 MJ/Nm^3 CO (Perry, 1973)

H_{L_fuel}: Lower heating value of the fuel used, MJ/kg fuel

❖ The heating value of combustible materials lost as **hydrocarbons in flue gas** is calculated as follows:

$$L_{CH} = C_mH_n * V_{fluegas,\ actual}^{0} * H_{L\_CmHn} / H_{L\_fuel} / 10{,}000 \qquad (C.22)$$

where,

L_{CH}: Total C loss with hydrocarbons, %

C_mH_n: C_mH_n concentration measured in flue gas as C_3H_8, ppm

H_{L_CmHn} = Lower heating value of C_3H_8 (ΔH_c^0, Heat of combustion), 91.31 MJ/Nm^3 C_3H_8 (Perry, 1973)

❖ The heating value of combustible material lost as **carbon in bottom ash** is calculated as follows:

$$L_{C,\,bed} = Ash_{\,bed} * C_{\,bed} * H_{L\_Char} / M_f / H_{L\_fuel} * 100 \quad (C.23)$$

where,

$L_{C,\,bed}$: Total C loss with carbon in bottom ash, %

$Ash_{\,bed}$: Amount of bottom ash formed during combustion, kg ash/h

$C_{\,bed}$: Unburnt carbon content in the bottom ash, kg C/ kg ash

H_{L_Char}: Lower heating value of char (ΔH_c^0, Heat of combustion), 32.79MJ/kg char (Perry, 1973)

M_f: Fuel feeding rate, kg fuel/h

❖ The heating value of combustible material lost as **carbon in fly ash** is calculated as follows:

$$L_{C,\,cyclone} = Ash_{\,cyclone} * C_{\,cyclone} * H_{L\_Char} / M_f / H_{L\_fuel} * 100 \quad (C.24)$$

where,

$L_{C,\,cyclone}$: Total C loss with carbon in fly ash, %

$Ash_{\,cyclone}$: Amount of ash held by cyclone, kg ash/h

$C_{\,cyclone}$: Unburnt carbon content in the fly ash, kg C/ kg ash

❖ Overall combustion efficiency (η) in % is calculated as follows:

$$\eta = 100 - (L_{CO} + L_{CH} + L_{C,\,bed} + L_{C,\,cyclone}) \quad (C.25)$$

The total thermal capacity of a combustor is calculated as follows:

$$Q_f = M_f * H_{L\_fuel} * (\eta/100) * (1\ h/3600\ sec) * (10^3\ kW/1\ MW) \quad (C.26)$$

where,

Q_f : Total thermal capacity of combustor, kW

APPENDIX D

SAMPLE CALCULATION FOR FLUE GAS COMPOSITION AND COMBUSTION EFFICIENCY

The pollutant concentrations in flue gas, combustion losses and combustion efficiency are calculated by using the equations given in Appendix C and the results are presented below. The results obtained by the co-combustion of fuel mixture containing 50 wt% olive cake and 50 wt% coal without secondary air injection are taken as an example. The pollutant concentrations are measured and recorded in every five seconds and twelve measurements are taken for a minute. They are expressed as average values of one-minute measurements.

The ultimate analyses of olive cake, coal and the fuel mixture containing 50 wt% olive cake and 50 wt% coal are given in Table D.1.

Table D.1 Ultimate analysis of olive cake, coal and fuel mixture

	Ultimate Analysis, on wet basis (wt%)		
	Olive Cake (O.C)	**Lignite Coal (C)**	**50 wt% O.C+ 50 wt% C**
C	47.93	46.29	47.11
H	5.46	3.37	4.42
N	1.19	1.14	1.17
O	34.42	16.75	25.59
S	0.08	1.87	0.98
ash	4.21	19.91	12.06
moisture	6.71	10.68	8.70
total	100.00	100.01	100.01

Volume of the flue gas that will form by complete combustion of fuel mixture is calculated below by using Equations C.1-1, C.2-2, C.3-3, C.4-4 and C.5 given in Appendix C for C, H, S, N, and O, respectively. The fuel composition given in Table D.1 is used for C, H, S, and O contents.

$V_{CO2} = 1.87 * C = 1.87 * 0.4711 = 0.88\ Nm^3/\ kg\ fuel$

$V_{H2O\ in\ flue\ gas} = 11.2 * H = 11.2 * 0.0442 = 0.49\ Nm^3/\ kg\ fuel$

$V_{SO2} = 0.7 * S = 0.7 * 0.0098 = 0.007\ Nm^3/\ kg\ fuel$

$V_{NO} = 1.6 * N = 1.6 * 0.0117 = 0.0188\ Nm^3/\ kg\ fuel$

$V_{O2} = 0.7$

$* O = 0.7 * 0.256 = 0.18\ Nm^3/\ kg\ fuel$

Equation C.5 is used in order to find the theoretical oxygen requirement of one kg of fuel mixture. The fuel is assumed to be completely burnt.

Theoretical air requirement for combustion;

The theoretical oxygen requirement for combustion has been found to be $O_{2,th} = 0.97\ Nm^3/\ kg$ fuel by using Eq. C.6 given in Appendix C.

O_2 in the atmosphere is assumed to be 20.90% by volume. According to the Eq. C.7, the theoretical air requirement for combustion is:

$V_{air,th} = (O_{2,th} / O_2\ atm) * (100\ \%) = 4.62\ Nm^3/\ kg\ fuel$

Actual air requirement for combustion;

If the combustion takes place with 50 % of excess air, then the excess air ratio (λ) is 1.5. The actual amount of air to be supplied to the combustor by using Eq. C.8 is:

$V_{air,actual} = V_{air,th} * \lambda = 6.93\ Nm^3/\ kg\ fuel$

N_2 supply from air to the combustor;

The amount of N_2 coming to the combustor with O_2 by using Eq. C.10 is:

$V_{N2} = V_{air,th} * [(100 - O_2 \text{ atm}) / (100\ \%)] = 3.65\ Nm^3/\text{ kg fuel}$

Calculation of the amount of flue gases formed at the end of the combustion process on dry basis;

The amount of flue gas formed on theoretical basis is calculated by using Eq. C.11.

$V_{fluegas,th(d.b)} = V_{CO2} + V_{SO2} + V_{NO} + V_{N2} = 4.56\ Nm^3/\text{ kg fuel}$

Calculation of the total amount of flue gases formed at the end of the combustion process on wet basis;

The volume of flue gas needs to be corrected for the moisture coming from the fuel and air and for the moisture formed during the combustion process by using Eq. C.13 and Eq. C.14 in Appendix C.

$V_{moisture\ in\ fuel} = (M.C._{fuel} / M.W._{H2O}) * (R * T / P)$

where;

$M.C._{fuel}$ =87 g moisture/kg fuel

$M.W._{H2O}$ = 18 g/mole

R = $8.205 * 10^{-5}$ atm-m^3/mole-K

T = 273 K

P = 1 Atm

$V_{moisture\ in\ fuel} = 0.11\ Nm^3/\text{ kg fuel}$

Saturation Mixing Ratio (SMR) at room temperature (20 ^{o}C) is found to be 14 g H_2O/kg of air according to (Lutgens, 1997). Relative Humidity (RH) is assumed to be 75%.

m_{H2O} = (SMR * RH) / 100 = 10.5 g H_2O/kg of air

X = (m_{H2O} / 1000) * ($M.W._{.air}$ / $M.W._{.H2O}$) * 100 = 1.68%, moleH2O/mole dry air

where;

$M.W._{.air}$ = 28.84 g/mole (20.9% of O_2 and 79.1% of N_2)

$M.W._{.H2O}$ = 18 g/mole

$V_{H2O\ in\ air}$ = X * (λ * $V_{air,th}$)/ 100 = 0.116 Nm^3/ kg fuel

The volume of the total amount of water vapor (moisture) in the flue gas becomes:

$V_{total,\ H2O}$ = $V_{H2O\ in\ flue\ gas}$ + $V_{moisture\ in\ fuel}$ + $V_{H2O\ in\ air}$ = 0.72 Nm^3/ kg fuel

If this amount is added on the volume of the dry flue gas, the following result is obtained:

$V_{fluegas,th(w.b)}$ = $V_{fluegas,th(d.b)}$ + $V_{total,\ H2O}$ = 5.28 Nm^3/ kg fuel

<u>Actual amount of flue gases formed at the end of the combustion process;</u>

The actual amount of flue gas formed due to the combustion process is calculated by taking the excess air also into consideration. Oxygen concentration in the flue gas is measured as 9.1 %. Excess air ratio is calculated according to the measured concentration of O_2 by using Eq. C.9.

λ = 20.9 / (20.9 - O_2 measured) = 1.77

Actual amount of flue gas formed (on volume basis) at the end of the combustion process is calculated by using Eq. C.18 and the result is given below:

$V_{fluegas,actual}^{0} = V_{fluegas,th,w.b.} + (\lambda - 1) * V_{air,th} = 8.84\ Nm^3/\ kg\ fuel$

where;

$V_{fluegas,actual}^{0}$ is the volume of flue gas formed for the combustion of one kg of fuel mixture.

The amount of CO_2 formed due to combustion (CO_2 concentration) is calculated as follows by using Eq. C.20:

$X_{CO2} = X_{CO2max} * [1 - (O_2\ measured / O_2\ atm)] = 10.78\ \%$

The concentrations of air pollutants in the flue gas are measured as "ppm_v" and the concentrations are expressed in mg/Nm^3 based on 6% by vol. O_2 content. This is also a requirement according to the Turkish Regulation RAPCIS(2004). The measured concentrations of air pollutants for the 50 wt% olive cake-50 wt% coal mixture are given in Table D.2.

Table D.2 Concentrations of air pollutants in the flue gas

	Concentrations	
	ppm	**mg/Nm^3**
CO	429.0	676.7
C_mH_n as C_3H_8	14.0	34.7
NO_x as NO_2	422.5	1,095
SO_2	452.5	1,631

Pollutant concentrations are converted from ppm_v to mg/Nm^3 by using the equation given below:

$$X\ (mg/Nm^3) = X\ (ppm) * [P / (R * T * 10^3)] * M.W._X * (\lambda_{ref} / \lambda) \quad (D.1)$$

where,

X (mg/Nm^3): Pollutant concentration expressed in mg/Nm^3

X (ppm): Pollutant concentration measured in ppm

M.W.$_X$: Molecular weight of pollutant, g/mole

λ_{ref}: Reference excess air ratio (according to 6% O_2), 1.4

λ: Calculated excess air ratio (according to measured O_2)

Calculation of Combustion Efficiency;

Combustion efficiency is calculated as follows:

- Firstly, the lower heating value of the fuel mixture (50 wt% olive cake-50 wt% coal) is calculated as follows:

H_{L_fuel} = [(% olive cake * $H_{L\_olive\ cake}$) + (% coal * H_{L_coal})] / 100
= [(50 * 19.44 MJ/kg) + (50 * 19.19 MJ/kg)] / 100
= 19.32 MJ/kg

- Secondly, the combustion loss due to **the formation of CO** is calculated by using Eq. C.21 as follows:

$L_{CO} = CO * V_{fluegas,\ actual}^{0} * H_{L\_CO} / H_{L\_fuel} / 10{,}000 = 0.25\%$

- Thirdly, the heating value of combustible materials lost as **hydrocarbons in flue gas** is calculated by using Eq. C.22 as follows:

$L_{CH} = C_mH_n * V_{fluegas,\ actual}^{0} * H_{L\_CmHn} / H_{L\_fuel} / 10{,}000 = 0.06\%$

At the end of the combustion of the fuel mixture, 5.3 g of bottom ash was collected within the bed material and 0.23 g of fly ash was collected by the ash hopper which is at the bottom of the cyclone. The combustion lasted 1.14 hours.

The ash sample was burned at 950 ^{o}C in order to find the unburnt-C content of the bottom ash. The difference in weight before and after the combustion at 950 ^{o}C, gave the unburnt amount of carbon in the ash sample. The unburnt carbon amount was found to be 2.32 wt%. The similar analysis is done for the ash sample from the cyclone. The result is 16.9 wt% unburnt C for the fly ash in the cyclone.
Thus;

Ash_{bed} = (5.3 g / 1.14 h) * (10^{-3} kg/g) = 4.6 * 10^{-3} kg ash/h

C_{bed} = 0.0232 kg C/ kg ash

$Ash_{cyclone}$: (0.23 g / 1.14 h) * (10^{-3} kg/g) = 0.2 * 10^{-3} kg ash/h

$C_{cyclone}$ = 0.169 kg C/ kg ash

M_f = 10 g fuel/min = 0.6 kg fuel/h

❖ The heating value of combustible material lost as **carbon in bottom ash** is calculated by using Eq. C.23 as follows:

$$L_{C,\,bed} = Ash_{bed} * C_{bed} * H_{L\_Char} / M_f / H_{L\_fuel} * 100 = 0.03\%$$

❖ The heating value of combustible material lost as **carbon in fly ash** is calculated by using Eq. C.24 as follows:

$$L_{C,\,cyclone} = Ash_{cyclone} * C_{cyclone} * H_{L\_Char} / M_f / H_{L\_fuel} * 100 = 0.01\%$$

❖ Finally, overall combustion efficiency (η) in % is calculated by using Eq. C.25 as follows:

$$\eta = 100 - (L_{CO} + L_{CH} + L_{C,\,bed} + L_{C,\,cyclone}) = 99.6\%$$

The total thermal capacity of a combustor (assuming that there is no heat loss) is calculated by using Eq. C.26 as follows:

$Q_f = M_f * H_{L\_fuel} * (\eta/100) * (1\ h/3600\ sec) * (10^3\ kW/1\ MW)$

= 3.2 kW